Spring 4-24-2015

TOWARD THE MEASUREMENT OF BIODISTRIBUTION OF ^{18}F-LABELED INDUSTRIAL CHEMICALS WITH POSITRON EMISSION TOMOGRAPHY (PET)

Katelyenn S. McCauley
University of Nebraska-Lincoln, kglaspy@huskers.unl.edu

TOWARD THE MEASUREMENT OF BIODISTRIBUTION OF ^{18}F-LABELED INDUSTRIAL CHEMICALS WITH POSITRON EMISSION TOMOGRAPHY (PET).

By

Katelyenn S. McCauley

A Thesis

Presented to the Faculty of

The Graduate College at the University of Nebraska

In Partial Fulfillment of Requirements

For the Degree of Master of Science

Major: Chemistry

Under the Supervision of Professor Stephen DiMagno

University of Nebraska

May 2015

TOWARD THE MEASUREMENT OF BIODISTRIBUTION OF ^{18}F-LABELED INDUSTRIAL CHEMICALS WITH POSITRON EMISSION TOMOGRAPHY (PET).

Katelyenn S. McCauley, M.S.

University of Nebraska, 2015

Advisor: Stephen DiMagno

Plasticizers are added to polymeric materials to increase flexibility and durability, thus they constitute a common, and widely used class of industrial chemicals. Plasticizers have been suspected of a number of adverse health effects including the interference with the endocrine system.[1] These substances have the tendency to migrate to the surfaces of materials, where they can be absorbed, ingested, or inhaled. [5] The iniquitousness of plasticizers and the daily contact with polymeric materials has given rise to concern about the toxicity and health effects of these substances. Many long-term and excessive-dose studies have been conducted on many of these chemicals, but little has been done to determine the short-term and small-dose effects of these types of compounds. [2,3,4] Classical methods of examining the biodistribution of such substances include autoradiography, as well as an array of other analytical techniques. While these methods can sufficiently provide biodistribution data, they suffers some limitations.

The majority of this thesis will argue that positron emission tomography (PET) is a potential replacement for classical techniques to monitor biodistribution and pharmacokinetics of widespread environmental contaminants. The work in this masters

thesis is focused on the preparation of three labeled model compounds: [^{18}F] 2-fluoro-4-(2-(4-hydroxyphenyl)propan-2-yl)phenol, [^{18}F] diethyl 4-fluorophthalate, and [^{18}F] bis(2-ethylhexyl) 4-fluorophthalate. Imaging of these compounds will be offered as proof of principle. Studies demonstrate that this approach is feasible, and that it can complement and replace many of the laborious animal studies used in current toxicology research.

Acknowledgements

First and foremost, I want to thank God for giving me the ability and strength needed to achieve this degree. Without Him, none of this would have been possible. Thank you for your love and grace.

Secondly, I would like to thank my family. Karina Allen, you are one exceptional lady. You kept me going when things became difficult. “Pull yourself up from your bootstraps, girl,” is a phrase I will never forget. To my dad, Jim Glaspy, thank you for reminding me that a day off every now and then is needed and should be taken advantage of. Abigail Glaspy, you have such a beautiful soul. You have blessed me with two amazing nieces. You are a great mother and an awesome sister. Thank you for your encouragement throughout this process. To my brother, Hunter Glaspy, you are a great guy. Thanks for being you, for making me laugh until I cry. Finally my grandparents, Wilson and Judy Gauntt, thank you so much for your prayers and support. You are both wise people and have taught me so much.

I want to send a special thanks to my friend, Ben Enns for following me around since undergrad. Thanks for being there and willing to help throughout all our academic struggles from C of O to UNL. I know you will find that special redheaded girl that loves tie-dye and fictional fairytale movies and videogames as much as you do!

To my coffee girls: Shaina and Veronika. Without those days that we took time to just get out of Hamilton for a coffee run, I would have probably lost my mind a long time ago. You both are exceptional chemists and I have no doubt that you can change the face

of chemistry. Thank you so much for your friendship and all the fun times. I wish you the best in all your endeavors.

To my husband, Jacob McCauley: you are my drive, my constant, and I am forever grateful for the sacrifices that you have made. Thank you so much for believing in me. Despite being 575 miles away from you for almost 2 years, you kept me going. You can always make a bad day better with just a phone call. I am so excited to take on life together! I look forward to having scientific debates in person. You pushed me to learn more and to be a better chemist. You kept my perspective on track. I love you so much.

Lastly, I would like to thank Dr. DiMagno and the group. Steve, you opened my eyes to many things about chemistry, and I am grateful for all the pep talks that redefined my purpose. Thank you for allowing me to have two great internships with your lab and then joining as a graduate student, where I have picked up many new skills. Thanks to Dr. Kiel Neumann for being my mentor and a great friend. Thank you for teaching me so much and for all that coffee! Dr. Bao Hu, "you da man!" Thanks for teaching me so many lab techniques, and standing beside me when I was worried about using pyrophoric compounds! Thanks to Jayson, Ethan, and Jordan for being there and understanding, and for all the borrowed glassware.

TABLE OF CONTENTS

LIST OF FIGURES

LIST OF TABLES

LIST OF SCHEMES

NOMENCALTURE AND ABBREVIATIONS

ADME	Absorption, distribution, metabolism and excretion
ADP	Adiponectin
AGD	Anogenital distance
AGI	Anogenital index
APCI	Atmospheric pressure chemical ionization
BBr_3	Boron tribromide
BPA	Bisphenol A
BPAQ	Bisphenol A *ortho*-quinone
CDC	Center for Disease Control and Prevention
DBP	Di-*n*-butyl phthalate
DBU	1, 8-Diazabicyclo[5.4.0]undec-7-ene
DCC	*N,N'*-dicyclohexylcarbodiimide
DCU	dicyclohexylurea
DEHP	Bis(2-ethyhexyl) phthalate
DEP	Diethyl phthalate
DMAP	4-dimethylaminopyridine
EOM	Ethoxy methyl
EPA	Environmental Protection Agency
ER	Estrogen receptor
FSH	Follicle stimulating hormone
GC	Gas chromatography

HPLC	High performance liquid chromatography
KF	Potassium fluoride
LC	Liquid chromatography
LH	Luteinizing hormone
MEHP	Mono(2-ethylhexyl) phthalate
MEP	Monoethyl phthalate
MOM	Methoxy methyl
MS	Mass spectrometry
MTBE	methyl-*tert*-butyl ether
NAD	Nicotinamide adenine dinucleotide
NADPH	Dihydronicotinamide-adenine dinucleotide phosphate
NFOBS	N-fluoro-*o*-benzenedisulfonimide
NFSI	N-fluorobenzenesulfonimide
NMR	Nuclear Magnetic Resonance
NTP	National Toxicology Program
PET	Positron Emission Tomography
PVC	Polyvinyl chloride
S_NAr	Aromatic substitution
TBAF	Tetrabutylammonium fluoride
TIPS	Triisopropylsilyl
TMAF	Tetramethylammonium fluoride
TMSOAc	Trimethylsilyl acetate
TMSOTf	Trimethylsilyl trifluoromethanesulfonate (triflate)

TMSTFA	Trimethylsilyl trifluoroacetate
TMS-X	Notation for general trimethylsilyl-anion ligand used for electrophilic activation
ZAG	Zinc-alpha2-glycoprotein

CHAPTER 1

Tools to Measure Biodistribution

1.1 Introduction

Plasticizers are added to polymeric materials to increase flexibility and durability, thus they constitute a common, and widely used class of industrial chemicals. These substances have the tendency to migrate to the surfaces of materials, where they can be absorbed, ingested, or inhaled. [5] The iniquitousness of plasticizers and the daily contact with polymeric materials has given rise to concern about the toxicity and health effects of these substances. One key element in evaluating the toxicity of a substance is to study its pharmacokinetics and biodistribution in animals and humans. There are several classical methods of measuring biodistribution. The majority of this thesis will argue that positron emission tomography (PET) is a potential replacement for classical techniques to monitor biodistribution and pharmacokinetics of widespread environmental contaminants. The work in this masters thesis is focused on the use three labeled model compounds: [^{18}F] 2-fluoro-4-(2-(4-hydroxyphenyl)propan-2-yl)phenol, [^{18}F] diethyl 4-fluorophthalate, and [^{18}F] bis(2-ethylhexyl) 4-fluorophthalate. Imaging of these compounds will be offered as proof of principle. Studies demonstrate that this approach is feasible, and that it can complement and replace many of the laborious animal studies used in current toxicology research.

1.2 Classical Methods of Measuring Biodistribution

Many classical techniques exist for measuring the absorption, distribution, metabolism and elimination (ADME) of a given substance. Some studies give information about exposure to circulating metabolites, identity of metabolites, rate at

which metabolites are excreted, and the route of elimination. Other studies have the ability to characterize the distribution of a compound/metabolites in a given tissue or organ sample at one given time point.

The most useful tool for measuring adsorption, distribution and metabolism is coupled gas chromatography and mass spectrometry. In its simplest form, GC/MS is used to evaluate the concentrations of a given substance in a bodily fluid or tissue. GC/MS analysis of multiple samples withdrawn at serial time points can provide an exceptionally accurate picture of the time course of the concentration profile *in vivo.* As an example, Hong-xia and co-workers used GC/MS to identify the active compound of a Chinese herbal medicine, *Gastrodia elata Blume*, and measure its biodistribution in mice. The animals were fed this compound, then urine and brain samples were collected. These samples were treated with acetic anhydride to enhance the volatility of the compound and its metabolite(s) and then injected into a GC/MS, which separated and identified the acetylated derivatives. [6]

Other methods have also been utilized to monitor biodistribution of a given compound including gas chromatography-mass spectrometry (GC/MS), (liquid chromatography- mass spectrometry (LC/MS), and mass spectrometry- mass spectrometry (MS/MS). Frias *et. al.* developed a GC/MS/MS method that was able to detect chlorocarbon pesticides in human serum samples, and Smeds and Saukko used GC/MS to measure these substances in adipose tissue.[7] The U.S. Center for Disease Control and Prevention (CDC) developed a high-throughput LC/APCI-MS/MS (Liquid chromatography/atmospheric pressure chemical ionization-mass spectrometry/mass spectrometry) to quantify eight phthalate metabolites in human urine.[7] The urine samples

were processed using enzymatic deconjugation of the glucuronides, followed by LC/APCI/MS/MS analysis. This method allowed for rapid detection of phthalate metabolites with relatively low detection limits. The CDC later further optimized this study by incorporating an isotopically labeled (^{13}C) internal standard for each of the eight analytes as well as a conjugated internal standard to monitor deconjugation efficiency

In absorption, distribution, metabolism and excretion (ADME) studies, it is common to radiolabel a compound in order to track it and its metabolites at the tracer level. In these cases, a variety of MS and GC instruments coupled to on- or off-line radioactivity detection can be employed. [^{14}C] Carbon and tritium, both beta-emitting isotopes, are commonly used for this type of analysis because their incorporation leads to virtually no change in the molecular structure or properties of the target compound. An example of the instrumentation used to measure radioactivity in an ADME study would be HPLC-MS/radiometry, which combines both radiochromatographic profiles for isotope quantification with mass spectral data of metabolites of a radiolabeled parent compound.[8]

MS-based techniques can provide information regarding identification, concentration and isotopic ratios in serum samples, but still suffer some limitations. These methods tend to require more work to obtain appropriate standards. Moreover, the extraction efficiency and characterization of various matrix effects on quantitation must be evaluated for each organ or tissue sample.[9] For MS samples, the compound needs to be ionized, which can cause different responses from metabolites than that of the parent compound. This creates a challenge for adequate quantification of specific metabolites and requires preparation of synthetic standards and calibration curves for each ion source.

[10] Most importantly, these techniques do not allow for direct visualization of biodistribution and binding of a given substrate in real time. In many cases, excretion and serum samples and animal sacrifice must be performed at various time points to retrieve complete information of adsorption, distribution, and metabolite quantification and qualification.

Autoradiography is another widely used tool to monitor the biodistribution of radiolabeled compounds. It has the benefit of permitting visualization of the distribution and binding of targets at various time points. This technique is used to localize radioactivity within a solid specimen, which provides data on distribution of a given substance and can ultimately assess whether a substance can be completely eliminated or not. In an autoradiography study, a subject can be sacrificed after injection of a radiolabeled ligand (*in vivo* autoradiography) or a target organ or tissue can be examined after treatment with a radiolabeled ligand (*in vitro* autoradiography). In either case, the collection of tissue samples is conducted by freezing the whole animal or organ and cryosectioning the subject. After treatment with the radio-ligand, these tissue sections are then exposed to a photographic emulsion or a phosphoimaging device that detects and quantifies the radioactivity in selected tissues. [10] The radionuclides of choice are typically [^{3}H] tritium (β decay), [^{14}C] carbon (β decay) or [^{125}I] iodine (γ decay). A typical dose supplied *in vitro* is around 160 μCi/kg. [8] In order to gather information about distribution, a statistically valid number of animals are injected with the same compound, and at least three at a time are sacrificed at each time point to determine biodistribution and pharmacokinetics.

While autoradiography can provide data on biodistribution, this method has a number of limitations. First, studies have shown that the use of tritium and iodine-125 as radioisotopes can be problematic in autoradiography analysis. Tritium has the tendency to undergo hydrogen exchange with water, and in many cases ^{125}I is not biologically benign *in vivo* and has shown to be liberated from the parent compound. [8,9] The extent of dissociation limits the accurate interpretation of the autoradiograph. The generation of carbon-14 can be difficult and time consuming. It requires labor-intensive operations to convert ^{14}C to graphite and is not readily adaptable to automation. This results in low throughput sample preparation and high cost analysis.[8] Therefore, many researchers often use ^{3}H or ^{125}I. Autoradiography is also limited by its inability to decipher between parent molecule, metabolites or degradation product, as it only detects total-substance radioactivity.[8] Finally, autoradiography does not allow for multiple time points to be observed in a single subject, rather at each time point, at least three subjects will be sacrificed. Thus, this technique cannot be applied for assessing ADME in human trials.

In summary, many experimental methods exist to monitor distribution of a compound *in vivo*. The above-mentioned methods have the capability of efficiently and accurately providing information on identity, substrate concentration, binding targets, metabolism and elimination. However, the major limitations of these methods warrant the need of a technique that allows for non-invasive, visualization of biodistribution over a series of time points in a single test subject. More recently, positron emission tomography has become increasingly popular in ADME studies because it is a less invasive technique, and can give an abundance of information relating to biodistribution and pharmacokinetics on a single, living subject. My research focuses on the application

of PET as a method to assess the distribution and toxicological profile of three industrial used plasticizers: bisphenol A, diethyl phthalate, and bis (2-ethylhexyl) phthalate. These compounds were selected as test cases for assessing PET as a standard tool in environmental toxicology, because there exists a wealth of data derived from classical biodistribution, pharmacokinetic, and pharmacodynamics studies.

1.3 Positron Emission Tomography

Positron Emission Tomography (PET) is a valuable, non-invasive nuclear imaging technique that allows for the visualization of physiological and biological processes *in vivo* in real time. While PET is commonly used for diagnostic confirmation and tumor localization, it is also useful as a means to determine pharmacokinetics and pharmacodynamics of early phase pharmaceuticals. PET holds advantages over methods like autoradiography, as it allows for the visualization of biodistribution in real time, and it also permits these measurements on a single subject at multiple time points. Also, the non-invasive nature of PET permits this method to be used in human studies, which is why tracer studies are commonly conducted for many pharmaceutical drugs before they enter Phase II or Phase III trials. [8]

PET has the potential to supplant classical methods such as autoradiography. Autoradiography is limited is its ability to also monitor kinetics, and multiple subjects must be used to get usable data for distribution studies. When using multiple subjects, there is much room for error. Different subjects may react differently to a compound, depending on sex, weight, blood type, etc. On the other hand, PET provides the investigator with the ability to perform multiple scans at various time points on a single,

living subject. This allows for more accurate kinetic studies as well as full visualization of the biodistribution of a compound. Figure 1-1 depicts a comparison of autoradiography and PET for the assessment of Alzheimer's patients. These studies utilized [^{18}F]-labeled THK523, a compound that recognizes and bind to tau proteins in the brain. Figure 1-1A shows the hippocampus of a 90-year-old woman who died of Alzheimer's disease.[11] Figure 1-1B are PET scans of three different levels of the brain of a 72-year-old woman who was diagnosed with Alzheimer's disease.[12] Essentially the same information can be drawn from a PET scan as from an autoradiogram, but PET can be conducted on a living patient to assess the efficiency of treatments, and monitor kinetics, distribution and binding of a specific compound over time.

A) **B)**

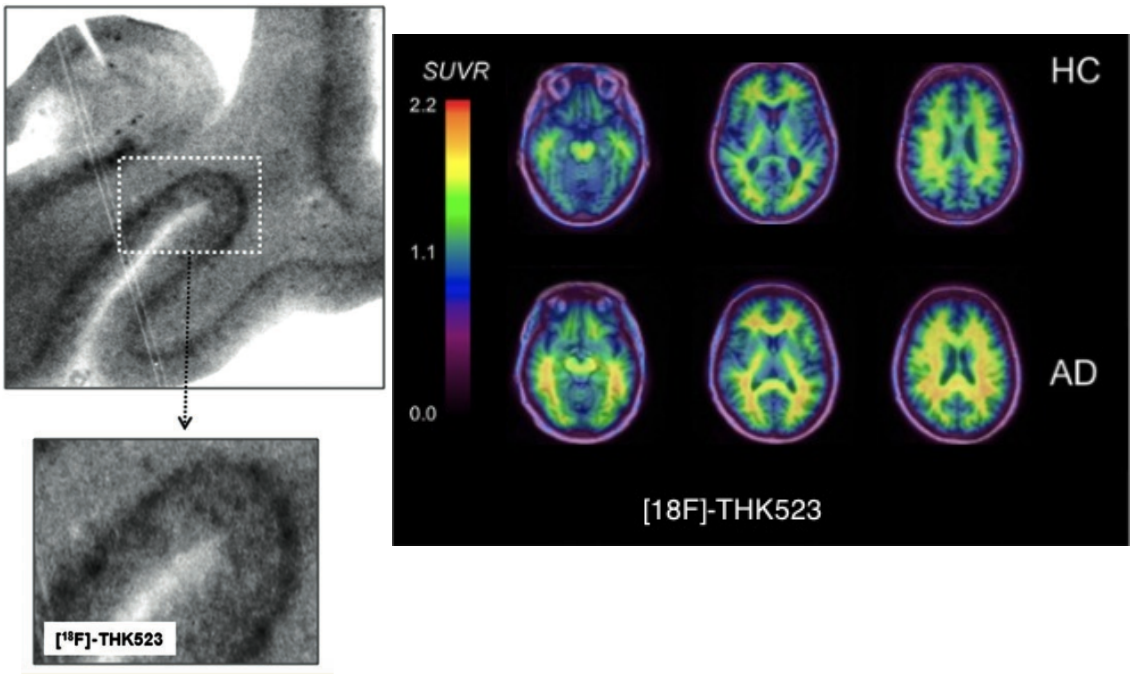

Figure 1-1: Comparison of autoradiograph and PET scan of Alzheimer's Disease patients. A) Autoradiogram of [^{18}F]THK523 binding to tau tangles.[11] B) PET scan of [^{18}F]THK523 binding to tau proteins. HC: healthy control; AD: Alzheimer's disease.[12]

PET imaging is performed after injecting a patient with a radiopharmaceutical that is labeled with a positron emitting radionuclide. As the radionuclide decays, a high kinetic energy positron is emitted, which, upon slowing down, captures an electron and cause an annihilation. This phenomenon releases two 511 keV gamma rays oriented at 180° from each other. The coincident λ-rays are detected by a circular scintillation detector that surrounds the patient. This concept is illustrated in Figure 1-2.

A. **B.**

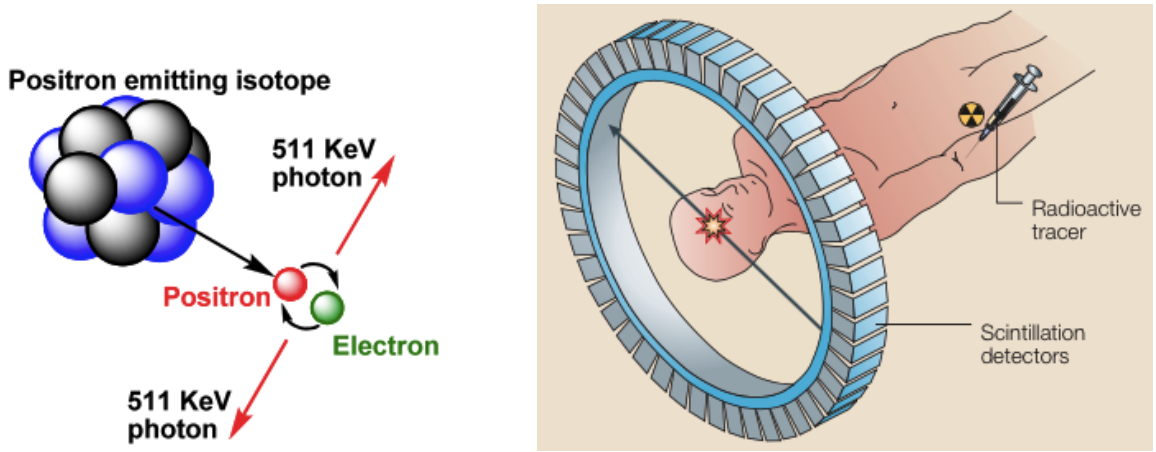

Figure 1-2: A) A representation of a positron-emitting nucleus and the annihilation phenomenon that occurs. Adapted from Z. Li, 2010.[13] B) A diagram of the detection of the emitted gamma rays by a scintillator. Adapted from C. West, 2004.[14]

Various radionuclides can be incorporated into radiopharmaceuticals to be used as PET agents, as seen in Table 1-1. It is common to utilize carbon-11 on molecules of interest because carbon is contained in all organic compounds, and thus it is believed that isotopic substitutions with a radioisotope of carbon does not affect biodistribution *in vivo*. A significant advantage of using [^{11}C] carbon is its relatively short half-life (20.3 min).

This short half-life means that the total radioactive dose given to the patient can be quite small. However, the short half-life poses a significant problem for the radiochemist; elaborate syntheses are typically ruled out. In contrast, using a radioisotope with a much longer half-life, such as [^{124}I] iodide (t ½ =4.18 d), the disadvantage is that dosimetry is less favorable. Of the nuclei mentioned in Table 1-1, [^{18}F] fluoride is the most useful to monitor short-term biodistribution. Advantages include: 1) a reasonable half-life of 109.7 minutes. This permits injection of the radiolabeled drug, a number of scans at various time points, and clearing of the radioactivity to occur in one day. 2) This radionuclide also has low positron energy (0.64 MeV) resulting in a relatively short range in tissue (maximum 2.2 mm) permitting high-resolution images. 3) ^{18}F-Fluoride can be produced in large amounts (>10 Ci) in a cyclotron, and 4) has acceptable radiation dosimetry for multiple studies in a patient.[15] Aryl florination of pharmaceuticals offers many advantages, which can include enhanced solubility, bioavailability and metabolic stability compared to non-fluorinated analogues.[19]

Isotope	**Half-life**	**Decay Mode**	**E_{β^+} avg. [KeV]**	**Maximum (avg) range in water [mm]**	**Max. Specific Activity [Gbq μmol^{-1}]**
^{11}C	20.39 min.	β^+ (99.8%) EC (0.24%)	385	3.8 (1)	3.4*10^5
^{13}N	9.96 min.	β^+ (99.8%) EC (0.2%)	491	5.0 (1.5)	7.0*10^5
^{15}O	122.24 sec.	β^+ (99.9%) EC (0.01%)	735	7.6 (2.7)	3.4*10^6
^{18}F	109.77 min.	β^+ (96.73%) EC (3.3%)	242	2.2 (0.3)	6.3*10^4
^{124}I	4.17 d.	β^+ (22.8%) EC (11.0%)	188	9.7 (3)	1.2*10^3

Table 1-1: Commonly used radio-nuclei for PET and their properties. [Adapted from Browne and Firestone (1986) and Brookhaven National Laboratory, Internet database, (2003).]

Aqueous [^{18}F] fluoride is produced by proton bombardment of a $^{18}OH_2$ target ($p^+ + {}^{18}O \rightarrow {}^{18}F + n$). The [^{18}F] fluoride so produced is solvated with water, which reduces its nucleaphilicity. To overcome this problem, [^{18}F] fluoride is trapped on an ion exchange resin to remove excess water and eluted with an aqueous solution of bicarbonate. To enhance the nucleophilicity and solubility of fluoride, the potassium ions are complexed by a cryptand, typically 1,10-diaza-4,7,13,16,21,24-hexaoxabicylco[8.8.8]hexacosane (Kryptofix 2.2.2) as shown in Figure 1-3. Water is removed by azeotropic distillation with a hydrophilic polar solvent, such as acetonitrile. Once the ^{18}F anion is dry, its nucleophilicity is enhanced so then it can participate in nucleophilic substitution reactions and related chemistries.

1.4 Methods of Fluoride Incorporation

Several methods are currently employed to incorporate ^{18}F-fluoride into aromatic compounds. Nucleophilic aromatic substitution (S_NAr) typically utilizes an "F -" source, such as tetramethyl ammonium fluoride (TMAF), tetrabutyl ammonium fluoride (TBAF), or Kryptofix 222 KF. A significant limitation of nucleophilic aromatic substitution is that the reaction occurs only in electron poor systems. In cases where electron-withdrawing groups are not present in the final product, multistep syntheses are required to transform or remove an "activating" group.

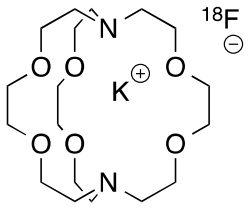

Figure 1-3: Structure of Kryptofix 222 KF, used in radiofluorination.

Direct electrophilic aromatic substitution utilizes an "F+" source such as NFSI[16], Selectfluor®[17], or NFOBS.[16, 18] This approach works reasonably well for electron rich arenes, but regioselectivity is sometimes an issue.[19] To conduct electrophilic reactions with ^{18}F, the synthesis of $^{18}F_2$ is generally required. This is a difficult reagent to prepare and handle routinely. In addition, its preparation involves dilution with ^{19}F. Use of this "carrier added" reagent leads to low specific activity compounds and the need to inject a significant amount of the imaging agent. This is a major limitation if highly potent compounds are being radiolabeled.

Another approach to incorporate fluoride into an arene is to employ a metal ion or main group atom fluorination reaction. The general mechanism for a metal catalyzed aryl fluorination is illustrated in Figure 1-4. This method can tolerate a variety of functional groups, but suffers from several constraints. Foremost among these is that the precursors are somewhat air-sensitive and unstable.

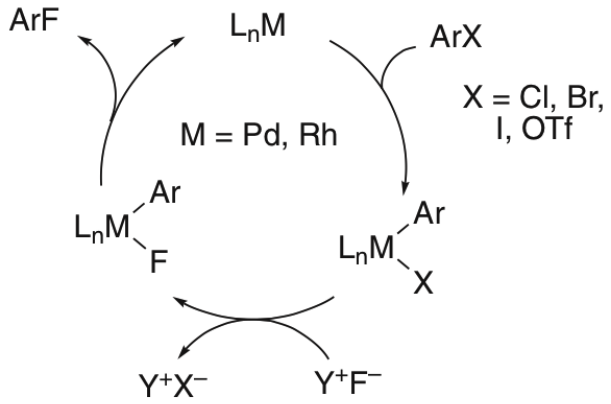

Figure 1-4: Metal catalyzed aryl fluorination. [20]

In the DiMagno group, the incorporation of ^{18}F-fluoride is conducted via thermolysis of diaryliodonium fluoride precursors. We have developed synthetic methods that permit very densely functionalized I(III) derivatives to be prepared. This method allows for metal-free incorporation of ^{18}F-fluoride in a no carrier added (n.c.a.) fashion. Incorporation of n.c.a. [^{18}F] fluoride results in a high specific activity product. Victor Pike was the first to incorporate n.c.a. ^{18}F by the thermolysis of a diaryliodonium salt.[21] In this study he found that reactions with n.c.a. [^{18}F] fluoride with diphenyliodonium chloride or triflate provided the first single-step method for the radiosynthesis of [^{18}F] fluorobenzene in high radiochemical yields. Diaryliodonium salt synthesis requires generation of a hypervalent I(III) center, such as that found in bis(acetoxy) I(III) anisole. These hypervalent compounds are relatively inexpensive to make, exhibit regioselectivity in their reactions, and can generally be used under mild conditions. [21] Hypervalent I(III) species are said to resemble the reactivity of Hg (II), Tl(III) and Pb(IV) cognates without the issue of toxicity. The mode of reaction of I(III), such as ligand exchange and reductive elimination, resembles that of the transition metal ion.[22] A general mechanism

of the synthesis and reductive elimination of diaryliodonium salts is shown in Figure 1-5. This illustration shows the two possible routes to prepare diaryliodonium salts that are used in our laboratory. First, an iodinated substrate can be oxidized to the hypervalent I(III) species, which is then coupled to a trifluoroborate arene to form a diaryliodonium salt. Alterntively, the desired substrate can be modified to a potassium trifluoroborate salt, which is then couple to a hypervalent I(III) arene to form a diaryliodonium salt. In both cases, TMS-X serves as a trimethyl silyl ligand to activate the I(III) center. These TMS-X groups act to "tune" the electrophilicty of the I(III) center, thus, the reaction can be "customized" for either electron poor or electron rich systems. In the DiMagno group, many TMS-X catalysts are used including TMS-TFA (trimethylsilyl trifluoro acetate), TMS-OTf (trimethylsilyl triflate) and TMS-OAc (trimethylsilyl acetate).

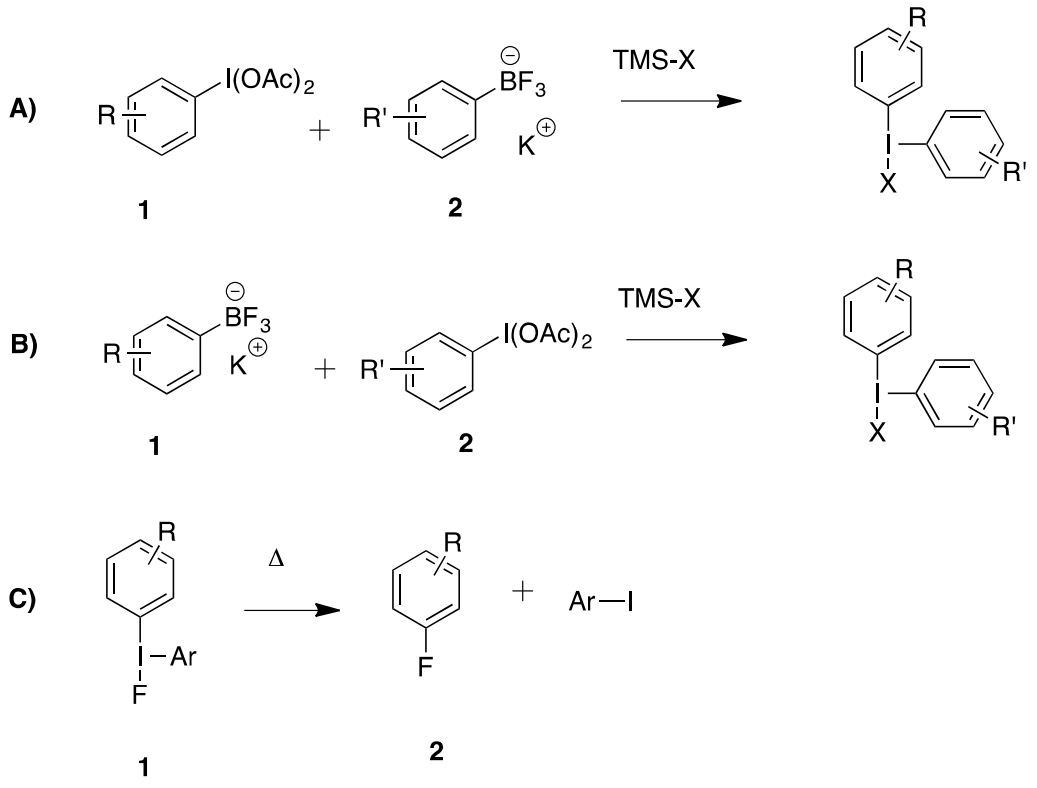

Figure 1-5: The synthesis and reductive elimination of diaryliodonium salts. **A)** A hypervalent I(III) substrate is coupled to a trifluoroborate arene to form a diaryliodonium salt. **B)** Trifluoroborate modified substrate is coupled to a hypervalent arene to form a diaryliodonium salt. **C)** Reductive elimination of an aryl iodide from a diaryliodonium fluoride to form a fluoroarene.

1.5 Conclusions

Classical methods of measuring biodistribution provide valuable information but still suffer from some limitations. PET imaging is potentially a complementary technique to visualize the distribution, adsorption and metabolism of compounds of interest. Unlike toxicokinetic measurement methods driven by GC/MS instruments, PET alone cannot identify and distinguish among metabolites. While PET can supplant such methods as autoradiography, methods to detect various metabolites will still be need to be utilized for biodistribution and toxicity studies. While there are multiple routes to incorporate ^{18}F onto a desire substrate for PET, for this work, the synthesis of a diaryliodonium salt precursor of diethyl phthalate, bis(2-ethylhexyl) phthalate and bisphenol A are explored for proof of principle studies. Once the diaryliodonium precursors are in hand, then biodistribution studies can be conducted to assess the efficiency of PET as a valuable, non-invasive tool for evaluating environmental toxicology of widely used industrial chemical.

CHAPTER 2

Diethyl Phthalate

2.1 Introduction

Diethyl phthalate (DEP) is a commonly used plasticizer. DEP is primarily used as a solvent or in cellulose acetate polymers. Unlike heavier chain phthalate esters, DEP is not used as a plasticizer in PVC because its low molecular weight makes it somewhat volatile. In 2008, approximately 5,200 of the 5,800 metric tons of consumed diethyl phthalate produced in the U.S. were used in cellulose acetate polymer formulations. These materials were used in films, tool handles and adhesives. [23] In 2010, the EPA reported that DEP was also found in a variety of other products including soaps, detergents, adhesives, sealants, rubber, and plastic products. DEP has also been found in cosmetics, epoxy resins, pharmaceutical and personal care products, children's toys, and insect repellents. DEP is also a component in fragrances.[23] The large number and variety of products in which DEP is found mean that consumers encounter this compound from multiple products on a daily basis. Moreover, this exposure to diethyl phthalate can occur through dermal absorption, inhalation and ingestion.

Diethyl phthalate exposure and the biodistribution of this compound in animals and human subjects are measured using the classical methods described in Chapter 1. The overall goal of this research is to develop an alternative, positron emission tomography (PET) based methodology to track this compound *in vivo.* The immediate goal of this project was to synthesize a diaryliodonium triflate precursor, which could be readily radiofluorinated to yield 4-[^{18}F]-fluorodiethyl phthalate. This radiotracer will be evaluated to determine if the behavior of the fluorinated compound exhibits comparable

biodistribution and pharmacokinetics compared to the nonfluorinated material. If so, 4-[^{18}F]-fluorodiethyl phthalate will be offered as a means to visualize the *in vivo* biodistribution of this environmental contaminant in real time.

2.2 Known Metabolism of Diethyl Phthalate

The major pathway of diethyl phthalate metabolism is hydrolysis to the monoester, which can be further hydrolyzed to phthalic acid or glucuronidated. Oxidation of the ester side chain also occurs as is outlined in Figure 2-1.[24] Hydrolysis of DEP occurs in the lumen of the gastrointestinal tract, in intestinal mucosal cells, or in the liver, kidneys and lungs after systematic absorption.[25]

Several studies have used ^{14}C-labeled DEP to monitor the biodistribution and metabolism of the parent compound. In 1976, Ioku and co-workers fed ^{14}C-labeled DEP to rats and mice and assessed its biodistribution by autoradiography at 48 hours post administration. The kinetics of the tissue distribution of DEP was also measured, and it was found that maximum radioactivity (at 20 minutes post administration) was found in the kidneys and liver, followed by blood, spleen and fat.[23, 25] The concentration of radioactivity was measured in excretion samples and it was found that there was a rapid decrease to trace amounts after 24 hours. Excretion was found to occur primarily through the kidneys; only about 3% of the total administered dose was elimination in feces. The authors identified two main metabolites: monoethylphthalate (MEP) (major) and phthalic acid (minor). This early study proves that DEP is cleared rapidly from rodents. This fact was used to argue that a single bolus of administered DEP carries little long term exposure risk.

A second study of the biodistribution of DEP in male rats probed the impact of dermal application of [^{14}C] DEP (5-8 mg/cm^2). Urine and fecal samples were collected and analyzed by liquid scintillation spectrophotometry every 24 hours for 7 days.[26] It was noted that 24% of the total dose was excreted within 24 hours. After animal sacrifice, radioactivity was detected in the brain, lungs, spleen, small intestines, kidneys, testis, blood and spinal cord, but each having a concentration less that 0.5% of the administer dose. It was noted that 86% of the given dose remained on the surface of the skin. This indicates that dermal absorption of DEP is very slow. This finding is significant considering that human exposure to DEP primarily occurs through application of fragrances and body lotions on the skin.

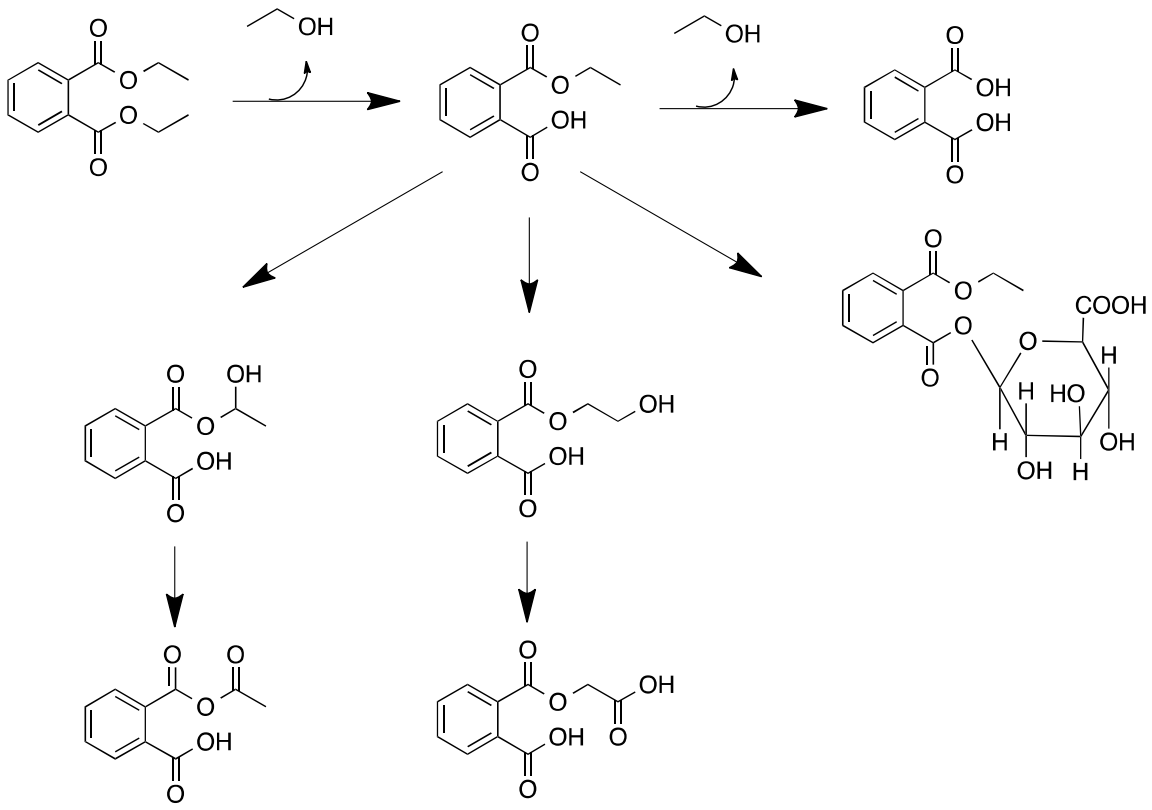

Figure 2-1: Pathways for metabolism of diethyl phthalate (DEP).

An experiment in 1975 by Singh and co-workers, monitored [^{14}C] diethyl phthalate in serum following intraperitoneal injection into 13 pregnant rats at either day 5 or day 10 of gestation. Analysis of withdrawn serum samples by liquid scintillation spectrophotometry showed that the distribution of radioactivity in maternal blood peaked at 24 hours then diminished quickly. A similar pattern was seen in fetal tissue and amniotic fluid. The rate of elimination was found to fit a first-order excretion curve. It was also suggested that radioactivity from the radiolabeled compound was transmitted through the placenta into the fetus. The [^{14}C] radioactivity was widely distributed and detected in maternal blood, amniotic fluid and the fetus (all <1%) at all gestational time points that were investigated.[24] This study is significant in that it shows that the mother and the fetus are both exposed to DEP, but it is also eliminated quickly from both the mother and fetus. Again, this suggests that prolonged exposure to DEP, even when administered by injection, is minimal.

The specific enzymes that are responsible for the hydrolysis of DEP have not yet been completely characterized for various species. However, DEP has shown to be hydrolyzed to the monoester by purified carboxylesterases isolated from human and rat liver. In 1987, Ashour *et. al.* demonstrated that microsomal carboxylesterase activity toward DEP was induced in mouse liver and rat kidneys.[25] Some major enzymes that are involved in the microbial metabolism of DEP include phthalate oxygenase, phthalate dioxygenase, phthalate dehydrogenase and phthalate decarboxylase.[27, 28, 29] In a study performed with commercially available porcine and bovine pancreatic cholesterol esterase (CEase, EC 3.1.1.13), it was found that DEP was hydrolyzed to MEP within 24

hours.[30] In 1997, Kayano and co-workers found that a novel esterase, ES46.5K, isolated from mouse hepatic microsomes demonstrated strong hydrolytic effects toward DEP and other short chain phthalate esters, but was less effective at hydrolyzing longer chain derivatives such as bis(2-ethylhexyl) phthalate (DEHP).[31] This esterase hydrolyzed only one of the ester groups of DEP; formation of phthalic acid was not observed even after prolonged incubation. From a study in 1998 by Hotchkiss and co-workers it was demonstrated that skin could also hydrolyze DEP to MEP using *in vitro* percutaneous absorption with rat and adult human skin. There are a variety of enzymes responsible for the metabolism of DEP and they are found in several areas of the body. All of these studies mentioned in this section confirm the efficient metabolism and rapid clearance of DEP from the body.

2.3 Potential Health Effects of Diethyl Phthalate

While there is an industrial demand for diethyl phthalate, some studies of human populations have suggested that its widespread use could be cause for concern. Diethyl phthalate and its commonly found metabolite, monoethyl phthalate (MEP) are found in population samples at levels often orders of magnitude greater than those of other phthalates such as bis (2-ethylhexyl) phthalate (DEHP) and di-*n*-butyl phthalate (DBP).[32] The prevalence of DEP in personal care products and its volatility, are thought to be responsible for the relatively elevated exposure to this compound.

Studies in animals and humans suggest that exposure to DEP may be responsible for a number of reproductive issues, especially in males. In dose-response studies performed by Duty (in 2003) and Hauser (in 2007) it was shown that damage to sperm

DNA was associated with high levels of MEP in urine samples in two groups of adult human males that were undergoing tests for infertility.[3] In 2005, Jonsson and coworkers evaluated urine, serum, and semen samples from 234 young Swedish males and found that men with the highest concentrations of MEP experienced 8.8% fewer sperm, 8.9% more immotile sperm, and lower serum luteinizing hormone values compared to men with lower levels of MEP.[3] However, the results of these studies were questioned because no data were reported for the actual exposure (amount or duration) to DEP each man experienced.

There are several other studies that correlate serum or urinary DEP metabolites to health effects. One of these was a 2005 study by Swan and co-workers reporting a significant association of MEP in samples in pregnant women with age-adjusted anogenital index (AGI) of postnatal males at 2-36 months of age. AGI, which describes the span of the perineum, the portion of the body between the anus and genitalia, has been suggested as a tool for identifying male sexual development vs. male feminization. It was concluded that MEP concentrations had an inverse relationship with AGI.[33] In a study in 2007, Stahlhut and co-workers correlated phthalate exposure with abdominal obesity and insulin resistance in adult males in the US. It was shown that MEP level was significantly associated with increased abdominal circumference and increased insulin resistance.[26] MEP is also suspected of being hepatocarcinogenic and teratogenic in mice who experience chronic exposure or administration of a large dose.[31] Again, these studies show that there may be a correlation between higher DEP metabolites in urine and serum samples and a shortened AGD in male offspring, obesity, diabetes and liver cancer.

However, it is difficult to give a definitive answer as to if DEP is indeed the cause of these health problems considering there was no record of the administered doses of DEP.

Several research studies have appeared in which accurate accounting of DEP exposure was recorded. In 1993, Jones investigated organelle changes in Leydig cells of rats that were exposed to four different phthalates including diethyl phthalate in a gavage dosage of 2000 mg/kg body weight once a day for two days.[24] Administration of DEP resulted in mitochondrial swelling, smooth endoplasmic reticulum focal dilation and vesiculation, and increased interstitial microphage activity associated with surface of the Leydig cells of rats. These data provide evidence that very large doses of DEP may be potentially damaging at the cellular level; however, the dose given is large that the relevance of these results on human exposure to DEP is questionable.

While earlier studies provided evidence suggesting that the dermal absorption of DEP was modest and slow, the National Toxicology Program (NTP) conducted a study observing the effects of dermal exposure to DEP over the course of 4 weeks. DEP was applied dermally to $B6C3F_1$ mice at doses of 12.5, 25, 50, and 100 μL (approximately 560, 1090, 2100 or 4300 mg/kg for males and 630, 1250, 2500 or 5000 mg/kg for females) 5 days/week. It was found that dermal application of undiluted DEP resulted in increased relative liver weight in mice.[25] Intriguingly, this study showed that adverse effects (increases in absolute and relative liver weights) only occurred in female test subjects. In another 4-week study performed by the NTP, DEP was applied to the skin of F344/N rats (200, 400, 800 or 1600 mg/kg for males and 300, 600, 1225, or 2500 mg/kg for females, given 5 days/week). This study showed increased relative liver weights in the higher dosed males and females.[25] These data suggest that prolonged exposure to

DEP at relatively high-doses could have a negative effect on the liver. Again, these doses and long-term exposure are not comparable to human exposure levels.

In summary, the above studies indicate there may be a correlation between DEP exposure and adverse health effects. DEP is suspected to be associated with sperm damage, shortened AGD in male offspring from mothers that were exposed during pregnancy, obesity, insulin resistance, and possible liver cancer. However, there was no reported data on the amount or duration at which those studied had been exposed to. Nonetheless, there are data suggesting that prolonged exposure to DEP in relatively high doses can have adverse effects toward rat livers and can be detrimental to organelles in rat cell lines.

I am interested in preparing a [^{18}F]-labeled DEP derivative to enable monitoring of the biodistribution and pharmacokinetics of DEP in mice using positron emission tomography (PET). [^{18}F]-DEP would be administered at a nanomolar concentration and assessed at various time points to verify if DEP or its metabolites are binding to any receptors in the body or if there is any evidence that this compound could be responsible for the speculated adverse health effects at relatively low doses, comparable to that of human daily exposure.

2.4 Synthetic Approach

The synthetic approach that was used to prepare the diethyl phthalate diaryliodonium salt and fluorinated analogue is illustrated in Scheme 2-1 below. The first step was to oxidize commercially available 4-iodoxylene to 4-iodophthalic acid following the methods proposed by Dudič.[34] Several esterification methods, including

thionyl chloride and ethanol resulted in mixtures that contained significant amounts of the monoester product. While the desired product could be readily separated from these reaction mixtures, it was found that esterification of 4-iodophthalic acid with *N,N'*-dicyclohexylcarbodiimide (DCC), 4-dimethylaminopyridine (DMAP) and ethanol provided an enhanced yield of the desired diester. Simple filtration through silica gel was sufficient to obtain the desired starting product in good yield and purity.

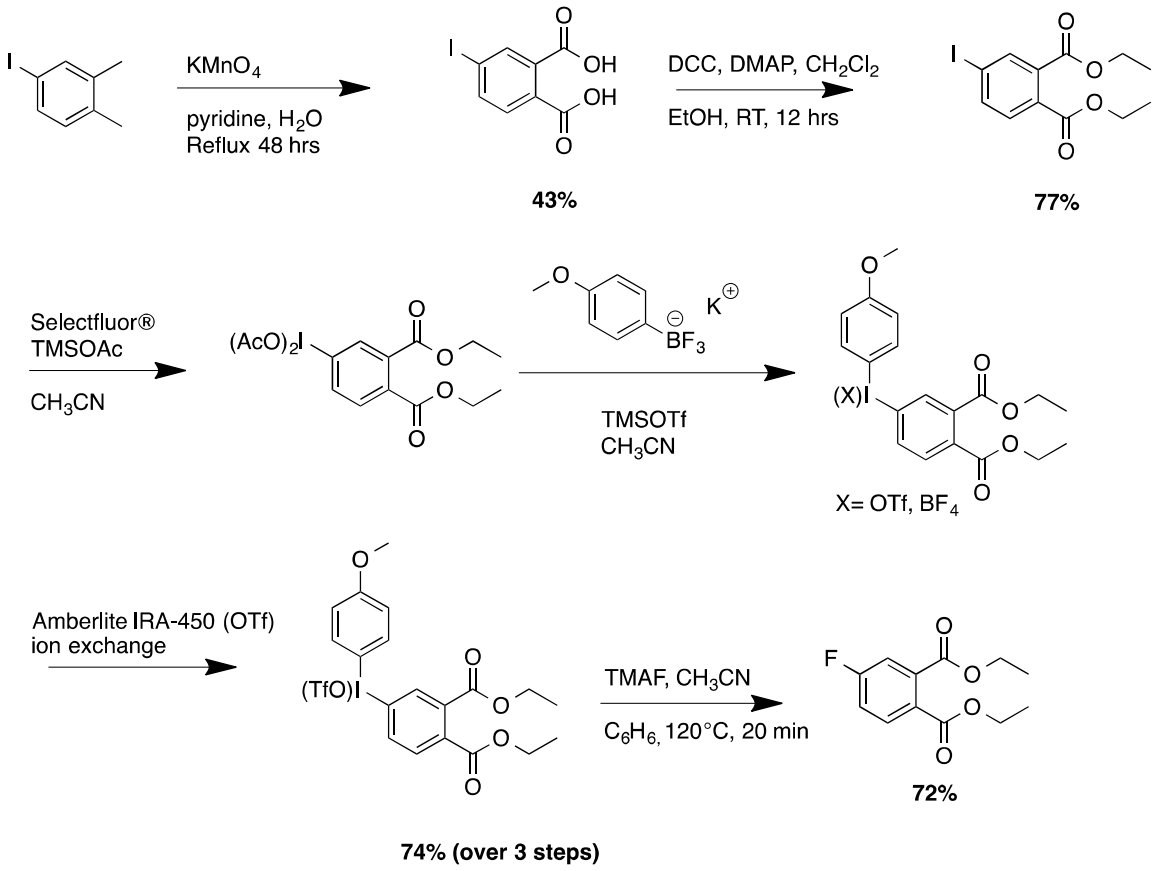

Scheme 2-1: Synthetic scheme of the synthesis of diethyl phthalate diaryliodonium triflate salt and conversion to the fluorinated analogue.

Once 4-iododiethyl phthalate was isolated, it was oxidized with Selectfluor® and TMSOAc in dry acetonitrile. Proton NMR spectroscopy was used to follow the progression of the oxidation reaction. After optimization of the reaction conditions, it was found that maximum conversion to the aryliodonium diacetate intermediate occurred at 24 hours at 60 °C. Once formed, the I(III) intermediate was treated with potassium trifluoro(4-methoxyphenyl)borate and TMS-OTf to form the diaryliodonium salt precursor. The desired product was easily purified by washing the solid product with methyl-*tert*-butyl ether (MTBE). Sonication of the mixture was used during the washing step to assist the removal of impurities that might be trapped in the solid matrix of the product.

High specific activity radiochemical syntheses generate vanishingly small amounts of material. In fact, standard UV-visible detectors on analytical HPLC equipment are insufficiently sensitive to detect the amount of radiotracer prepared be the methods we use in our group. Therefore, a "cold" fluorination standard sample of every compound must be prepared to help the radiochemist establish the identity of the radiolabeled product. The first preparation of the standard used a model reaction of the radiosynthesis: the diaryliodonium salt precursor was treated with 0.8 equivalents of tetramethylammonium fluoride (TMAF) in dry acetonitrile for about 15 minutes to effect an ion exchange and prepare the corresponding diaryliodonium fluoride. The solvent was removed and replaced with dry C_6D_6 and the mixture was heated at 120 °C for 10-20 minutes. It was found that the optimal temperature and time needed for maximum conversion was 20 minutes at 120°C. The final product was analyzed by HPLC (275 nm

UV detection, mobile phase: 65% acetonitrile : 1% acetic acid in water, Phenomonex, Luna, C18 column). The HPLC trace of the isolated standard is given in Figure 2-2.

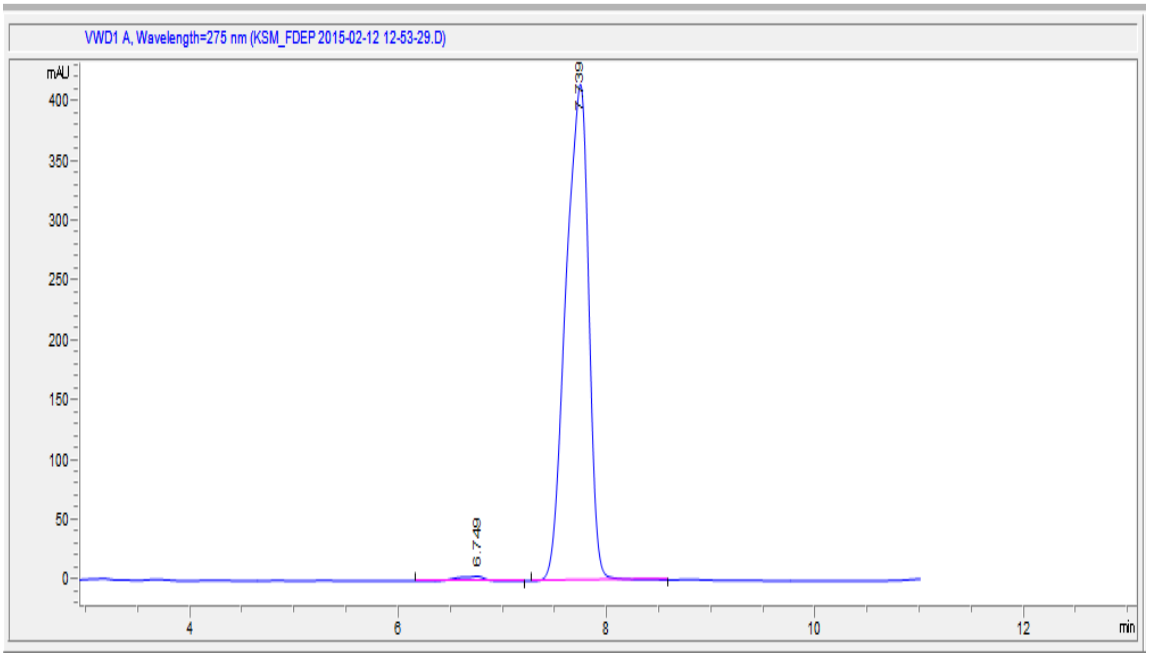

Figure 2-2: HPLC trace of 4-fluorodiethyl phthalate.

2.5 Conclusions

In summary, diethyl phthalate is a widely utilized industrial chemical that can be found in everyday consumer items such as soaps, detergents, sealants, fragrances, lotions and plastic products, such as children's toys. Routes of exposure to DEP include dermal absorption, ingestion, and inhalation. Diethyl phthalate has been reported to metabolize and eliminated from the body quickly. The metabolism of DEP is mainly through hydrolysis to the monoester, which can be hydrolyzed to phthalic acid or glucuronidated. Ethyl side chain oxidation products are also formed. While it has been reported to metabolize rapidly, the widespread use of DEP by consumers, can correlate to having a

high concentration of DEP or its metabolites in urine and serum samples. DEP has been speculated of being responsible for a number of adverse health effects, as mentioned above. While there may be evidence of DEP metabolites present in many of these studies, there was little evidence that DEP was solely responsible for many of the conditions discussed, or the DEP doses were incredibly large. It is also unclear why males would be more susceptible to DEP than female subjects.

The focus of this project was to prepare the diaryliodonium triflate salt precursor, which could be exposed to late-stage radio-fluorination to yield [^{18}F] 4-fluoro-diethyl phthalate. The radiotracer could then be injected into a test subject at nanomolar concentrations and visually assess the biodistribution in real time using PET. This could give vision to where diethyl phthalate is going through the body at reasonable concentrations. PET scans can also give insight to if there is any occurrence of target binding that may be associated with these speculated health effects, however other qualification tests would need to be conducted to know to what extent, and to where, exactly, a compound is binding.

2.6 Experimental Data

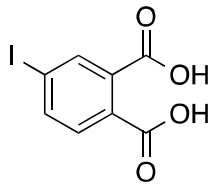

4-iodophthalic acid

This is a known compound (CAS 6301-60-6) but was synthesized according to the procedure reported by Dudič.[34] In a 1L round bottom flask, 4-iodo-1,2-dimethylbenzene (11.0 mL, 77.4 mmol) was diluted in160 mL of pyridine. Potassium permanganate (146.7 g, 928.8 mmol) and 340 mL of deionized water were added and the reaction mixture was allowed to reflux for 72 hrs. After the mixture cooled to RT, the reduced manganese salts were removed by filtration, and the filtrate was acidified carefully with concentrated hydrochloric acid to pH 1-2. Upon acidification, a white precipitate was formed and extracted with ethyl acetate. Extraction of the reaction mixture with ethyl acetate followed by evaporation of the solvent *in vacuo* produced a light pink solid. The crude product was dissolved sodium carbonate, and the aqueous solution was washed with ethyl acetate (3 X 50 mL). The aqueous solution was adjusted back to pH=1 with concentrated hydrochloric acid, precipitating the purified product. The mixture was extracted with ethyl acetate and the solvent was removed under reduced pressure and dried *in vacuo* to yield 9.70 g (43%) of the colorless product. ^{1}H NMR (D_2O+CH_3CN, 400 MHz, 25°C) δ 8.26 (d, J= 1.6, 1H), δ 8.12 (dd, J_1= 1.6, J_2= 8.2, 1H), δ 7.68 (d, J= 8.2, 1H); ^{13}C NMR (D_2O+CH_3CN, 100 MHz, 25°C) δ 170.4, 169.7, 140.8, 137.7, 133.8, 131.1, 130.8, 98.1; HRMS (ESI): Calcd $C_8H_5O_4I$ $[M-H_2O]^+$ 274.9205; found 274.9173.

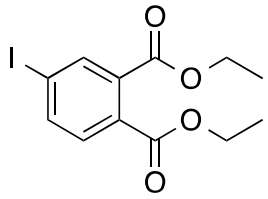

Diethyl-4-iodophthalate

This compound is known (CAS 67193-51-5) but was prepared using the esterification reaction modeled after that used by Buchwald.[74] In a 250 mL round bottom flask, 4-iodophthalic acid (2.32 g, 7.94 mmol) was dissolved in 15 mL of dichloromethane. Ethanol (0.93 mL, 15.9 mmol) and DMAP (0.24 g, 1.96 mmol) was added to the reaction flask, which was cooled to 0 °C. N,N'-dicyclohexylcarbodiimide (DCC) (3.44 g, 16.7 mmol) was dissolved in 10 mL of dichloromethane and added to the cooled reaction mixture in a drop-wise fashion. The reaction was stirred and allowed to warm to RT slowly for 12 hours. A white precipitate had formed as a result of an insoluble DCC by-product, DCU, which was filtered off of the reaction mixture. The filtrate was stirred for an hour with hexanes, producing more DCU solid, which was removed by filtration. The filtrate was subjected to reduced pressure removing the solvent and the desired product was purified by column chromatography (5% EtOAc: Hexanes). After removal of solvent, 2.13 g of a clear oil was obtained in a 77% yield. ^{1}H NMR (CD_3CN, 400 MHz, 25°C) δ 8.04 (d, J= 2.0, 1H), 7.96 (dd, J_1= 8.0, J_2= 1.6, 1H), 7.47 (d, J= 8.0, 1H), 4.30 (q, J= 7.2, 2H), 4.29 (q, J= 7.2, 2H), 1.31 (t, J= 7.2, 3H), 1.30 (t, J= 7.2, 3H); ^{13}C NMR (CD_3CN, 100 MHz, 25°C) δ 167.7, 166.9, 141.2, 138.3, 135.1, 132.4, 131.4, 98.0, 62.9, 62.8, 14.4; HRMS (ESI): Cald $C_{12}H_{13}IO_4$ $[M+Na]^+$: 370.9756; found 370.9774

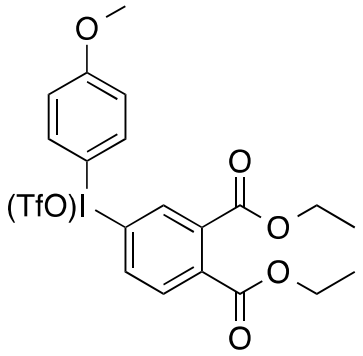

[3,4-Bis(ethoxycarbonyl)phenyl]-(4'-methoxyphenyl)iodonium triflate

In a N_2 charged atmosphere, in an oven dried Schlenk flask, diethyl-4-iodophthalate (2.08 g, 5.98 mmol) was dissolved in 60 mL of dry acetonitrile. In a 20 mL scintillation vial, Selectfluor® (2.75 g, 7.76 mmol) was dissolved in 10 mL of dry acetonitrile, followed by trimethylsilyl acetate (2.33 mL, 15.5 mmol) that was diluted in 10 mL of dry acetonitrile and was allowed to mix for 3-5 mins. The Selectfluor® solution was added to the reaction mixture in a drop-wise fashion. This mixture was sealed and stirred at 60 °C for 24 hrs. In a inert atmosphere, potassium trifluoro(4-methoxyphenyl)borate (1.28 g, 5.98 mmol) was dissolved in a minimal amount of dry acetonitrile and added to the reaction flask. In a 20 mL scintillation vial, trimethylsilyl trifluoromethanesulfonate (1.0 mL, 5.8 mmol) was diluted in 10 mL of dry acetonitrile and added to the reaction flask in a drop-wise fashion. The flask was sealed and reacted at RT for 12 hours. The solvent was removed under reduced pressure. The mixture was dissolved in dichloromethane and washed with deionized water (3 X 50 mL). The organic layer was dried over sodium sulfate, and upon removal of the solvent produced a colorless solid. The solid was ultrasonicated in methyl-tert-butyl ether (3 X 50 mL) and dried *in vacuo*. The resulting white solid was subjected to a triflate ion exchange column (Amberlite IRA-450 (OTf)) in a solution of acetonitrile/water (80:20). The solvent was removed under high dynamic vacuum overnight. This resulted in 2.67 g (73%) of a colorless solid. ^{1}H NMR (CD_3CN, 400 MHz, 25°C) δ 8.37 (d, J=1.6 Hz, 1H), 8.21 (dd, J_1= 2.0, J_2= 8.4, 1H) 8.05 (d, J= 9.2, 2H) 7.75 (d, J= 8.4, 1H) 7.07 (d, J= 9.2, 2H) 4.32 (q, J= 7.2, 2H) 4.32 (q, J= 7.2, 2H) 3.84 (s, 3H), 1.31 (t, J= 6.8, 3H) 1.30 (t, J= 6.8, 3H); ^{13}C NMR (CD_3CN, 100 MHz, 25°C) δ 167.0, 165.8, 164.6, 139.1, 138.6, 137.1, 135.9, 135.5, 132.9, 119.3, 118.4, 116.8, 102.6,

63.5, 63.4, 56.8, 14.3, 14.3; ^{19}F NMR (CD_3CN, 376 MHz, 25°C) δ-80.9. HRMS (ESI): Cald $C_{20}H_{20}F_3O_8IS$ $[M\text{-}OTf]^+$: 455.0356; found 455.0366.

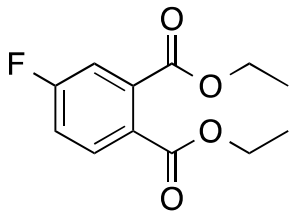

Diethyl 4-fluorophthalate

This compound is known (CAS 320-96-7) but preparation by this route has not been previously reported. In an N_2 charged glove box, diethyl 4-((4-methoxyphenyl)(((trifluoromethyl)sulfonyl)oxy)-λ^3-iodanyl)phthalate (0.3 g, 0.5 mmol) and tetramethyl ammonium fluoride (0.04 g, 0.40 mmol) was dissolved in dry acetonitrile (15 mL) in a 50 mL Schlenk tube. The solution was allowed to stir at room temperature for 5 minutes and the solvent was evaporated under high dynamic vacuum. The reaction mixture was then dissolved in dry benzene (15 mL) and heated to 120 °C for 20 minutes. The solvent was evaporated and the product mixture was purified by column chromatography (5:95; Ethyl acetate: Hexanes). This yielded a clear oil (0.07 g) in 72% yield. ^{1}H NMR (CD_3CN, 400 MHz, 25°C) δ 7.81 (dd, $^3J_{H\text{-}H}$= 8.6, $^4J_{H\text{-}F}$= 5.4, 1H), 7.41 (dd, $^3J_{H\text{-}F}$= 8.9, $^4J_{H\text{-}H}$= 2.5, 1H), 7.33 (td, $^3J_{H\text{-}F}$= 8.4, $^3J_{H\text{-}H}$= 8.4, $^4J_{H\text{-}H}$= 2.5, 1H) δ 4.31 (q, J= 7.2, 4H), δ 1.32 (t, J= 7.2, 3H) δ 1.31 (t, J= 7.2, 3H); ^{13}C NMR (CD_3CN, 100 MHz, 25°C) δ 167.5 (d, $^4J_{C\text{-}F}$= 2.2 Hz) 167.2, 164.9 (d, $^1J_{C\text{-}F}$= 251 Hz), 136.6 (d, $^3J_{C\text{-}F}$= 8.1 Hz), 132.8 (d, $^3J_{C\text{-}F}$= 8.9 Hz), 129.0 (d, $^3J_{C\text{-}F}$= 3.5 Hz), 118.9 (d, $^2J_{C\text{-}F}$= 21.9 Hz), 116.8 (d, $^2J_{C\text{-}F}$= 24.3 Hz), 63.0, 62.7, 14.4, 14.4; ^{19}F NMR (CD_3CN, 376 MHz, 25°C) δ -109.03 (td, $^3J_{H\text{-}F}$= 8.6 Hz, $^4J_{H\text{-}F}$= 5.4Hz); HRMS (ESI): Cald $C_{12}H_{13}FO_4$ $[M+Na]^+$: 263.0696; found 263.0692.

CHAPTER 3

Bis(2-ethylhexyl) phthalate

3.1 Introduction

Bis(2-ethylhexyl) phthalate, commonly referred to as di(2-ethylhexyl) phthalate or DEHP, is common plasticizer that has had a wide range of uses. This colorless liquid has an aqueous solubility of 41 μg/L at room temperature. It is miscible with mineral oil and liquid hydrocarbons, such as hexane. According to a 1999 report from Mannsville Chemical Products Corporation, 95% of DEHP is used as a plasticizer for polyvinyl chloride (PVC) products to induce flexibility.[2] Examples of these PVC products include floor tiles, upholstery, wall coverings, shower curtains, swimming pool liners, garden hoses, plastic toys, rainwear, packaging film and sheets, and sheathing for wire and cables. DEHP is also widely used in medical tubing, blood storage bags, disposable medical examination gloves, surgical gloves, and dialysis tubing.[2] Less commonly, DEHP is used as a plasticizer in natural and synthetic rubbers. Non-plasticizer uses of DEHP include acting as solvent in erasable inks, as an acaracide in orchards, pesticides, and as an ingredient in cosmetics, vacuum pump oil ingredient, and dielectric fluids. It has also been used to detect leaks in respirators and for testing air filtration systems.

DEHP can enter the environment through disposal of industrial and municipal wastes, and by leaching into consumer products that have been stored in material containing DEHP. This compound has been shown to sorb strongly to soil and sediment. The most frequent route of exposure to humans is through ingestion.[2] However, the greatest risk of acute exposure to DEHP occurs during medical procedures such as blood transfusions (estimated upper bound limit of 8.5 mg/kg/day) and hemodialysis (estimated

upper bound limit of 0.36 mg/kg/day).[2] According to the U.S. Food and Drug Administration (2001) it was proposed the DEHP can leach from these plastic medical equipment into biological fluids and then into the patient.[2] Due to an increase in the awareness of potential health concerns associated with DEHP, many companies have discontinued use of this phthalate.[2]

It is important to note that the presence of DEHP in commonly used analytical equipment makes it difficult to accurately measure the relatively low levels of the compound in laboratory samples. The ubiquitous nature of DEHP can lead to false positives during assays, and also introduce significant uncertainty in the amount of DEHP contaminant present.

The focus of this project was to synthesize a diaryliodonium triflate precursor of bis(2-ethylhexyl) phthalate for the purpose of preparing radiolabeled DEHP. Once prepared, the radio-fluorinated DEHP analogue shall be administered to laboratory animals, and the pharmacokinetics and biodistribution of the compound will be measured using positron emission tomography (PET).

3.2 Known Metabolism of Bis(2-ethylhexyl) phthalate

The metabolism of bis(2-ethylhexyl) phthalate is much like that of diethyl phthalate. The main metabolite detected in urine and serum samples is the corresponding monoester, MEHP, which can undergo further hydrolysis to phthalic acid or aliphatic side chain oxidation. The metabolic pathways for degradation of DEHP are illustrated in Figure 3-1 below. DEHP is more lipophilic than MEHP and it should readily absorb in the gastrointestinal tract. However, a 1980 study by White and co-workers indicated that

only the monoester was adsorbed in the small intestines of rats.[35] This finding suggested the presence of a hydrophilic barrier in the lining of the small intestine that limits the amount of the parent compound being absorbed. Another report by Sjoberg and co-workers in 1986 suggested that absorption of the orally administered dose of DEHP is age-dependent.[36] This study showed that younger rats had the ability to absorb more MEHP through the small intestine than older rats when administered 2.7 mmol of DEHP/ kg/ day.

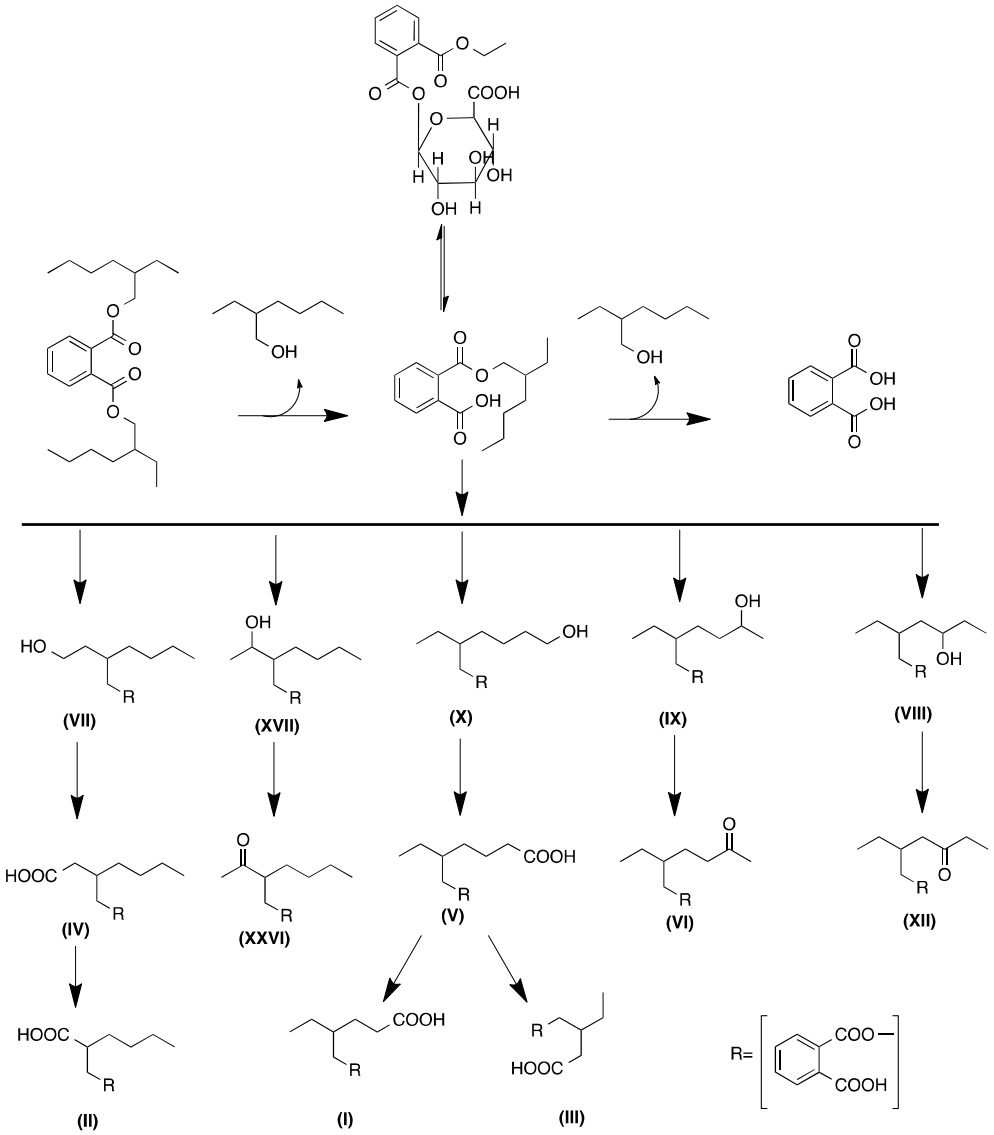

Figure 3-1: Metabolic pathway of DEHP.

Bis(2-ethylhexyl) phthalate is hydrolyzed to MEHP and 2-ethylhexanol in the gastrointestinal tract by the combined actions of pancreatic lipase and an intestinal mucosa lipase.[2] Other lipases, found in the liver, kidney, lungs and plasma have been reported to hydrolyze DEHP to MEHP.[37] A small amount of MEHP is further hydrolyzed to phthalic acid while the remainder undergoes ω- and ω-1-oxidation of the aliphatic side chain.[37] The products of ω-oxidation can undergo α- or β-oxidation, reducing the number of carbons in the side chain. The oxidized metabolites can also be glucuronidated and excreted. In a study performed on two humans in 1985, Schmid and Schlatter administered 30 mg of DEHP orally to two human volunteers and analyzed urine samples by mass spectrometry.[38] From the metabolites in Figure 3-1, it was found that 20% was 2-ethyl-5-oxyhexyl phthalate (VI), 30% was 2-ethyl-5-hydroxyhexyl phthalate (IX) and 30% was 2-ethyl-5-carboxypentyl phthalate (V) of the total excreted material. MEHP accounted for up to 12% of excreted DEHP metabolites; the remaining metabolites accounted for less than 5% of the total excreted material.

It has been suggested that similar metabolic pathways are involved when DEHP is inhaled or dermally administered due to the lipases present in alveolar cells and the epidermis. In 1989, Elsisi and co-workers administered a dermal dose of 30 mg/kg/day for 7 days to rats.[26] Only 5% was excreted (3% in urine and 2% in feces) and 95% was recovered from the skin surface. This study demonstrated that transdermal absorption of DEHP was not extensive, suggesting that skin exposure is of relatively little concern. Secondly, the fact that 40% of the absorbed portion was found in the feces reflects the importance of biliary excretion.[2]

Other enzymes are responsible for further hydrolysis and oxidation of MEHP. For the hydrolysis of the monoester to phthalic acid, an esterase (primarily microsomal) is implicated. MEHP can be reversibly glucuronidated, with the formation of the glucuronide catalyzed by UDP-glucuronyltransferase (Figure 3-1). Regeneration of the aglycone, from the glucuronide, is catalyzed by β-glucuronidase. Oxidation of MEHP to the primary and secondary hydroxyl products is catalyzed by NADPH-dependent microsomal monooxygenases in a manner analogous or identical to fatty acid ω- and (ω-1) hydrolases.[37] Albro has postulated that the hydroxylated products are substrates for alcohol dehydrogenase, which produce aldehyde-containing metabolites. These compounds can be oxidized to di-acids by aldehyde dehydrogenase and NAD. The diacids can be further oxidized to form shorter acids with the help of α- and β-oxidation enzymes, cofactors, mitochondria and/or peroxisomes.[37]

Because medical procedures significant exposure to DEHP, several studies were conducted to analyze the metabolism of intravenously administered plasticizers. When a single dose of ^{14}C-DEHP was administered intravenously to rats, the majority of the dose was recovered in the urine and feces, indicating that the major excretory pathways for rats were urine and bile.[2] In 1975, Rubin and Schiffer demonstrated that humans who were administered a bolus of DEHP during a blood transfusion showed rapid clearance of the compound from the blood.[39] Patients receiving an injection of platelets stored in a vinyl plastic pack displayed an initial DEHP plasma concentrations ranging from 0.34 to 0.83 mg/dL. These concentrations decreased rapidly; the mean rate of DEHP clearance was 2.83% per minute and the plasma half-life of the compound and related metabolites was 28 minutes.

3.3 Potential Health Effects of Bis(2-ethyhexyl) Phthalate

In a study of prematurely born infants who required mechanical ventilation, it was found that the infants displayed unusual lung function similar to that of hyaline membrane disease, which is caused by insufficient surfactant production in the lungs.[2] In 1991, Klimisch and co-workers exposed rats to 1,000 mg/m^3 of DEHP aerosol for 6 hrs/day, 5 days/week, for 4 weeks and found evidence of increased lung weight, thickening of aveolar septa and proliferation of foam cells in male rats.[40] These effects were found to be reversed 8-weeks post exposure. The female lab subjects did not display any of these symptoms. There are also reports that suggest that DEHP in house duct work can be responsible for the onset of asthma, wheezing, and eczema.[32]

The toxicity of DEHP itself is presumed to be low, but several of its monoester metabolites are presumed to exhibit toxicity. Oral ingestion of DEHP is associated with a number of health effects. While no direct human studies were located, Barry and co-workers observed a potential human cardiac muscle contractility effect in an in vitro study in 1990.[41] The monoester of DEHP, MEHP, displayed a dose-dependent negative inotropic effect of human atrial trabecule. This work suggests that high MEHP serum levels could lead to cardiotoxic effects in humans. However, because of the rapid metabolism and excretion of MEHP, the long-term exposure to this metabolite would be minimal.

In 2009, a study was conducted with clinically relevant concentrations of DEHP on neonatal rat cardiomyocytes.[42] It was found that applying DEHP to a confluent, synchronously beating cardiac cell network, caused a loss of gap junction connexin-43, a

gap junction protein necessary for many physiological processes such as depolarization of cardiac muscles and the conducted response in microvasculature. This led to a marked, concentration-dependent decrease in conduction velocity, which is the speed at which an electrochemical impulse propagates down a nerve pathway. This ultimately caused the cells to beat out of sync. This experiment also showed that DEHP affected the mechanical movement of myocyte layers, which resulted in a decrease of triton-insoluble vimentin, leading to stiffness of underlying fibroblasts.

Experiments on rats and mice reported that liver mass increased in response to DEHP oral administration. DEHP triggered rapid cell division along with some liver cell enlargement.[2] Morphological changes caused by DEHP include fat deposits to the periportal area, a decrease in centrilobular glycogen deposits, and structural changes in the bile ducts. Hepatic cell enlargement and fat deposits are indicators of cellular lipid peroxidation.[2] It has also been noted by Mitchell and co-workers that rats exposed to 50 mg/kg/day of DEHP show an increase in hepatic peroxisomes in the centrilobular and periportal areas of the liver, which ultimately leads to cellular hypertrophy.[43] These changes were only observed in male rats, even up to doses of 200 mg/kg/day, indicating that male rats are more susceptible to the hepatotoxic effects of DEHP than females. The reason why males are more susceptible is unclear.

DEHP is a well-known peroxisome proliferator. Peroxisomes are organelles that utilize molecular oxygen to produce hydrogen peroxide during the catabolism of a substrate. Peroxisomal fatty acid oxidation follows the same pathway utilized by mitochondria, with the exception that ATP is not produced and hydrogen peroxide is produced in place of water. There are several studies that indicate that the activity of the

enzymes responsible for fatty acid catabolism is increased in rodents up to 1,500% after exposure to DEHP in doses greater that 11 mg/kg/day and longer than 2 weeks.[2] When peroxisomal catabolism of fatty acids is not accompanied by an increase of the liver detoxifying hydrogen peroxide, the excess hydrogen peroxide can begin to react with cellular lipids, proteins, and nucleic acids. Marker of lipid reactions with peroxides, namely, lipofuscin deposits, were identified in high-dose studies in rats through their lifetime.[44] These data suggest that some hepatic damage caused by DEHP can be attributed to the reaction of excess hydrogen peroxide with cellular lipids.

When studies were conducted on the endocrine effects of DEHP in rats, it was found that, in some cases, thyroid structure and activity were altered. In 1986 when Hinton orally exposed male rats with 2,000 mg/kg/day for as little as 3 day, there was a significant decrease in serum thrytoxine (T4) levels at all time points observed.[2] Electron microscopy also revealed a considerable increase in the number and size of lysosomes, signs of mitochondria damage and enlargement of the Golgi apparatus. These ultrastructural changes are consistent with hyperactivity of the thyroid. These results are consistent with a study done in 2009 by Ghisari and co-workers.[1] In this report, *in vitro* studies were conducted on thyroid hormone-dependent GH3 cells and MVLN cells derived from human breast cancer cells for estrogen receptor binding. Here, the thyroid hormone disrupting potential of DEHP was determined by the effect on the TH-dependent rat pituitary GH3 cell proliferation and the estrogenic activity was assessed in MVLN cells, transfected with an estrogen receptor (ER) luciferase reporter vector.

Several rodent studies suggest that the testes are primary target tissues for DEHP in doses beyond 100 mg/kg/day. Many of these studies reported decrease in testicular

weight and tubular atrophy, along with weight reductions for seminal vesicles, epididymis, and prostate gland.[2] In a study from Albro and co-workers in 1989 [45], acute testicular atrophy occurred when a single dose of DEHP (2.8 g/kg) or MEHP (0.8 g/kg) were orally given to young male rats and to testicular cells for *in vitro* studies. When testicular cells were subjected to ^{14}C-labelled MEHP (8 μM), it was found that the cells could not metabolize MEHP beyond slight hydrolysis to phthalic acid after 24 hours. Sjoberg also suggests that MEHP, the metabolite of DEHP, is responsible for these testicular effects.[36] There is also evidence from multiple rat studies that indicate sperm DNA damage and sperm malformations.[2]

There are few data on the effects of DEHP on female fertility. In a short-term study feeding female rats 140 mg/kg/day for 126 days resulted in a complete loss of fertility.[46] When the rats were sacrificed, a significant decrease in the weights of ovaries, oviducts and uterus in females, as well as a decrease in sperm concentration and an increase in testicular atrophy in males was observed. These data suggest that DEHP had adverse effects toward reproductive organs in rats. In 1994, Davis and co-workers reported a decrease in serum estradiol levels, an increase in FSH levels and the absence of LH surges, which is necessary for ovulation, when given a one-time dose of 2,000 mg/kg. This led to hypoestrogenic anovulatory cycles and the development of polycystic ovaries in female rats.[47]

There are a plethora of studies on potential developmental effects caused by DEHP exposure, but only a few will be mentioned. In 2005, Swan and co-workers conducted a study examining the anogenital distance (AGD) and other genital measurements on humans in relation to prenatal exposure to phthalates.[33] It was found

that the oxidized metabolites of DEHP were those responsible for shortening of the AGD. A report from Colón in 2000, correlated phthalate metabolites in serum with pre-mature breast development in Puerto Rican girls younger than 8 years old with no other signs of puberty displayed.[48] In this study several phthalates were screened and the monoester of DEHP accounted for 68% of phthalate metabolites present.

Bis(2-ethylhexyl) phthalate is noted to reduce fetal testosterone, and insulin-like growth factor-3, which results in male reproductive abnormalities in humans. These abnormalities include shortened AGD, and malformations of the epididymis, vas deferens, semina lvesciles, and prostate, along with signs of hypospadias and cryptorchidism.[32] These are all symptoms of a condition that has come to be named the "phthalate syndrome."

The Carcinogen Assessment Group of the Environmental Protection Agency (EPA) classified DEHP as "probable human carcinogen". When examining for carcinogenic potential it was found that the 2-ethylhexyl moiety is associated with hepato-carcinogenic activity in rodents.[2, 49] In several chronic, high-dose feeding studies, it was noted that there was a clear dose-dependent increase in the appearance of liver tumors, and in some cases pancreatic islet cell adenomas were also observed.[2]

3.4 Synthetic Approach

The synthetic route to prepare the bis(2-ethylhexyl) phthtalate diaryliodonium triflate is depicted in Scheme 3-1 below. Initially, the esterification reaction to form bis(2-ethylhexyl) 4-iodophthalate was conducted in the same manner as 4-iododiethyl phthalate with DCC, DMAP and 2-ethylhexanol (Scheme 3-2). In this reaction, the DCC

by-product formed, dicylcohexylurea (DCU), typically precipitates out of the dichloromethane solvent.

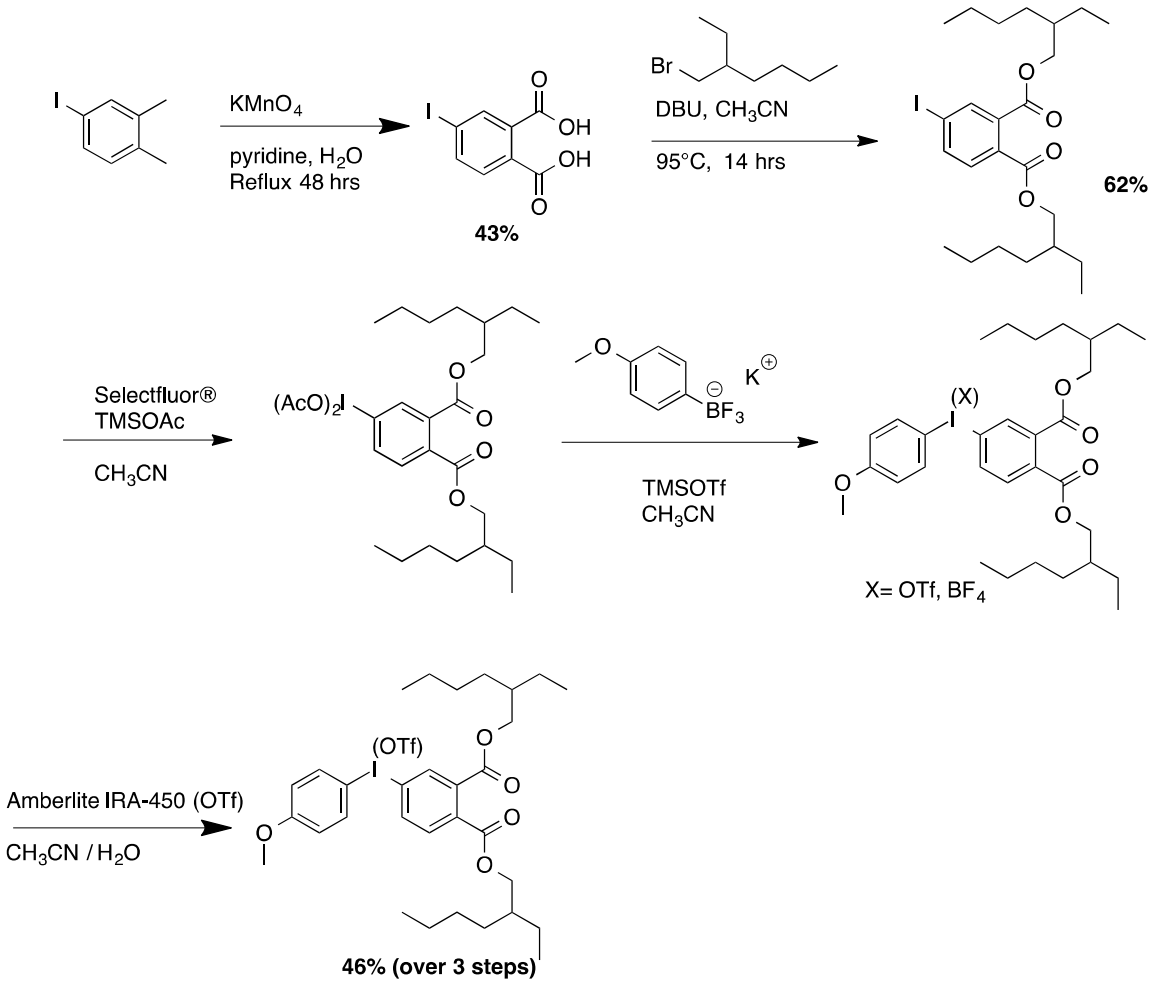

Scheme 3-1: Synthetic route to prepare [3,4-bis(((2-ethylhexyl)oxy)carbonyl)phenyl]-(4'-methoxyphenyl)iodonium triflate

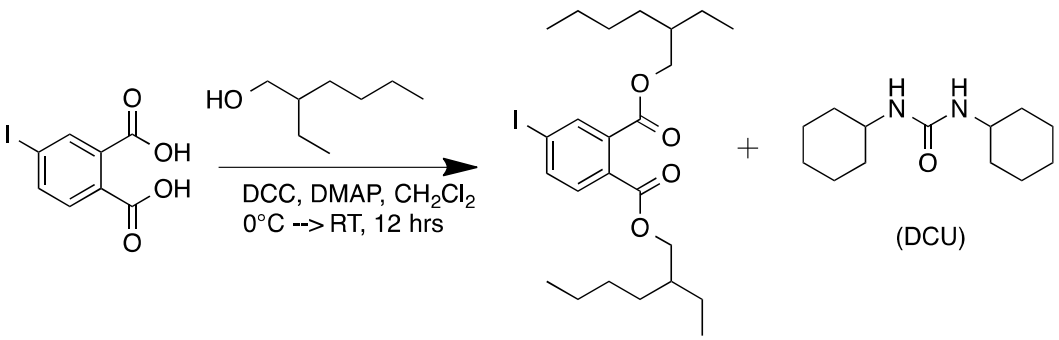

Scheme 3-2: Initial route explored to synthesize bis(2-ethylhexyl) 4-iodophthalate.

Multiple filtration, precipitations, and column chromatography was not efficient to remove the residual DCU, as indicated in the ^{1}H NMR in Figure 3-2.

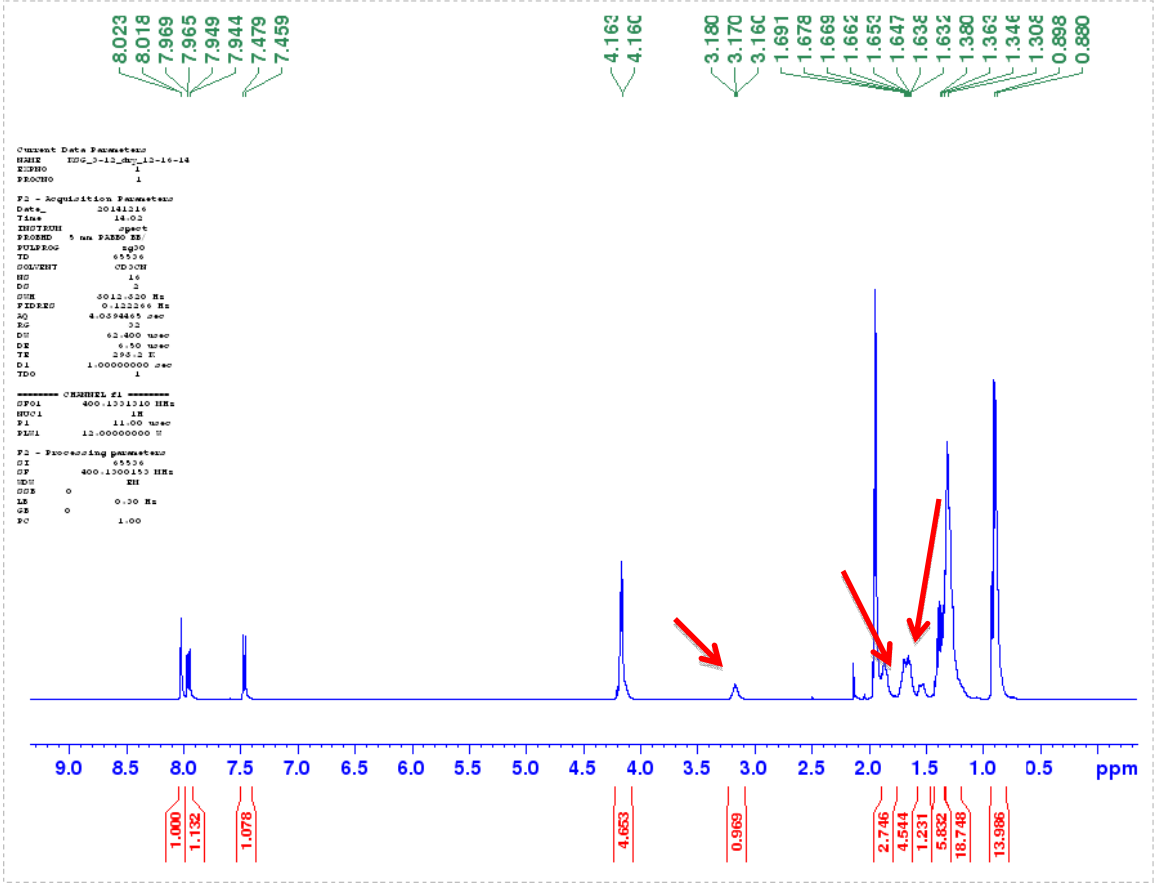

Figure 3-2: ^{1}H NMR data representing the presence of DCU (indicated by red arrows) after column chromatography.

To solve this problem, a second, a DCC-free esterification method was developed. 4-Iodophthalic acid was treated with thionyl chloride to form 4-iodophthaloyl chloride. The thionyl chloride was removed and the resulting solid was dissolved in dichloromethane and treated with 6 equivalents of 2-ethylhexanol and pyridine in dichloromethane to form the desired diester in 12 hours. (Scheme 3-3). An aqueous

workup followed by solvent removal under high dynamic vacuum left the product contaminated with residual pyridine and excess alcohol, which were observed by ^{1}H NMR. The reaction mixture was subjected to column chromatography in 100% hexanes, which removed the pyridine but not the residual alcohol. An aliquot was heated to 45 °C and stirred under high dynamic vacuum for 12 hours. There was no observable change in the ratio of alcohol to product following this treatment. Further heating (60 °C for 2.5 days) resulted in significant decomposition.

Esterification of 4-iodophthaloyl chloride was also performed with triethylamine in chloroform as was reported by Navarro.[50] The amount of alcohol used was also reduced to 2.2 equivalents. Unfortunately, when reduced amounts of the alcohol were used, a mixture of mono- and di-substituted products was obtained.

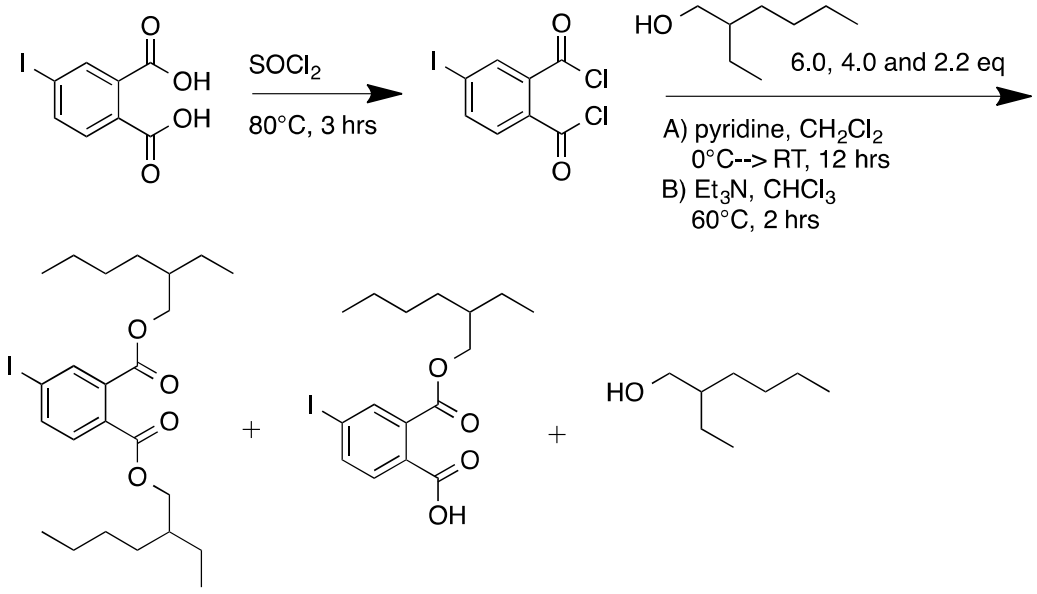

Scheme 3-3: Esterification route from the di-acyl chloride species with modifications of the amount of 2-ethylhexanol used and various conditions (A &B).

While each of the prior esterification methods suffered from significant problems in product isolation and purification, the method of Kelber and co-workers [51] provided the desired product in sufficient purity. In this route, 4-iodophthalic acid was dissolved in acetonitrile and treated briefly with 1, 8-diazabicyclo[5.4.0]undec-7-ene (DBU) under an inert atmosphere before 2-ethylhexyl bromide was added. After the mixture was heated to 95 °C for 14 hours, it contained a large amount of the desired ester with a minimal amount of the mono-substituted analogue. These products were easily separated from each other and from residual 2-ethylhexyl bromide by column chromatography. The bis(2-ethylhexyl) 4-iodophthalate so isolated (62%), was treated with Selectfluor® and TMSOAc, the general oxidation conditions developed in our laboratory, to provide bis(2-ethylhexyl) 4-(diacetoxy-λ^3-iodanyl)phthalate. This I(III) intermediate was coupled with potassium trifluoro(4-methoxyphenyl)borate, using TMSOTf as a catalyst to provide [3,4-Bis(((2-ethylhexyl)oxy)carbonyl)phenyl]-(4'-methoxyphenyl)iodonium triflate, the DEHP diaryliodonium triflate salt, which was obtained as a paste-like compound that proved to be difficult to recrystallize. Despite the luck of crystallinity of this diaryliodonium salt, I decided to forge ahead with model fluorination studies. A sample of [3,4-Bis(((2-ethylhexyl)oxy)carbonyl)phenyl]-(4'-methoxyphenyl)iodonium triflate (0.30 g) was treated with 0.8 equivalents of TMAF in 15 mL of acetonitrile, evaporated, then dissolved in benzene and heated form 20 minutes at 120 °C. This reaction produced the I(I) species, bis(2-ethylhexyl) 4-iodophthalate, along with the desired fluorinated DEHP, bis(2-ethylhexyl) 4-fluorophthalate and 4-iodo-anisole (Scheme 3-4). When this reaction was conducted on an NMR scale (0.02 g) and treated with 0.8 equivalents of TMAF, formation of the iodophthalate was still observed. Because of the lack of 4-

fluoroanisole as a major by-product, it was determined that "aryl-swapping" could be occurring at 120°C.

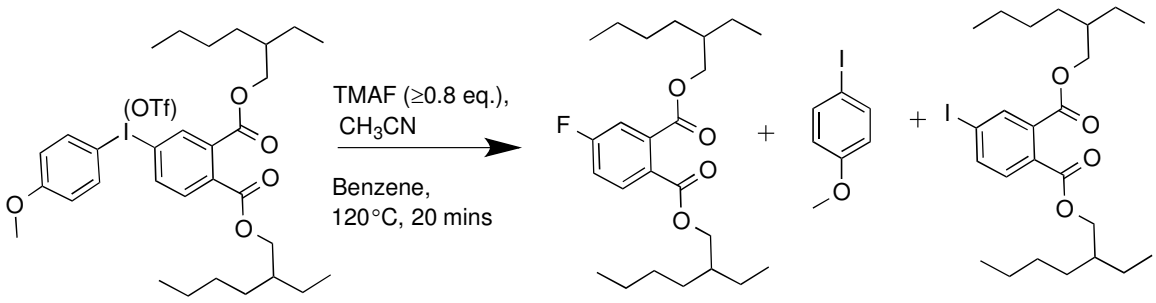

Scheme 3-4: Fluorination reaction with 0.8 equivalents of TMAF with DEHP OTf salt.

The suggested mechanism for aryl swapping for DEHP can be seen in Scheme 3-5, based on a report by DiMagno.[52] This article reports that at 80°C in benzene, these aryl-exchange products can be observed, and even more so at higher temperatures. This could have been a result of an impurity in the triflate salt, thus recrystallization conditions for the triflate salt were explored.

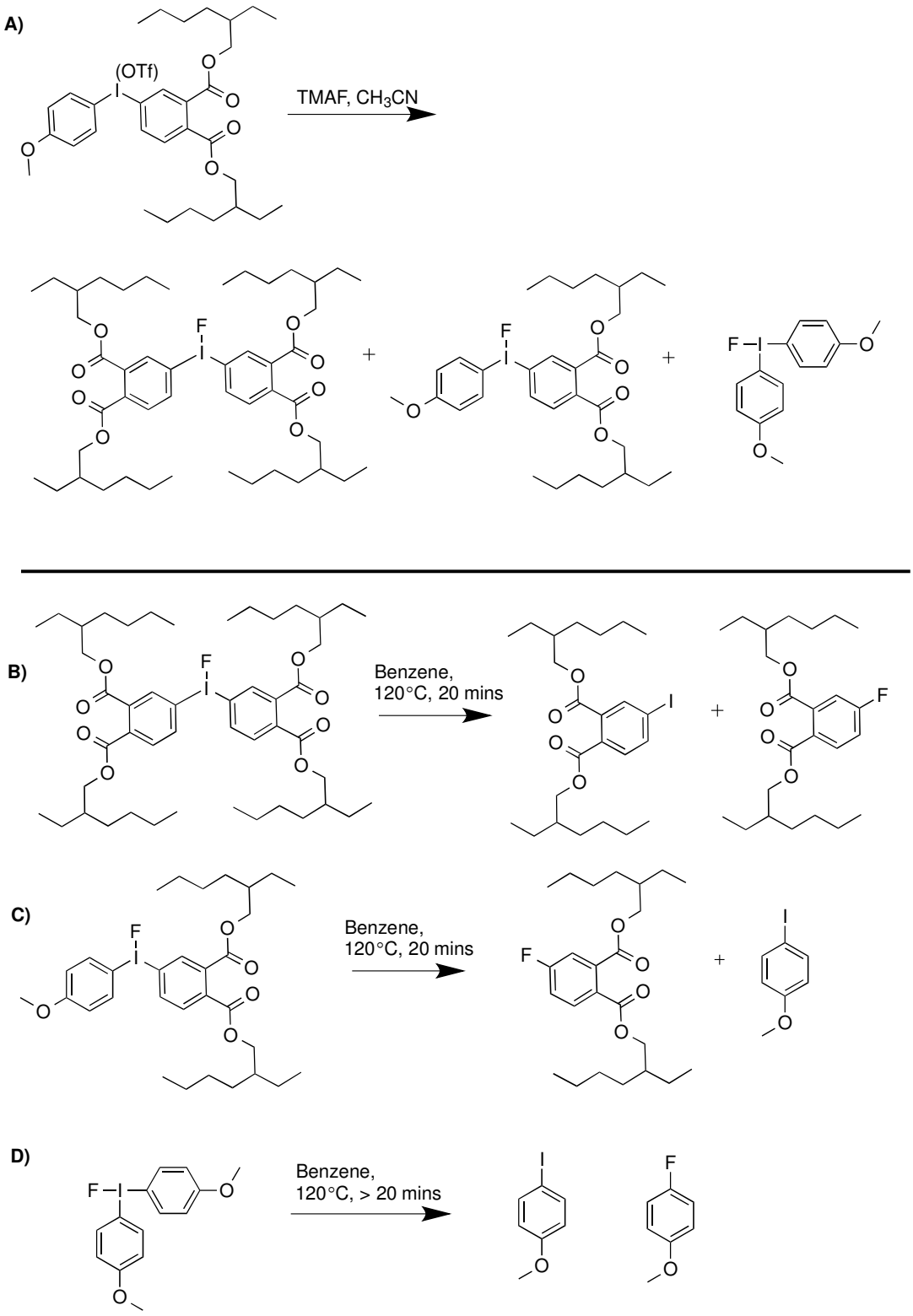

Scheme 3-5: A) Possible aryl exchange products when subjected to fluoride anion. **B-D)** decomposition products for each scenario.

Another fluorination route was investigated utilizing commercially available 4-fluoro-o-xylene, which was oxidized to 4-fluorophthalic acid. The product was esterified in the same fashion as mentioned above for bis(2-ethylhexyl) 4-iodophthalate in good yield (Scheme 3-6). This fluorinated standard was analyzed by HPLC (275 nm UV detection, mobile phase: 100 % acetonitrile, Phenomonex, Luna, C18 column). The HPLC trace of the isolated standard is given in Figure 3-3.

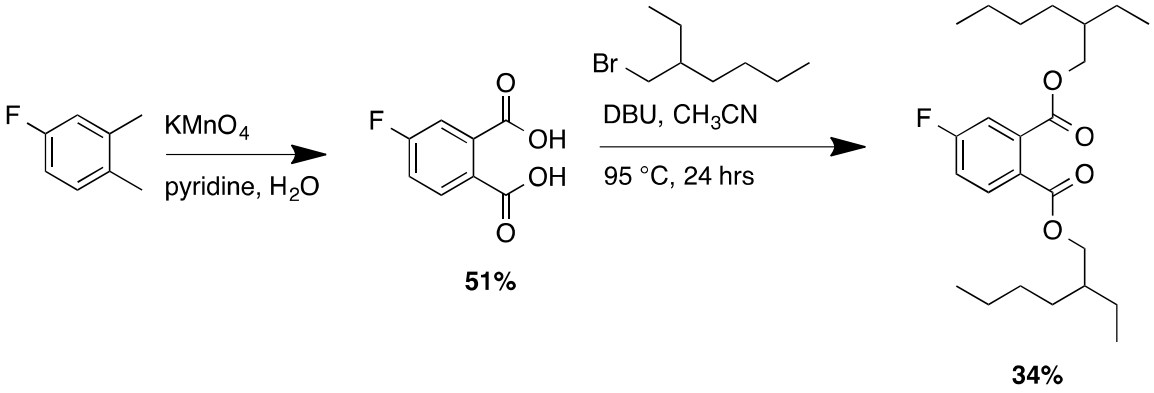

Scheme 3-6: Synthesis of bis(2-ethylhexyl) 4-fluorophthalate.

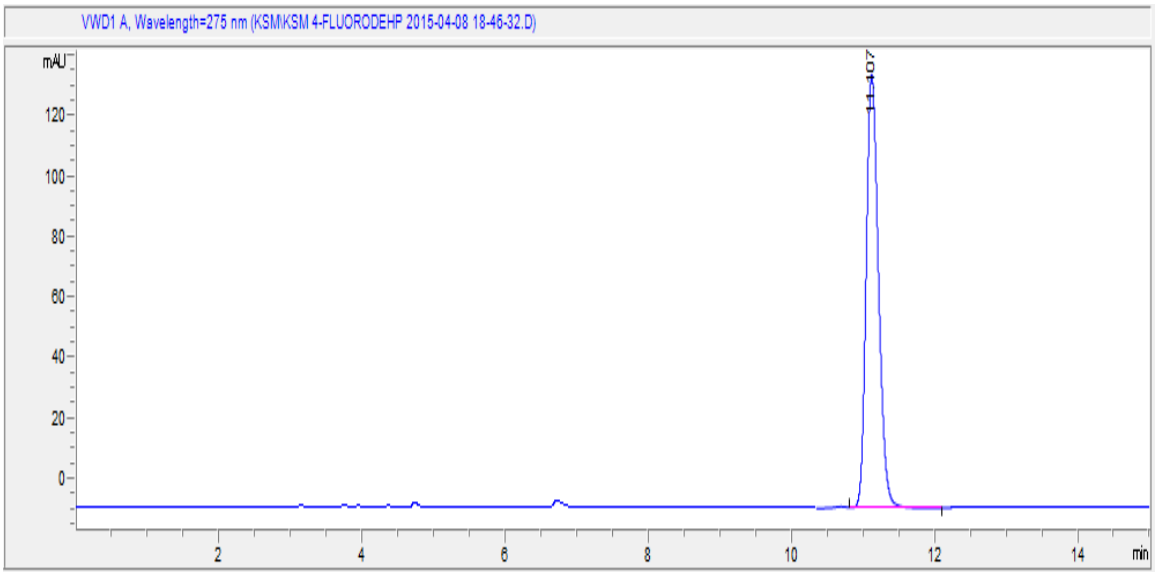

Figure 3-3: HPLC trace of 4-fluoro-bis(2-ethylhexy)phthalate.

3.5 Conclusion

Bis(2-ethylhexyl) phthalate is a widely used plasticizer found in a number of everyday household PVC items. It is also widely used in medical tubing, blood storage bags, disposable medical examination gloves, surgical gloves, and dialysis tubing.[2] Bis(2-ethylhexyl) phthalate has also been reported to be used in non-plasticizer manners as well.

DEHP is metabolized to the corresponding monoester, MEHP, which can then undergo further hydrolysis to yield phthalic acid or oxidation to give several oxidized metabolites (Figure 3-1). Some studies show that the metabolites of DEHP may be the cause of some associated health concerns. However, due to the rapid metabolism and elimination of DEHP and its metabolites, long-term exposure is minimized reducing any potential hazards. In most of the metabolism and distribution studies mentioned above, most, if not all, of the administered dose was accounted for in one form or another. This leaves little evidence of long-term binding to target receptors.

Studies have shown that DEHP exposure is associated with a number of health concerns, especially in males. The testes have shown to be a target organ for MEHP, resulting in a number of component malformations and sperm DNA damage. The reason behind why males are more at risk for health effects caused by DEHP exposure is unclear. Nonetheless, DEHP studies in female rodents have reported reproductive complications, such as decrease fertility. The main health concern that could be of heightened risk would be the inhalation of DEHP during mechanical ventilation, especially in premature infants. This can sometimes be a prolonged procedure. Evidence

has proved to be directly correlated inhaled DEHP to insufficient production of surfactant in the lungs of premature infants. Other medical exposures to DEHP, like blood transfusions, have the capacity to be metabolized more quickly.

The goal of this project was to prepare the bis(2-ethylhexyl) phthalate diaryliodonium triflate aslt as a precursor for radio-fluorination to yield bis(2-ethylhexyl)-[^{18}F]-4-fluorophthalate. The radiotracer could then be injected into a test subject then undergo PET scans to analyze the short-term biodistribution of the compound at any given time point. This imaging technique has the ability to overcome current limitations of classical analytical methods for measuring biodistribution.

3.6 Experimental Data

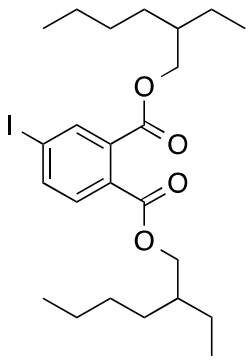

Bis(2-ethylhexyl) 4-iodophthalate

This compound was esterified following the method of Kelber.[51] In an oven dried Schlenk tube in a N_2 charged atmosphere, 4-iodophthalic acid (5.0 g, 17 mmol) and 1,8-diazabicyclo[5.4.0]undec-7-ene (DBU) (5.10 mL, 34.2 mmol) was dissolved in 100 mL of dry CH_3CN. To this solution, 2-ethylhexyl bromide (10.8 mL, 51.4 mmol) was added dropwise. The reaction vessel was sealed and heated at 95 °C for 14 hrs. The solvent was removed under high dynamic vacuum and the reaction mixture was washed with DI

water (100 mL) and extracted with ethyl acetate (4 X 100 mL). The organic layer was washed with DI water (1 X 100 mL), then the ethyl acetate was dried over sodium sulfate, gravity filtered, and the solvent was removed from the product. Bis(2-ethylhexyl) 4-iodophthalate was isolated by column chromatography with a gradient of 100 % hexanes to 5% EtOAc: hexanes. This yielded a pale yellow oil (5.45 g) in a 62% yield. ^{1}H NMR (CD_3CN, 300 MHz, 25°C) δ 8.01 (d, J= 1.2, 1H), 7.93 (dd, J_1= 1.5, J_2= 8.1, 1H), 7.46 (d, J= 8.4, 1H), 4.16 (d, J= 5.7), 4H), 1.66-1.62 (m, 2H), 1.42-1.30 (m, 17H), 0.92-0.87 (m, 13H); ^{13}C NMR (CD_3CN, 75 MHz, 25°C) δ 167.8, 167.1, 141.3, 138.4, 135.2, 132.5, 131.5, 98.1, 69.2, 69.0, 39.7, 39.7, 31.2, 31.2, 29.8, 29.7, 24.6, 24.6, 23.8, 14.4, 11.4. HRMS (ESI): Cald $C_{24}H_{37}IO_4$ $[M+Na]^+$: 539.1634, found: 539.1623.

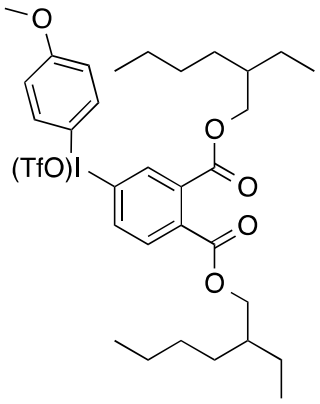

[3,4-Bis(((2-ethylhexyl)oxy)carbonyl)phenyl]-(4'-methoxyphenyl)iodonium triflate

In an N_2 charged glove box, in an oven dried Schlenk tube, bis(2-ethylhexyl) 4-iodophthalate was dissolved in approximately 100 mL of dry acetonitrile. In an oven dried round bottom flask, Selectfluor® (4.46 g, 12.6 mmol) was dissolved in 100 mL of dry acetonitrile. Trimethylsilyl acetate (TMS-OAc) (3.80 mL, 25.2 mmol) was slowly added via syringe. This mixture was allowed to stir for 3-5 mins, and added drop-wise to

the reaction mixture. The reaction vessel was sealed and heated to 60 °C for 24 hrs. Potassium trifluoro(4-methoxyphenyl)borate (2.07 g, 9.68 mmol) was added to the reaction mixture. Trimethylsilyl triflate (TMS-OTf) (1.7 mL, 9.2 mmol) was diluted in dry acetonitrile (5 mL) and added in a drop-wise fashion to the reaction tube. This mixture was allowed to stir at room temperature for 1 hour. The solvent was removed under high dynamic vacuum and the reaction mixture was washed with DI water (100 mL) and extracted with dichloromethane (4 X 50 mL). The organic layer was dried over sodium sulfate and the solvent was removed *in vacuo*, leaving 3.42 g of a light pink paste in a 46% yield. ^{1}H NMR (CD_3CN, 300 MHz, 25°C) δ 8.27 (d, J= 1.8, 1H), 8.20 (dd, J_1= 1.8, J_2= 8.4, 1H), 8.05 (d, J= 9.0, 2H), 7.76 (d, J= 8.4, 1H), 7.08 (d, J= 9.3, 2H), 4.20 (d, J= 5.4, 2H), 4.19 (d, J= 5.7, 2H), 3.851 (s, 3H), 1.67-1,603 (m, 2H), 1.39-1.30 (m, 17H), 0.92-0.87 (m, 13H); ^{13}C NMR (CD_3CN, 75 MHz, 25°C) δ 167.1, 165.9, 164.7, 139.3, 138.5, 137.3, 135.6, 135.6, 135.5, 132.9, 119.4, 116.7, 102.3, 69.6, 69.6, 56.9, 39.6, 31.2, 31.1, 29.7, 24.6, 24.5, 23.7, 14.4, 14.4, 11.4; ^{19}F NMR (CD_3CN, 282 MHz, 25°C) δ -79.29; HRMS (ESI): Cald $C_{32}H_{44}F_3IO_8S$ $[M\text{-}OTf]^+$: 623.2234 found: 623.2219.

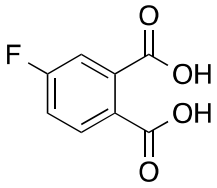

4-fluorophthalic acid

This is a known compound (CAS 320-97-8) but was prepared following the methods of Dudič.[34] In a 250 mL round bottom flask, 4-fluoro-o-xylene (2.0 mL, 16 mmol) was mixed with potassium permanganate (30.54 g, 193.3 mmol), pyridine (32 mL, 16 mmol)

and deionized water (32.0 mL) and refluxed for 48 hrs. After the mixture cooled to RT, the reduced manganese salts were removed by filtration, and the filtrate was acidified carefully with concentrated hydrochloric acid to pH 1-2. Extraction of the reaction mixture with ethyl acetate followed by evaporation of the solvent *in vacuo* produced a colorless solid. The crude product was dissolved in a minimal amount of ethyl acetate and stirred while hexanes was added to the mixture drop-wise. A white precipitate formed and was dried under high dynamic vacuum yielding 1.52 g (51%) of the pure product as a colorless solid. ^{1}H NMR (CD_3CN, 300 MHz, 25°C) δ 9.13 (s, 2H), 7.85 (dd, $^{3}J_{H-H}$= 8.5 Hz, $^{4}J_{H-F}$= 5.4 Hz, 1H), 7.44 (dd, $^{3}J_{H-F}$= 8.5 Hz, $^{4}J_{H-H}$= 2.6 Hz, 1H), 7.32 (td, $^{3}J_{H-F}$= 8.6 Hz, $^{3}J_{H-H}$= 8.6 Hz, $^{4}J_{H-H}$= 2.6 Hz, 1H); ^{13}C NMR (CD_3CN, 75 MHz, 25°C) δ 168.4, 168.211, 165.0 (d, $^{1}J_{C-F}$= 251 Hz), 136.56 (d, $^{3}J_{C-F}$= 8.2 Hz) 133.24 (d, $^{3}J_{C-F}$= 9.2 Hz) 128.29 (d, $^{4}J_{C-F}$= 3.4 Hz), 118.96 (d, $^{2}J_{C-F}$= 21.9 Hz) 117.00 (d, $^{2}J_{C-F}$= 24.4 Hz); ^{19}F NMR (CD_3CN, 282 MHz, 25°C) δ 108.53 (td, $^{3}J_{H-F}$= 8.6 Hz, $^{4}J_{H-F}$= 5.4 Hz); HRMS (EI): Cald $C_8H_5FO_4$ $[M]^+$: 184.0172 found: 184.0175.

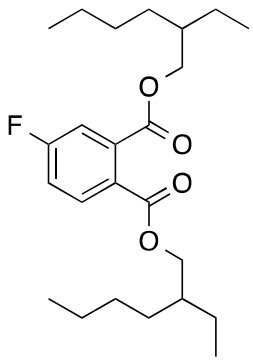

Bis(2-ethylhexyl) 4-fluorophthalate

This compound was esterified following the method of Kelber.[51] Under inert atmosphere, in a 100 mL Schlenk tube, 4-fluorophthalic acid (1.01 g, 5.43 mmol) and 1,8-

diazabicyclo[5.4.0]undec-7-ene (DBU) (1.6 mL, 11 mmol) were dissolved in dry acetonitrile (32 mL). 1-Bromo-2-ethylhexane (3.5 mL, 16 mmol) was added drop-wise to the solution. The reaction vessel was sealed and heated to 95 °C for 24 hrs. The solvent was removed and the resulting orange oil was treated with deionized water (50 mL) and extracted with ethyl acetate (3 X mL). Ethyl acetate was removed under reduced pressure and the product was isolated by column chromatography (95%hexanes: 5% ethyl acetate). The product obtained was 0.76 g of a colorless oil (34% yield). ^{1}H NMR (CD_3CN, 300 MHz, 25°C) δ 7.80 (dd, $^{3}J_{H-H}$= 8.6 Hz, $^{4}J_{H-F}$= 5.4 Hz, 1H), 7.39 (dd, $^{3}J_{H-F}$= 8.8Hz, $^{4}J_{H-H}$= 2.6 Hz, 1H), 7.32 (td, $^{3}J_{H-H}$= 8.4, $^{3}J_{H-F}$= 8.4 Hz, $^{4}J_{H-H}$= 2.6 Hz, 1H), 4.18 (m, 4H), 1.65 (m, 2H), 1.34 (m, 17H), 0.90 (m, 13H); ^{13}C NMR (CD_3CN, 75 MHz, 25°C) δ 167.5 (d, $^{4}J_{C-F}$= 2.3 Hz), 167.2, 164.8 (d, $^{1}J_{C-F}$= 251 Hz), 136.7 (d, $^{3}J_{C-F}$= 8.1 Hz) 132.8 (d, $^{3}J_{C-F}$= 9.0 Hz), 129.0 (d, $^{4}J_{C-F}$= 3.4 Hz) 118.9 (d, $^{2}J_{C-F}$= 21.9 Hz) 116.8 (d, $^{2}J_{C-F}$= 24.3 Hz) 69.2, 68.9, 39.7, 39.7, 31.2, 31.2, 29.8, 24.6, 24.6, 23.8, 14.5, 11.4; ^{19}F NMR (CD_3CN, 75.5 MHz, 25°C) δ -108.8 (td, $^{3}J_{H-F}$= 8.4 Hz, $^{4}J_{H-F}$= 5.2 Hz); HRMS (ESI): Cald $C_{24}H_{37}FNaO_4$ $[M+Na]^+$: 431.2574 found: 431.2570

CHAPTER 4

Bisphenol A

4.1 Introduction

Bisphenol A (BPA) is a commodity chemical used primarily as a polymer backbone component in polycarbonate plastics and epoxide resins, a class of polymers found in food and drink packaging, food can liners, bottle tops, water bottles, water supply pipes, and flame-retardants. BPA is also used in the processing of PVC plastics, the recycling of thermal paper, in infant feeding bottles, and in microwave ovenware.[4, 53] Exposure to BPA mainly occurs orally. Other exposure routes include inhalation and skin absorption. It has been shown that young children and infants are exposed to the highest doses of BPA.[53] BPA has been known to migrate to the surface of plastic or resin containing products and leach into liquids and foods, including infant formulas.[1]

Low levels of BPA ranging from 2-8 μg/L can be found in the environment from the release of effluent from wastewater treatment plants. Bisphenol A dust particulates are typically well-contained in workplaces reducing the release of air-born BPA into the environment. BPA has an aqueous solubility ranging from 0.120-0.300 g/L and this value can increase when in alkaline environments.[54]

There are several health concerns associated with BPA that will be discussed in Section 4.3. Analyses have quantified the amount of BPA that the general public is exposed to through urine, serum, and tissue samples. BPA is suspected as being an endocrine disruptor, but the mechanism by which this could occur is unclear.

The focus of this project was related to the projects described in the two previous chapters: to synthesize a bisphenol A diaryliodonium triflate precursor for the efficient

preparation of ^{18}F-labelled BPA. From here the [^{18}F] labeled analogue can be injected into a test subject to visualize the biodistribution of the compound in real-time, on a single subject, at multiple time points. Based on preliminary data, ^{18}F-BPA also shows potential as biomarker for liver function, since it undergoes rapid clearance and is subjected to enterohepatic recirculation. Once ^{18}F-BPA is efficiently synthesized, its use as a probe to assess liver function and damage will be explored.

4.2 Known Metabolism of Bisphenol A

The metabolism of BPA mainly occurs in the gut and liver where the major metabolite, glucuronidated BPA is observed. Other minor metabolites, sulfonated-BPA, and the ortho-quinone of BPA, have also been observed.[55] These metabolites are shown in Figure 4-1. BPA is extensively absorbed in the gastrointestinal tract, then glucuronidated in the liver and gut in rats and mice, which limits the internal exposure to the aglycone form, which is the form suspected of being an endocrine disruptor. In rodents, enterohepatic recirculation of the glucuronidated BPA occurs, which prolongs the serum lifetime of the compound.

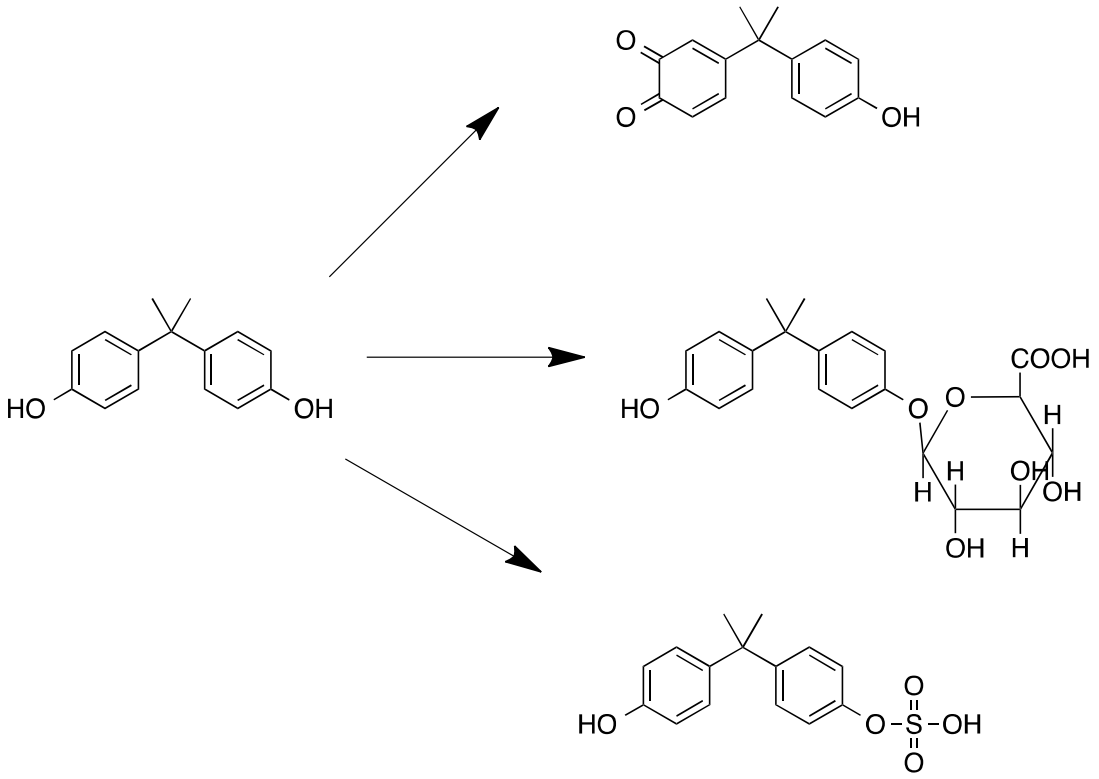

Figure 4-1: Observed BPA metabolites.

The enzymes responsible for the glucuronidation of BPA include a number of uridine diphosphate glucuronosyltransferase isoforms, which are located in the endoplasmic reticulum in vertebrates. The major isoform responsible for the glucuronidation of BPA in the human liver is 2B15. Human, rat and mouse hepatocytes, along with microsomes from rat and human liver and intestine have been shown to catalyze the conversion of BPA to its glucuronidated conjugate. Sulfonation of BPA is catalyzed by sulfotransferase isoforms 1A1, 2A1 and 1E1.[55] Evidence show that most of these enzymes are present in very low concentrations, or even absent altogether, in prenatal and perinatal humans.[55, 56] The BPA-*o*-quinone is generated by a cytochrome P450 isoform, 1B1.[56, 57] Hydroxylation of BPA yields 3-hydroxybisphenol A, which is

oxidized to the *ortho*-quinone (BPAQ). This metabolite is suspected to be genotoxic. In 2012, Kolsek and co-workers studied the reaction of BPAQ with deoxyadenosine and glutathione to elucidate the mechanism by which BPAQ interacts with DNA.[57] It was determined that BPAQ reacts preferentially with guanine sites of DNA. It will also act as an electrophile toward glutathione if it is available, contributing to glutathione depletion in cells. Edmonds and co-workers performed a similar study in 2004 in which herring testes DNA and deoxyguanosine in aqueous buffer (pH 7) were treated with BPAQ resulting in a BPAQ-guanine-N7 adduct. It was suggested that metabolic oxidation of BPA could be as effective as estrogen oxidation in the generation of *ortho*-quinones that covalently bind to DNA.[59]

In a study conducted by Yoo in 2001[60] female rats were administered 100 μg/kg of BPA intravenously, and rapid elimination of the aglycone form was observed. The half-life of BPA was determined to be 0.66 hours. In 2010, Doerge and co-workers administered 0-200 μg/kg of BPA orally and observed linear pharmacokinetics, enterohepatic recirculation of the conjugated BPA form, but not the aglycone form. There was also a significant inverse relationship observed between postnatal age and measures of internal exposure to aglycone BPA in rats with the elimination half-time decreasing with postnatal age. Measurements of the BPA analogues from urine, serum and feces were examined by LC/MS/MS. Doerge also concluded that oral exposure of BPA to rats attenuates internal exposure to aglycone BPA to below 1% of the total administered dose.[60] These findings highlight the significant differences between the elimination of BPA in rats by biliary secretion compared to non-human primates and humans, which eliminate BPA primarily in urine. This study also noted that the maximum concentration

of algycone BPA in neonatal and adult rats from a one-time dose of 100 μg/kg, was found to be 0.4 nM-30 nM. When comparing oral and intravenous administration, Doerge noted that orally administered BPA resulted in a much lower percentage of algycone BPA (5% of dose) than intravenously administered BPA (45%).

Another study monitored and compared the biodistribution of orally and intravenously administered ^{14}C-labeled BPA in rats at doses of 100 or 0.1 mg/kg. It was determined that the ^{14}C-BPA derived radioactivity was tightly bound to plasma protein and preferentially distributed to the plasma with a blood/plasma ratio of 0.67. This study also reported finding free BPA in feces.[62] The author conducted a similar study using Cynomolgus monkeys in 2002. The monkeys were subjected to a single oral or intravenous dose of ^{14}C-BPA (100 μg/kg). It was reported that 79-85% of the dose was excreted in the urine over 7 days, with most of the urinary excretion recovered after the first 24 hours after administration. Radioactivity measured in fecal matter only accounted for 1.8-3.1% of the total radioactive dose. The unchanged ^{14}C-BPA half-life was somewhat shorter for male monkeys ($t_{1/2}$= 0.57 hr) than that for females ($t_{1/2}$= 0.39 hr). The authors concluded from these studies that the aglycone form was fractionated into adipose tissue after intravenous injection, and ^{14}C-BPA derived radioactivity also bound tightly to plasma protein.[63] For these studies, radioactivity was determined by liquid scintillation counting and the identification and quantification of metabolites were determined by HPLC analysis.

4.3 Potential Health Effects of Bisphenol A

A large amount of data have been generated on the potential toxic effects of BPA, and a number of reproductive and developmental effects have been associated with exposure to this compound. While, BPA is typically described as being "weakly" estrogenic, a number of studies indicate a number of additional biological activities.[53] Xin and co-workers conducted a study in which they treated INS-1 cells with various doses of BPA (0, 25, 50 or 100 μM) and assessed subsequent DNA damage by nuclear comet assays, gel electrophoresis, and western blot analysis. The results indicated that BPA is associated with a dose-dependent increase in DNA strand breaks at higher doses and with greater DNA migration from the nucleus into the comet tail. DNA damage was also suggested by the observation of a significant increase in the expression of DNA repairing proteins.[64]

Three epidemiological studies in humans reported associations with high urinary BPA metabolite concentrations and reduced semen quality.[4] A study conducted on factory workers in China found that those who worked with BPA were found to have reduced sperm count and decreased sperm concentration. A 2010 study on fertile males in the US determined that there was an inverse relationship with BPA urine concentration and sperm count and motility of sperm. A third study conducted on infertile males also concluded that there was an inverse relationship with urinary BPA concentration and sperm count and sperm motility. This study also reported that there was also a positive correlation with abnormal sperm morphology.

BPA exposure has been correlated with a number of cardiovascular and neuronal disorders. Michaela and co-workers investigated the effects of BPA on T-type calcium

channels, which are vital regulatory elements in both the cardiovascular and neuronal systems. The whole-cell patch clamp technique was used to measure calcium current through T-type calcium channels expressed in HEK 293 cells. It was found that BPA inhibited the current through calcium channel subtypes in a concentration-dependent manner. The concentration range resulted in a physiological response that corresponds to that found in human fluids.[65]

There has been some correlation between BPA exposure and a decrease in glucose metabolism. In 2013, Zhang and co-workers, studied the effects of BPA on glucose metabolism and adipokine expression in female offspring of pregnant rats that had been exposed to BPA. Pregnant rats were exposed to aqueous BPA at doses of either 1 μg/mL or 10 μg/mL from the sixth day of gestation to the end of the lactation period. Body weight, fasting serum glucose levels, insulin, adiponectin (ADP) (adipokine needed for glucose metabolism), Zinc-alpha2-glycoprotein (ZAG) (body weight regulator), ADP mRNA, and protein expression from the adipose tissue of 7 week old female offspring were examined. It was observed that the female offspring had higher body weight, significantly higher serum glucose and insulin levels, lower serum ADP and plasma ZAG protein levels, and lower ADP and ZAG mRNA and protein expression as compared to the control group. It was concluded that BPA exposure during early development has long-term effects on body weight and glucose metabolism in rats.[66]

A study of BPA exposure in pregnant rats being exposed to BPA revealed similar results as Zhang's work. In 2010, Alonso-Magdalena and co-workers treated pregnant rats with 10 or 100 μg/kg/day during day 9-16 of gestation.[67] Glucose tests performed on both the mother and offspring divulged that BPA aggravated the insulin resistance

produced during pregnancy, increased plasma insulin, triglycerides, and leptin concentrations in comparison to controls. Six-month old male offspring exposed to BPA *in utero* expressed decreased glucose tolerance increased insulin resistance and altered blood parameters. As a result, the authors of the study suggested that BPA exposure may be linked to an increased risk of diabetes.

In 2014, Khalil and co-workers investigated whether BPA is correlated with obesity and metabolic changes in human liver.[68] A cross-sectional study was conducted on 39 obese and overweight children (3-8 years old) indicated that a higher BPA concentration in overweight children was associated with an increase in free thyroxine levels. In male candidates, there was a correlation of serum BPA (1.82 μg/g) and elevated levels of the liver enzyme aspartate aminotransferase, elevated diastolic blood pressure, and insulin resistance.

A 2014 study showed that colorectal cancer SW480 cells exposed to nanomolar to micromolar concentrations of BPA (10^{-8} M and 10^{-5} M) exhibited changes in the expression of more than 56 proteins relevant to structure, motility, cell proliferation, production of ATP, oxidative stress, and protein metabolism. It was also suggested that BPA increased migration and invasion of cancer cells, as well as triggered transformations from epithelial to mesenchymal transitions of colorectal cancer cells.[69]

There is a substantial body of work indicating that BPA is an endocrine disruptor, but the mechanism by which BPA could function in such a capacity in unclear. BPA's estrogenic activity is weak; its binding affinity to ER-alpha and ER-beta are more than 10,000 times lower than that of estradiol. However, as the above studies show, cellular responses are induced by very low concentrations of BPA. In a study in which pregnant

rats were fed 0.025 μg/kg/day and 0.25 μg/kg/day, masculinization of a brain region essential for cyclic gonadotropin release in female offspring was observed. This suggests that BPA could have acted as an estrogen in specific areas of a developing brain that are important for sexual differentiation.[70]

Vom Saal and Hughes reviewed several low dose rodent BPA studies in 2005. Several health effects, including increased postnatal growth, early onset of sexual maturity in females, altered plasma luteinizing hormone levels, an increase in prostate size in male offspring, and stimulation of mammary gland development in female offspring were observed. Other health effects included increased mortality of embryos, altered immune function, increase in progesterone receptor mRNA levels, modulation of somatostatin receptors in the brain, and behavioral changes such as hyperactivity, an increase in aggressiveness, altered reactivity to pain, and impaired learning.[71]

4.4 Preliminary Data and Synthetic Short Comings

Preliminary studies conducted in the DiMagno lab focused on the routes relying on the dimethylether protected BPA derivative. The synthesis of the diaryliodonium salt, which was developed by Dr. Kiel Neumann, relied heavily upon a selective iodoarylation method that was recently published by our research group.[72] A synthetic shortcoming of using a diaryliodonium salt precursor, featuring methyl ether protective groups, was that aggressive deprotection conditions were required, involving the use of a strong acid. These conditions led to destruction of the parent molecule, perhaps by aryl ring protonation and the generation of a stabilized cumyl cation. The radio-fluorination and deprotection procedure that Dr. Neumann developed is shown in Scheme 4-1. While the

deprotection conditions used in this synthesis provided radio-fluorinated BPA, BBr_3 proved to be aggressive toward the radiosynthesis equipment and the yields were quite low. To pursue imaging studies with ^{18}F-BPA, a better synthesis was needed. It was proposed that a more acid-labile phenol-protecting group be used. We selected ethoxy methyl (EOM) as a more acid-labile alternative to methyl ether. Chloromethyl ethyl ether is preferred over other acid-labile protecting groups, like methoxy methyl (MOM), because it is less volatile and thus, less hazardous to work with.

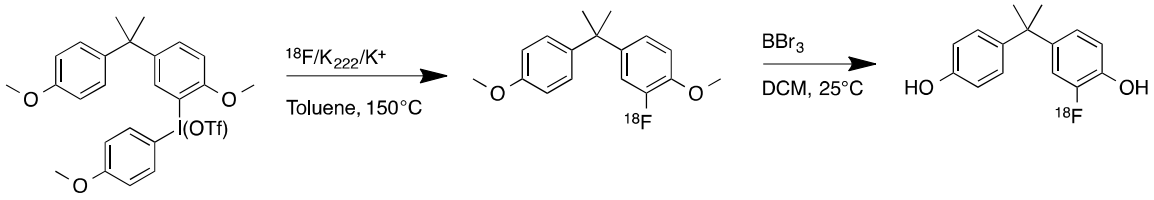

Scheme 4-1: Radiosynthetic route of [^{18}F] FBPA.

Dr. Neumann's preliminary PET imaging data of [^{18}F] BPA in mice suggests that BPA has promising potential as a biomarker for liver function. The PET scan of a healthy mouse can be seen in Figure 4-2. This is a PET scan taken 60 minutes post-intravenous injection. These data show that the most concentrated areas of radioactivity are in the stomach and intestines. This is indicative of rapid metabolism and clearance of the radiolabelled compound from the bloodstream. In Figure 4-3, it is shown that at 10 minutes and 22 minutes post injection, there is a spike in radioactivity in the intestine followed by a slight decrease. This is indicative of enterohepatic recirculation occurring. The highest concentration of radioactivity in the intestine was at approximately 53

minutes. This suggested rapid metabolism of the majority of the radioactive compound. No data was acquired on rate or amount of radioactivity excreted during this experiment. At 55 minutes the mouse was sacrificed and each organ was weighed and counted for radioactivity. In Figure 4-4, the *ex vivio* biodistribution of [^{18}F]-FBPA is illustrated at 150 minutes post-injection. These data indicate that the radioactive compound has recirculated back into the liver yet again. This is also evident of the advantages of utilizing PET as tool to monitor biodistribution and pharmacokinetics, over classical methods such as *ex vivo* biodistribution. PET allowed for the visualization of the biodistribution of [^{18}F] BPA and the rate at which the enterohepatic recirculation took place. The classical *ex vivo* method can only give information on where radioactivity resides at the time of death.

Figure 4-2: Representative PET imaging at 60 min post injection of [^{18}F]FBPA in normal, healthy mouse.

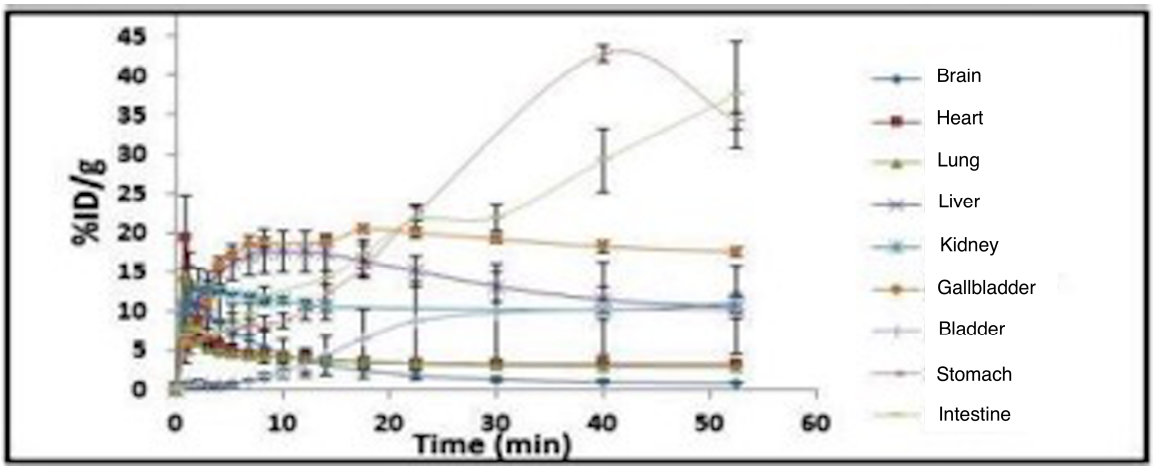

Figure 4-3: Time activity curve of major organ in 60 min dynamic scan (n=3)

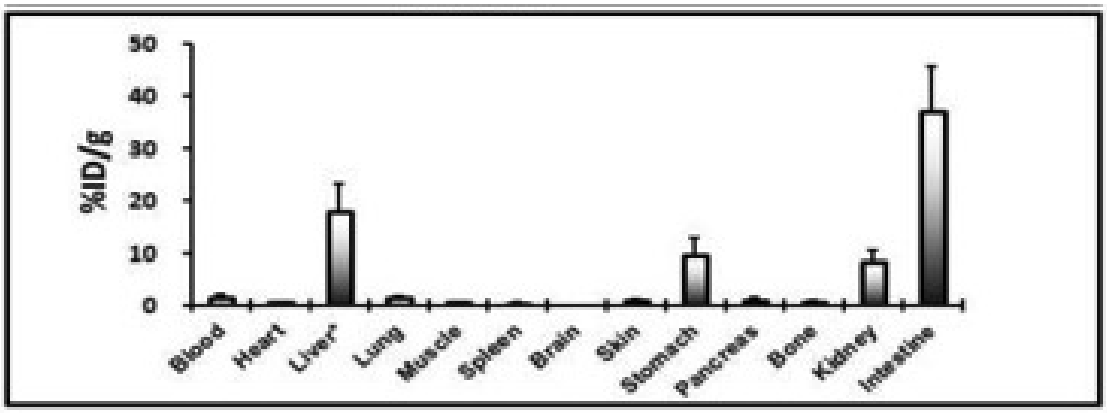

Figure 4-4: *Ex vivo* biodistribution data of healthy mice 150 min post-injection (n=3), *%ID/g in liver includes gall bladder.

4.5 Synthetic Approach

I explored several synthetic routes towards (2-(ethoxymethoxy)-5-(2-(4-(ethoxymethoxy)phenyl)propan-2-yl)phenyl)(4-methoxyphenyl)-λ^3-iodanyl trifluoromethanesulfonate. The first route is illustrated in Scheme 4-2. Here,

commercially available bisphenol A was protected with chloromethyl ethyl ether. Next, I conducted a heteroatom-directed *ortho*-lithiation, followed by transmetalation with trimethyl borate. The obtained aryl borate was treated with potassium bifluoride to hydrolyze the borate esters and form the corresponding potassium trifluoroborate. However, lithiation was not efficient and the desired product was only obtained in 8% yield. Nonetheless, this compound was carried forward. Coupling with bis(acetoxy)iodoanisole took place in excellent yields. However, because the trifluoroborate derivative was formed in such poor yields, other avenues toward the synthesis were explored.

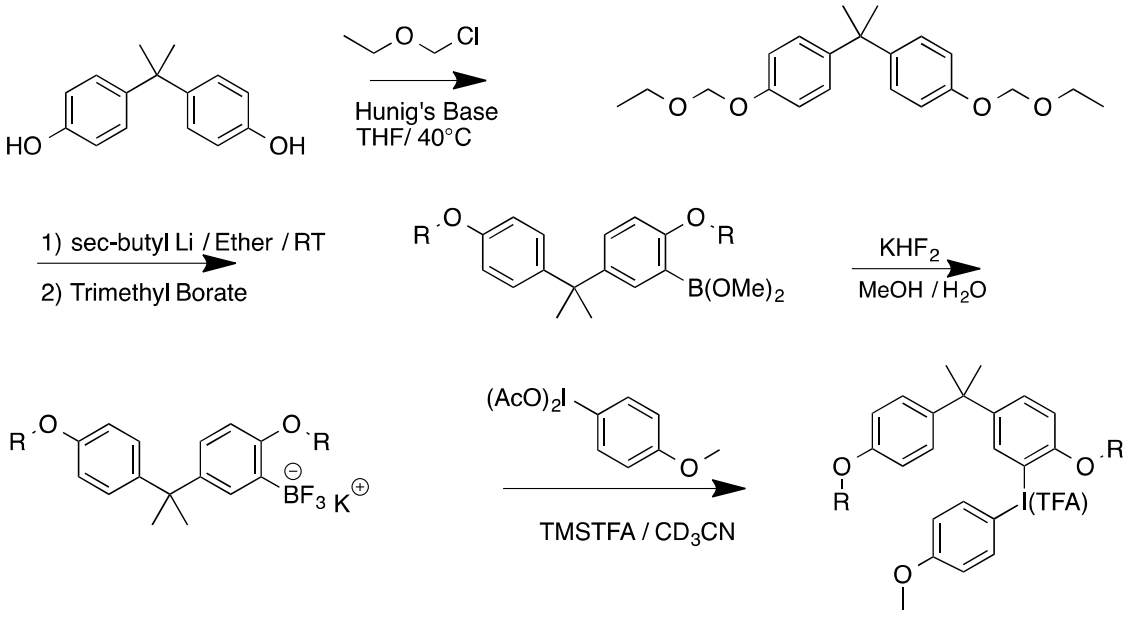

Scheme 4-2: First synthetic route attempted to form a BPA diaryliodonium salt.

Several iodination reactions were employed to find a suitable method to selectively iodinate 4,4'-(propane-2,2-diyl)bis((ethoxymethoxy)benzene). Because of the symmetrical nature of this compound, selective, mono-substitution was not achieved

when using I_2 and TMSI as iodinating agents under the conditions shown in Scheme 4-3.

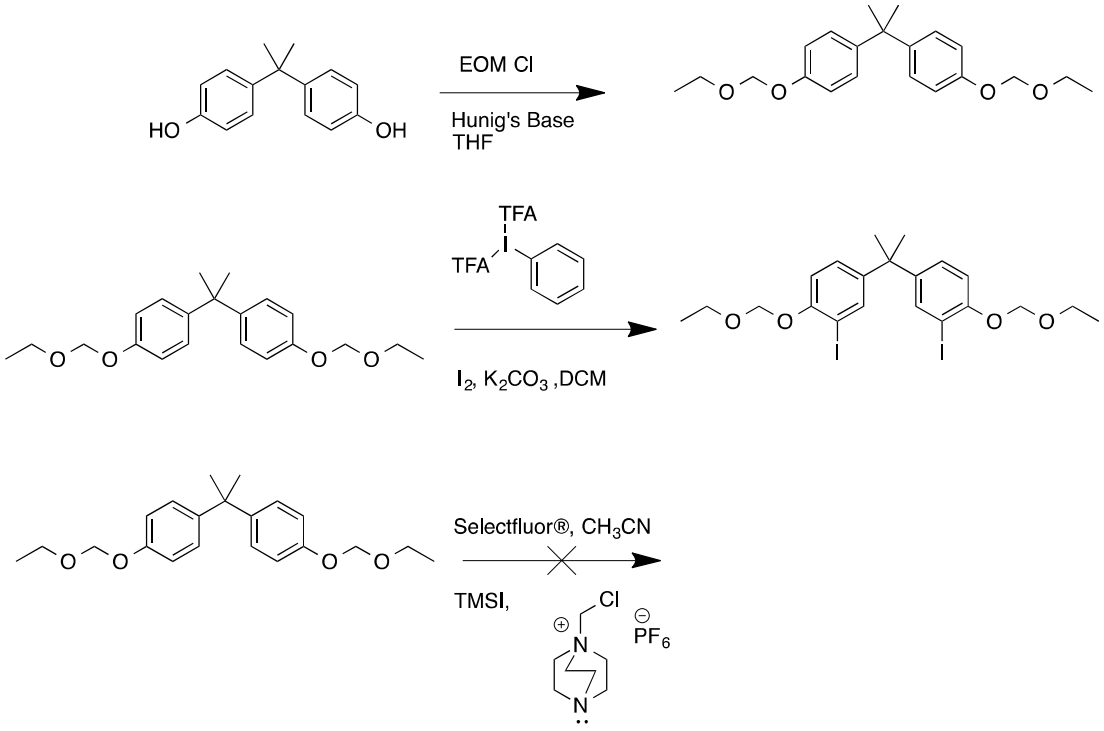

Scheme 4-3: Iodination methods investigated for 4,4'-(propane-2,2-diyl)bis((ethoxymethoxy)benzene).

Because the bulky triisopropylsilyl (TIPS) protecting group has been shown to inhibit ortho halogenation in heterocyclic systems,[73] I thought that preparation of a selectively protected BPA derivative, in which only one phenolic oxygen was silylated, might allow for selective iodination. Mono-TIPS substituted BPA was subjected to several iodination methods using I_2 and NIS as the iodine source (Scheme 4-4) but a mixture of iodinated isomers were observed in each case.

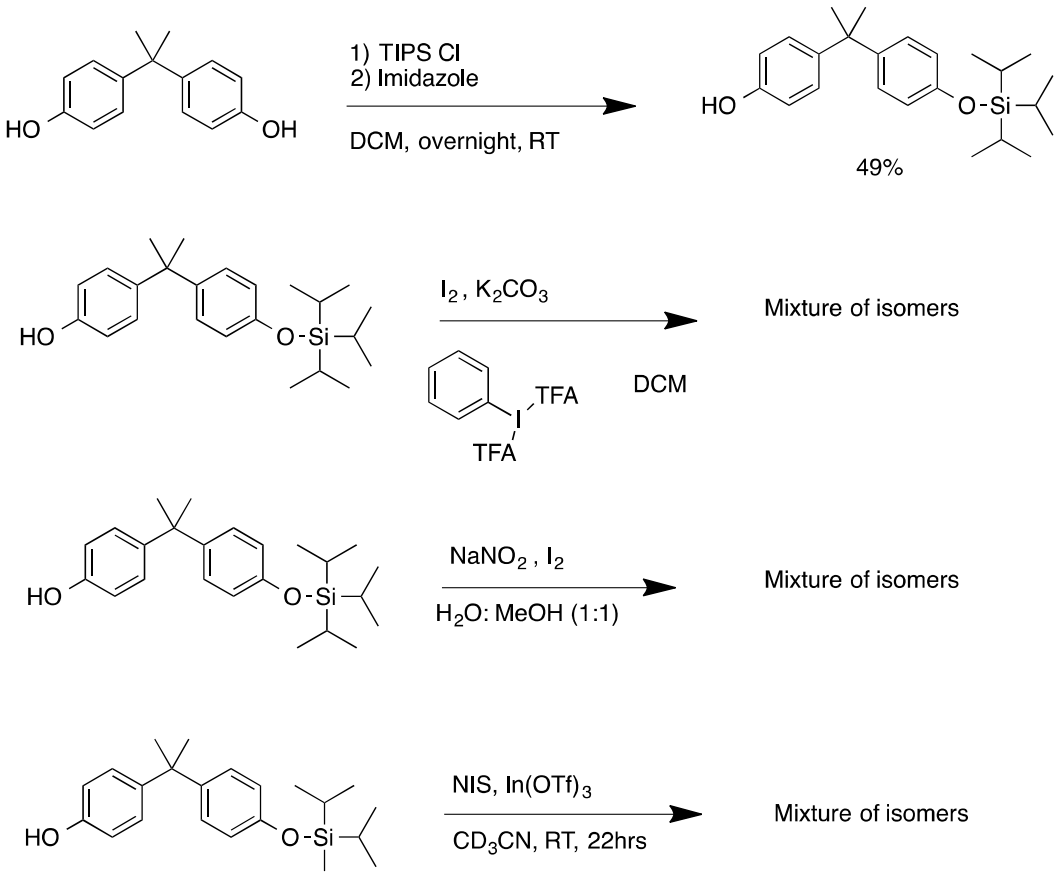

Scheme 4-4: Attempted selective iodination of mono-substituted TIPS BPA.

Iodoarylation was also attempted with 4-methoxyphenyl iodonium diacetate in the presence of 1-(chloromethyl)-1,4-diazabicyclo[2.2.2]octan-1-ium hexafluorophosphate(V), which acts as a weak base to scavenge any acid that could be potentially generated. (Scheme 4-5). Activation of 4-methoxyphenyl iodonium diacetate with TMS-TFA gave no reaction. Even after 24 hour at 40°C, there was no conversion. When TMS-OMS was used as the catalyst, there was an instant color change to light green and the NMR data from time = 15 minutes indicated complete conversion of $ArI(OAc)_2$ to ArI and no production of the desired diaryliodonium salt. The result was the same when TMS-OTf was used, but the color change was from clear to brown. It

was thought that 1-(chloromethyl)-1,4-diazabicyclo[2.2.2]octan-1-ium hexafluorophosphate(V) could have potentially been interacting with the TMS-X groups or the bis(acetoxy) iodoanisole, so the reaction was attempted without the base. This reaction resulted in decomposition of the I(III) center to I(I) but no noticeable sign of deprotection.

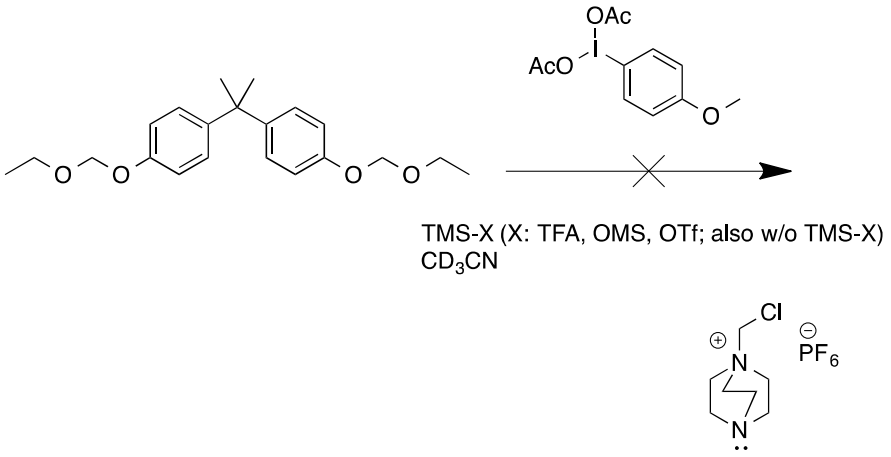

Scheme 4-5: Attempted iodoarylation of 4,4'-(propane-2,2-diyl)bis((ethoxymethoxy)benzene), with various TMS-X groups in the presence of 1-(chloromethyl)-1,4-diazabicyclo[2.2.2]octan-1-ium hexafluorophosphate(V).

In the end, we elected to perform the initial iodination on a dimethyl ether protected derivative of BPA using chemistry developed by Dr. Neumann. [72] Once the selectively iodinated, the compound was deprotected with BBr_3 and protected with chloromethyl ethyl ether and the iodine center was oxidized with Selectfluor®. Coupling of the aryliodonium diacetate with potassium trifluoro(4-methoxyphenyl)borate gave the corresponding diaryliodonium salt (Scheme 4-6). The only major difficulty encountered

in this synthesis was discovering the optimal recrystallization conditions for the diaryliodonium triflate salt.

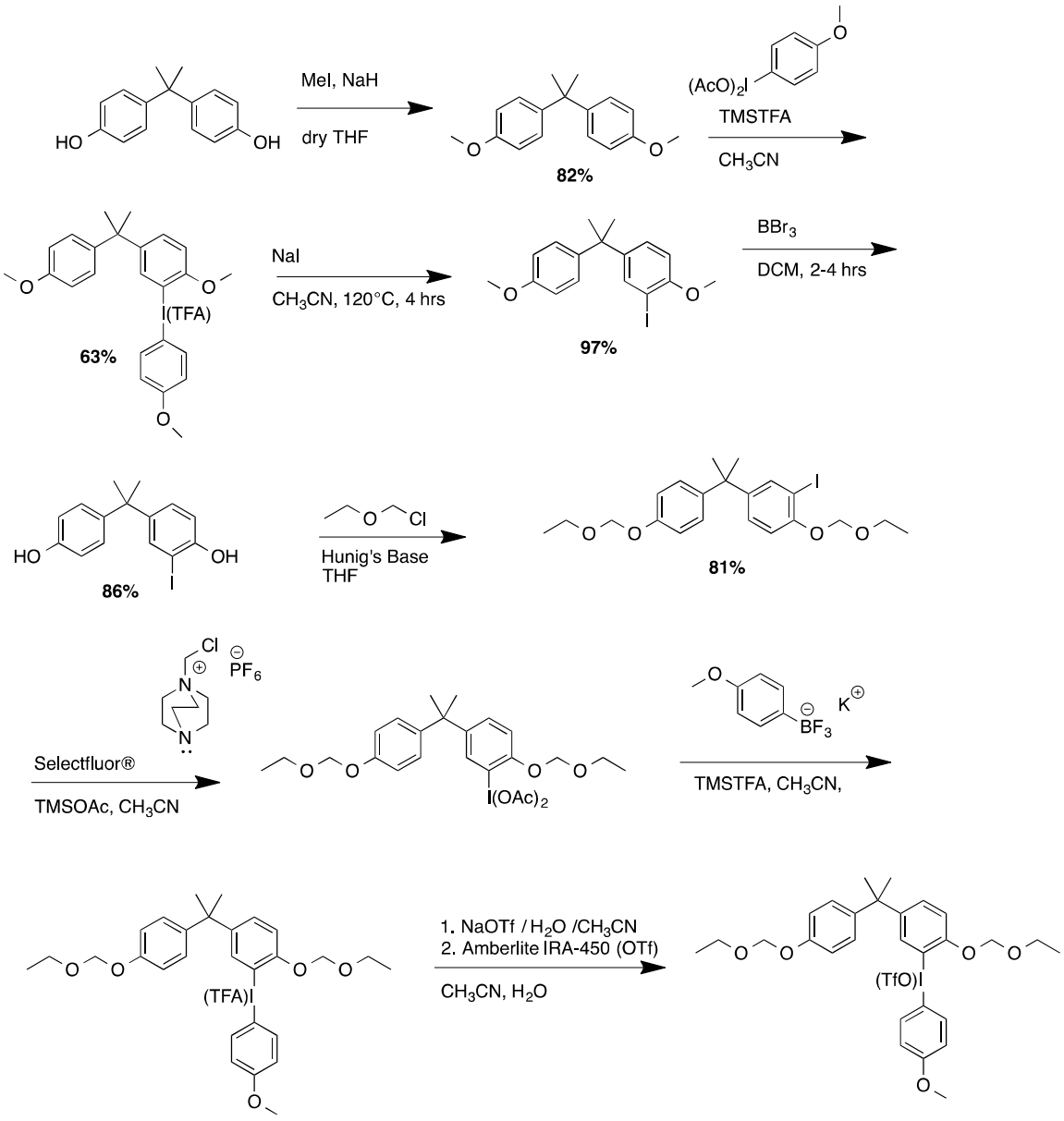

Scheme 4-6: Total synthesis of (2-(ethoxymethoxy)-5-(2-(4-(ethoxymethoxy)phenyl)propan-2-yl)phenyl)(4-methoxyphenyl)-λ^3-iodanyl trifluoromethanesulfonate.

4.6 Conclusions

In summary, bisphenol A is a widely used industrial compound found in a number of everyday consumer products. BPA is metabolized primarily in the gut and liver where the major metabolite is the guluronidated conjugated and minor metabolites include sulfonated-BPA and the 3,4-quinone-BPA. BPA and its metabolites have been associated with several health effects including damage to sperm DNA and morphology, cardiovascular and neuronal disorders, obesity, insulin resistance, and altered glucose metabolism, high blood pressure, and was reported to accelerate the invasion and metastasis of colorectal cancer cells. BPA was also shown to act as an estrogen in specific areas of the brain responsible for sexual differentiation. It was also associated with an early onset of sexual maturity in female rats, increased prostate size in male rats, and altered immune function and behavioral changes.

Preliminary data generated by Dr. Kiel Neumann suggests that BPA has great potential as a biomarker for liver function. Most importantly, it suggests that BPA is cleared remarkably fast and does not bind to any target receptor with high affinity in mice. While the synthetic methods used to generate [^{18}F] FBPA were successful, the deprotection conditions with BBr_3 proved to be harsh toward the radiosynthesis equipment. This research was designed to synthesize a BPA diaryliodnium salt precursor with a more acid-labile protecting group. The synthesis of this precursor will allow for late-stage radio-fluorination and application to the monitoring of biodistribution of BPA in animal models with both healthy and damaged livers and visualize liver function.

4.7 Experimental Data

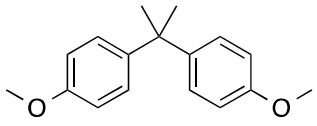

4,4'-(propane-2,2-diyl)bis(methoxybenzene)

This compound is known (CAS 1568-83-3) and the synthesis was modeled after the methods of Kubo.[75] In an oven dried, Schlenk tube, with a magnetic stir bar, under a N_2 atmosphere, 4,4'-(propane-2,2-diyl)diphenol (3.00 g; 13.1 mmol) was dissolved in 25 mL of dry THF and this solution was cooled to 0 °C. Sodium hydride (0.95 g; 39.4 mmol) was added slowly and this mixture was stirred at 0 °C for 30 mins. Methyl iodide (2.3 mL; 53 mmol) was added dropwise to the reaction mixture at 0 °C. The tube was sealed, transferred to an oil bath and heated at 75 °C overnight. The reaction was monitored by TLC with an elution of 30% ethyl acetate in hexanes and gave an R_f value of 0.79. The reaction was cooled to RT then quenched with DI H_2O. The solvent was removed *in vacuo* then the product was extracted with dichloromethane (3 X 25 mL). The organic layer was dried over sodium sulfate, gravity filtered, and evaporated to yield a colorless solid. Any residual starting material was removed by dissolving it in hexanes (with sonication) and filtering the remaining solid. The solvent was removed from the filtrate, yielding 2.78 g (82.4% yield) of colorless, prism-like crystals. ^{1}H NMR (CD_3CN, 400 MHz, 25°C) δ 7.15 (d, J=8.6 Hz, 4H), 6.82 (d, J=8.6 Hz, 4H), 3.74 (s, 6H), 1.62 (s, 6H); ^{13}C NMR (CD_3CN, 100 MHz, 25°C) δ 158.6, 144.1, 128.7, 114.3, 55.8, 42.3, 31.4; HRMS (EI): calcd for $C_{17}H_{21}O_2$ $[M+H]^+$: 257.1542; found 257.1543.

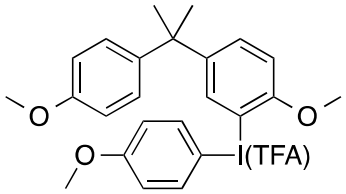

2,2,2-trifluoro-1-((2-methoxy-5-(2-(4-methoxyphenyl)propan-2-yl)phenyl)(4-methoxyphenyl)-□^{3}-iodanyl)ethan-1-one

This compound was synthesized following the procedure reported by Hu.[76] In a N_2 charged glove box, in an oven dried Schlenk flask, 4,4'-(propane-2,2-diyl)bis(methoxybenzene) (6.01 g; 23.5 mmol) was dissolved in 50 mL of dry acetonitrile. In dry acetonitrile (50 mL) (4-methoxyphenyl)-□^{3}-iodanediyl diacetate (3.30 g; 9.38 mmol) was added to the reaction flask. In a scintillation vial, trimethylsilyl trifluoro acetate (3.2 mL; 19 mmol) was diluted in dry acetonitrile (50 mL). This solution was then added slowly to the reaction mixture. The flask was sealed and stirred at 80 °C for 24 hrs. The solvent was removed under high dynamic vacuum. A small amount of ethyl acetate was added to the resulting orange viscous oil and subjected to sonication. Methyl-tert-butyl ether (100 mL) was added to the flask and subjected to sonication for 20 mins. A colorless solid was precipitated out of the solution. The solution was decanted off into a round bottom flask and the volume was reduced by 10% forming more solid precipitate. The solid was dried under high dynamic vacuum giving 3.48 g (63%) of the desired product. ^{1}H NMR (CD_3CN, 300 MHz, 25°C) δ 7.88 (d, J=9.2 Hz, 2H), 7.67 (d, J=2.3 Hz, 1H), 7.430, (dd, J_1=8.7 Hz, J_2=2.3 Hz, 1H), 7.08 (d, J=2.2 Hz, 2H), 7.05 (d, J=8.6, Hz 1H), 6.95 (d, J=9.3 Hz, 2H), 6.80 (d, J=8.7 Hz, 2H), 3.89 (s, 3H), 3.83 (s, 3H), 3.76 (s, 3H), 1.60 (s, 6H); ^{13}C NMR (CD_3CN, 75 MHz, 25°C) δ 163.6, 158.8, 155.6, 147.9, 142.6, 138.5, 135.0, 133.6, 128.6, 114.4, 113.1, 106.6, 103.9, 57.9,

56.6, 55.9, 42.8, 30.9; ^{19}F NMR (CD_3CN, 282 MHZ, 25 °C), -75.48; HRMS (HREI): Calcd for $C_{26}H_{26}F_3IO_4$ $[M\text{-}TFA]^+$: 489.0938; found 489.0929.

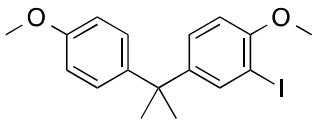

2-iodo-1-methoxy-4-(2-(4-methoxyphenyl)propan-2-yl)benzene

This compound is known (CAS 1501940-95-9) and was prepared following the procedure of Hu.[76] In a N_2 charged atmosphere, in a Schlenk flask, 2,2,2-trifluoro-1-((2-methoxy-5-(2-(4-methoxyphenyl)propan-2-yl)phenyl)(4-methoxyphenyl)-□^{3}-iodanyl)ethan-1-one (3.51 g; 5.98 mmol) and sodium iodide (2.69 g; 17.9 mmol) were dissolved in dry acetonitrile (60 mL). The Schlenk flask was sealed and stirred for 4 hours at 120 °C. The flask was cooled to RT. The solvent was removed *in vacuo* and the compound was isolated by column chromatography (100 % hexanes). The R_f value for the desired product was 0.47. After removal of solvent, the product was 2.29 g of a pale yellow oil (96.8% yield). ^{1}H NMR (CD_3CN, 300 MHz, 25°C) δ 7.62 (d, J=2.4 Hz, 1H), 7.23 (dd, J_1=8.6 Hz, J_2= 2.4 Hz, 1H), 7.15 (d, J=8.8 Hz, 2H), 6.83 (d, J=8.7 Hz, 1H), 6.83 (d, J=8.7 Hz, 2H), 3.79 (s, 3H), 3.74 (s, 3H), 1.59 (s, 6H); ^{13}C NMR (CD_3CN, 75 MHz, 25°C) δ 158.6, 157.0, 146.5, 143.3, 138.5, 128.9, 128.6, 114.3, 111.7, 86.0, 57.0, 55.8, 42.1, 31.1. HRMS (HREI): Calcd $C_{17}H_{19}IO_2$ M^+: 382.0430; found 382.0447.

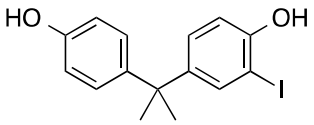

4-(2-(4-hydroxyphenyl)propan-2-yl)-2-iodophenol

This compound is known (CAS 88953-17-7) but was prepared by a different route. In a Schlenk tube with a magnetic stir bar that had been purged with nitrogen gas, 2-iodo-1-methoxy-4-(2-(4-methoxyphenyl)propan-2-yl)benzene (2.22 g; 5.79 mmol) was dissolved in dry dichloromethane (20 mL) and cooled to 0 °C. An excess of boron tribromide (2.19 mL; 23.2 mmol) was added drop-wise to the reaction mixture. The flask was sealed and stirred at 0 °C for 2 hrs. The solution was gently poured over 5 grams ice. The aqueous layer was washed with dichloromethane (3 X 20 mL), which was washed with pH 5 deionized water (2 X 25mL). The organic layer was dried over sodium sulfate, and the solvent was removed *in vacuo* yielding1.76 g (86%) of a colorless solid. ^{1}H NMR (CD_3CN, 400 MHz, 25°C) δ 7.2 (s, 1H), 7.07 (dd, J_1=8.3 Hz, J_2=2.3 Hz, 1H), 7.05 (d, J=8.6 Hz, 2H), 6.78 (d, J=8.4 Hz, 1H), 6.71 (s, 1H), 6.71 (d, J=8.6 Hz, 2H), 1.57 (s, 6H); ^{13}C NMR (CD_3CN, 100 MHz, 25°C) δ 155.7, 154.7, 146.0, 142.6, 138.0, 129.1, 128.6, 115.6, 115.4, 84.1, 42.1, 31.14. . HRMS (HREI): Calcd for $C_{15}H_{15}IO_2$ M^+: 354.0117, found 354.0126

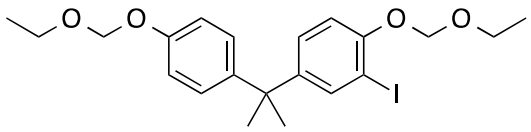

1-(ethoxymethoxy)-4-(2-(4-(ethoxymethoxy)phenyl)propan-2-yl)-2-iodobenzene

In an oven-dried 25 mL Schlenk storage tube purged with nitrogen, 4-(2-(4-hydroxyphenyl)propan-2-yl)-2-iodophenol (1.76 g; 4.96 mmol) was dissolved in dry THF (17 mL). Hunig's base (3.50 mL; 19.9 mmol) was added drop-wise to this solution, and the reaction mixture was stirred for 10 minutes and cooled to 0 °C followed by the drop-wise addition of chloromethyl ethyl ether (1.50 mL; 19.9 mmol). The tube was sealed and

transferred to an oil bath to react at 40 °C for 48 hrs. The solvent was removed *in vacuo,* and the product was extracted with dichloromethane (3 X 20 mL) from deionized water. The organic aliquots were combined and washed with an aqueous solution of $NaHCO_3$ (pH 8). The dichloromethane was dried over sodium sulfate, and the solvent was removed *in vacuo*. TLC was conducted in 10% ethyl acetate in hexanes, giving an R_f value of 0.52 for the desired product. The product was isolated by column chromatography (10:90; ethyl acetate: hexanes) yielding 1.88 g (80.7%) of a pale yellow oil. ^{1}H NMR (CD_3CN, 400 MHz, 25°C) δ 7.67 (d, J=2.4 Hz, 1H), 7.19 (dd, J_1=8.6 Hz, J_2= 2.3 Hz, 1H), 7.16 (d, J= 8.6 Hz, 2H), 6.99 (d, J=8.8 Hz, 1H), 6.94 (d, J=8.8 Hz, 2H), 5.23 (s, 2H), 5.18 (s, 2H), 3.72 (q, J=7.0, 2H), 3.69 (q, J=7.0, 2H), 1.61 (s, 6H), 1.17 (t, J=7.0, 6H); ^{13}C (CD_3CN, 100 MHz, 25°C) δ 156.2, 154.8, 147.2, 144.1, 138.2, 128.8, 128.4, 116.6, 115.3, 94.56, 93.86, 87.66, 65.35, 64.77, 42.22, 31.19, 15.62, 15.66. HRMS (ESI): calcd for $C_{21}H_{27}IO_4$ $[M+Na]^+$: 493.0852, found 493.0834.

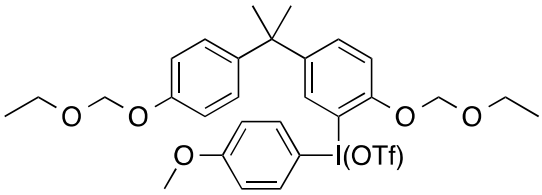

(2-(ethoxymethoxy)-5-(2-(4-(ethoxymethoxy)phenyl)propan-2-yl)phenyl)(4-methoxyphenyl)-λ^3-iodanyl trifluoromethanesulfonate

In an N_2 charged glove box, in an oven-dried 100 mL Schlenk tube, 1-(ethoxymethoxy)-4-(2-(4-(ethoxymethoxy)phenyl)propan-2-yl)-2-iodobenzene (1.80 g; 3.82 mmol) was dissolved in 40 mL of dry CH_3CN. 1-(chloromethyl)-1,4-diazabicyclo[2.2.2]octan-1-ium hexafluorophosphate(V), (0.58 g; 1.91 mmol) was added to the reaction flask. In a separate vial, Selectfluor® (1.76 g; 4.97 mmol) was dissolved in 20 mL of dry CH_3CN,

followed by the addition of trimethylsilyl acetate (1.50 mL; 9.95 mmol) in a drop-wise fashion. This mixture was shaken for 3-5 mins and slowly added to the reaction flask. The flask was sealed and allowed to stir at RT for 21 hrs. Potassium trifluoro(4-methoxyphenyl)borate (0.64 g; 2.97 mmol) was dissolved in a small amount of dry CH_3CN followed by trimethylsilyl trifluoroacetate (0.33 mL; 1.93 mmol) diluted in 10 mL of dry CH_3CN was added to the reaction flask. This mixture was stirred at RT for 12 hrs. The solvent was evaporated, leaving behind ~5-10 mL of CH_3CN, which was poured into an aqueous solution of sodium acetate (basic pH). The product was extracted from the aqueous layer with dichloromethane (3 X 30 mL). The organic aliquots were combined and washed with deionized water (1 X 50 mL). The water layer was washed with dichloromethane again (2 X 30 mL). The organic aliquots were combined and dried over sodium sulfate. The solvent was removed *in vacuo*, yielding a brown, viscous oil, which was dissolved in hexanes (2 X 100 mL) and subjected to sonication. The hexanes solution was poured off of the oil. The oil was treated with methyl-tert-butyl ether with sonication. The solution was poured off and placed under high dynamic vacuum. This produced a tan colored foam. The solid was dissolved in a minimal amount of acetonitrile and transferred to a 1M solution of sodium trifluoromethane sulfonate (30 mL). This mixture stirred for 30 mins, and extracted with dichloromethane (3 X 30 mL), dried over sodium sulfate, gravity filtered, and then the solvent was removed under reduced pressure. To insure that all trifluoroacetate ions were exchanged with triflate ions, the orange product was passed through an ion exchange resin. The ion exchange column was loaded with Amberlite IRA-450 (Cl) and a mixture of acetonitrile/water (8:2 by volume). The solution was allowed to drain slowly. A 1.0 M solution (100 mL) of sodium triflate

was passed through the ion exchange resin very slowly (~1 drop/15 sec). Dry 1-((2-(ethoxymethoxy)-5-(2-(4-(ethoxymethoxy)phenyl)propan-2-yl)phenyl)(4-methoxyphenyl)-λ^3-iodanyl)-2,2,2-trifluoroethan-1-one was dissolved in a solution of acetonitrile and water (8:2 by volume) and loaded onto the ion exchange resin. The solution was passed through the column very slowly at a rate of approximately 1 drop/ 30 seconds and collected. The (2-(ethoxymethoxy)-5-(2-(4-(ethoxymethoxy)phenyl)propan-2-yl)phenyl)(4-methoxyphenyl)-λ^3-iodanyl trifluoromethanesulfonate solution was dried under reduced pressure overnight. The product was 1.48 g of a tan solid that was found in 95 % purity (41 % yield). ^{1}H NMR (CD_3CN, 300 MHz, 25°C) δ 7.92 (d, J=9.2 Hz, 2H), 7.69 (d, J=2.2 Hz, 1H), 7.47 (dd, J_1=8.6 Hz, J_2=2.2 Hz, 1H), 7.23 (d, J=8.6 Hz, 1H), 7.09 (d, J_1=8.9 Hz, 2H), 7.01 (d, J_1=9.1 Hz, 2H), 6.92 (d, J_1=8.8 Hz, 2H), 5.35 (s, 2H), 5.20 (s, 2H), 3.85 (s, 3H), 3.68 (q, J_1=7.1 Hz, 2H), 3.62 (q, J_1=7.1 Hz, 2H), 1.62 (s, 6H), 1.16 (t, J_1=7.0 Hz, 3H), 1.11 (t, J_1=7.0 Hz, 3H); ^{13}C NMR (CD_3CN, 75 MHz, 25°C) δ 164.3, 156.6, 153.5, 149.1, 143.6, 139.0, 134.9, 134.3, 128.7, 119.0, 116.9, 116.1, 105.3, 100.9, 95.2, 94.0, 66.1, 65.0, 56.8, 43.1, 30.8, 15.5, 15.4; ^{19}F NMR (CD_3CN, 282 MHz, 25°C) -79.3; HRMS (LR-FAB): calcd for $C_{29}H_{34}IO_8S$ $[M\text{-}OTf]^+$: 577.1451, found 577.1448

APPENDIX A: List of NMR Spectra

^{1}H NMR Spectrum of 4-iodophthalic acid

^{13}C NMR Spectrum of 4-iodophthalic acid

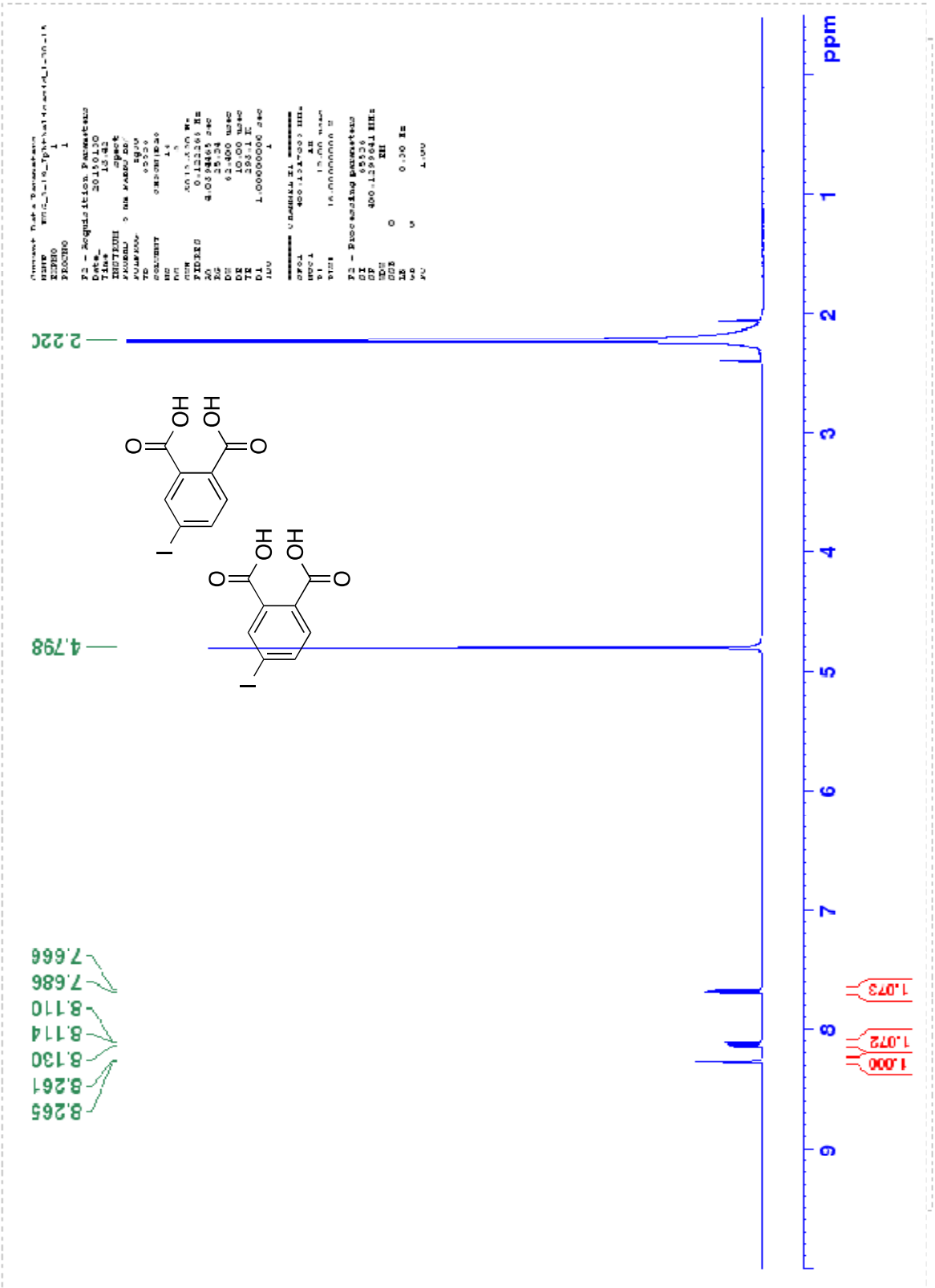

^{1}H NMR Spectrum of diethyl-4-iodophthalate

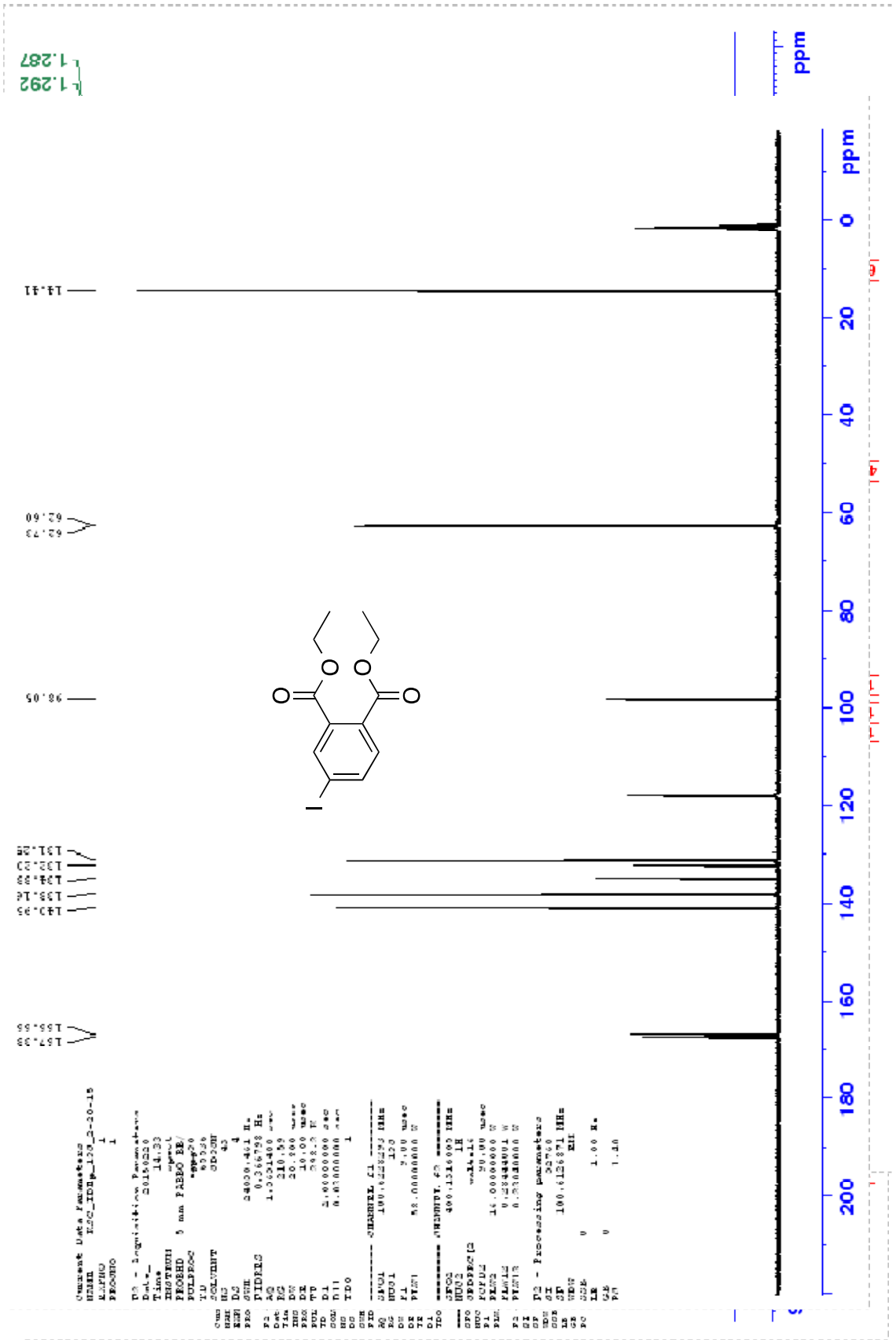

^{13}C NMR Spectrum of diethyl 4-((4-methoxyphenyl)(((trifluoromethyl)sulfonyl)oxy)-λ^3-iodanyl)phthalate

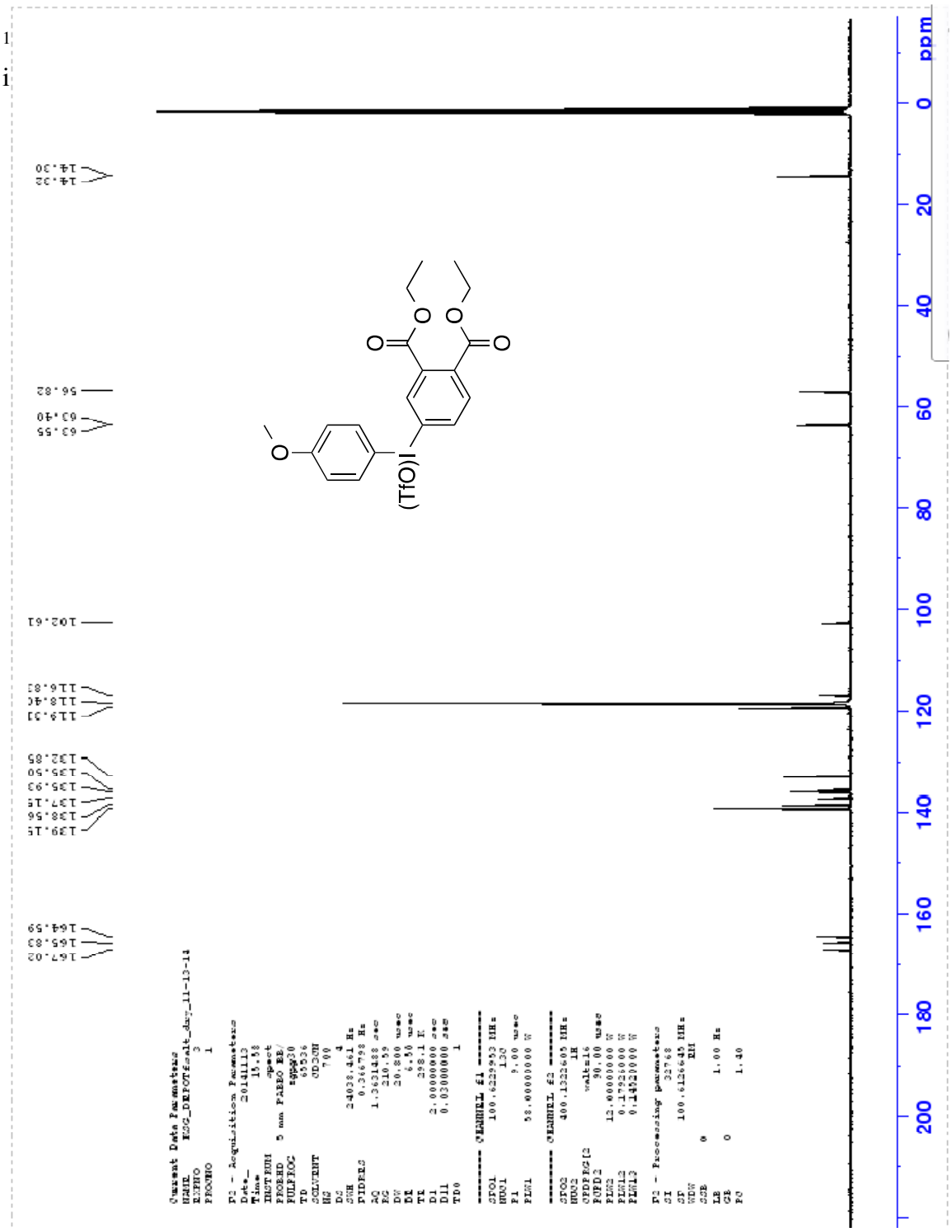

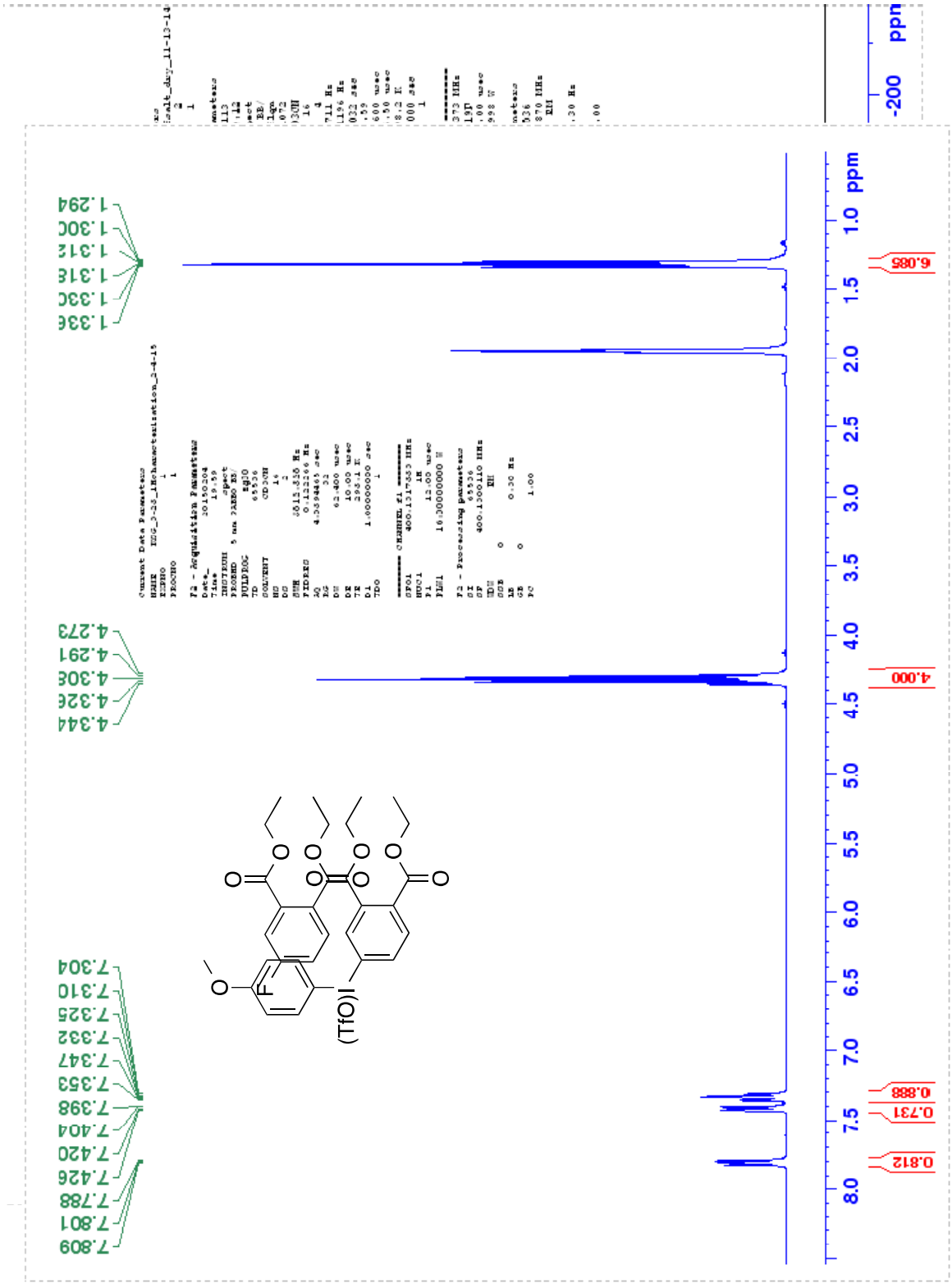

^{13}C NMR Spectrum of diethyl 4-fluorophthalate

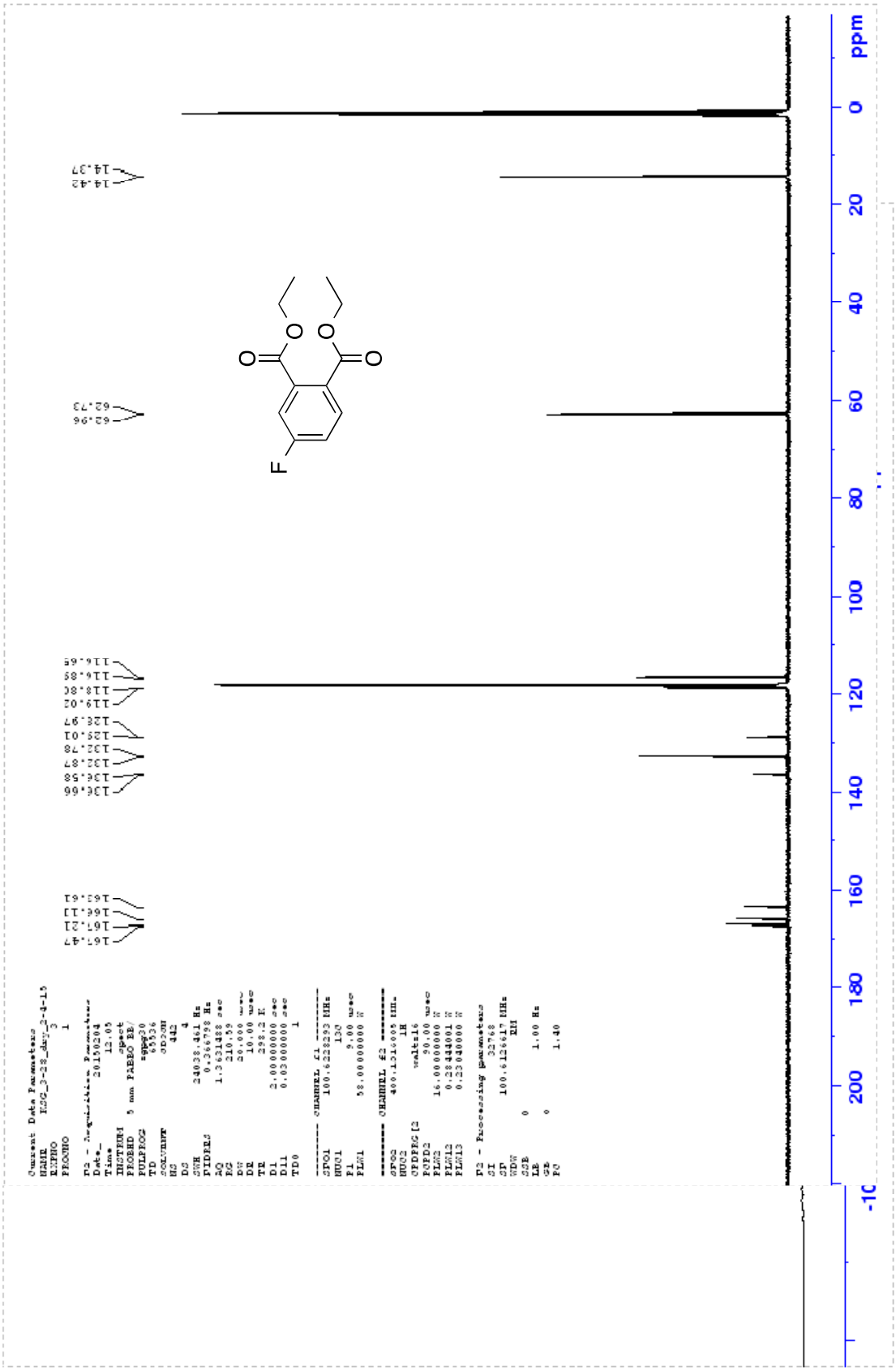
ppm
0
20
40
60
80
100
120
140
160
180
200
-10
14.42
14.37
62.96
62.73
136.66
136.58
132.87
132.78
129.01
128.97
119.02
118.80
116.89
116.65
167.47
167.21
166.13
163.61
F
O
O
O
O

^{1}H NMR Spectrum of bis(2-ethylhexyl) 4-iodophthalate

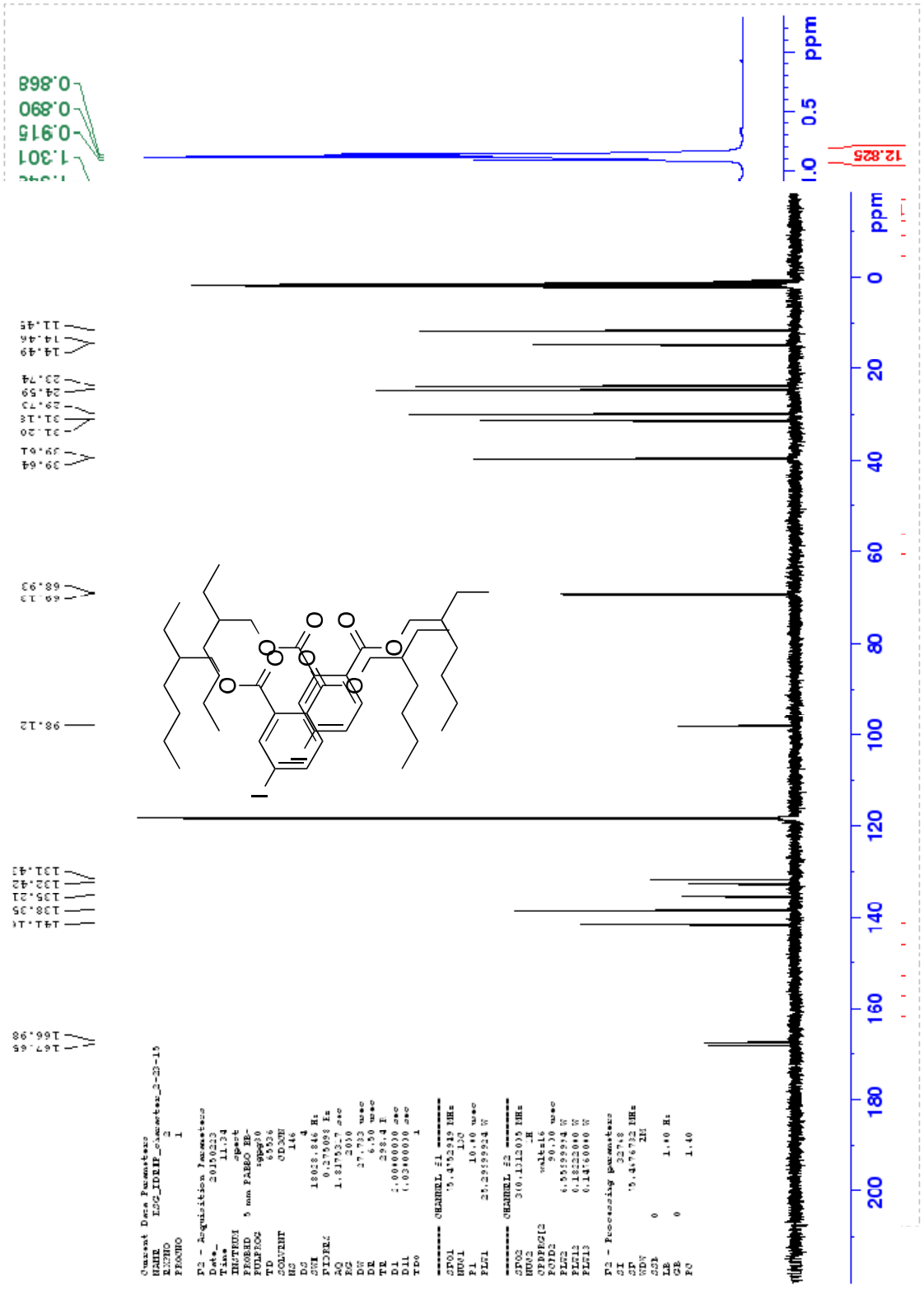

^{1}H NMR Spectrum of bis(2-ethylhexyl) 4-iodosylphthalate compound with 1-methoxy-4-((trifluoromethyl)sulfonyl)benzene (1:1)

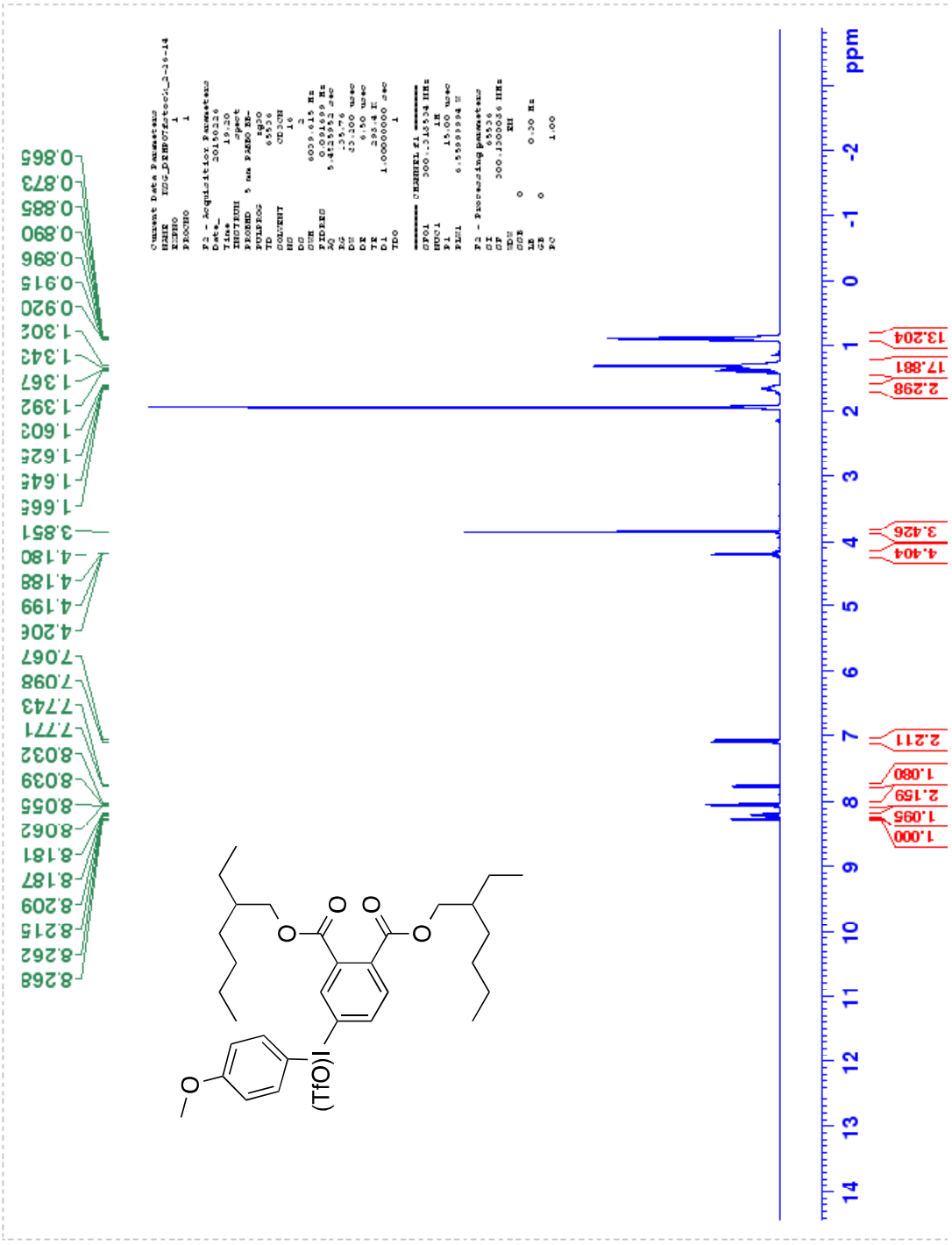

^{13}C NMR Spectrum of bis(2-ethylhexyl) 4-iodosylphthalate compound with 1-methoxy-4-((trifluoromethyl)sulfonyl)benzene (1:1)

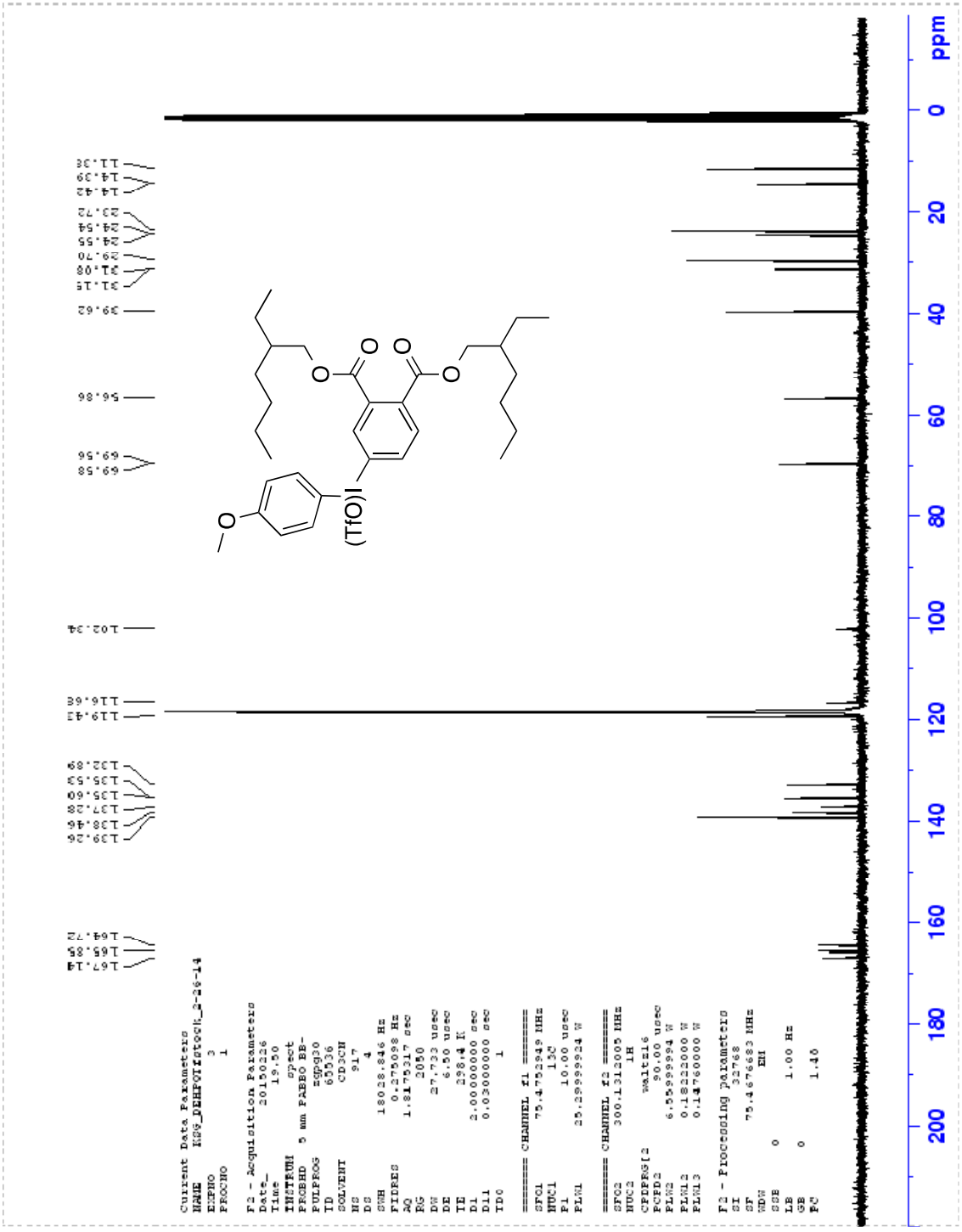

^{19}F NMR Spectrum of bis(2-ethylhexyl) 4-iodosylphthalate compound with 1-methoxy-4-((trifluoromethyl)sulfonyl)benzene (1:1)

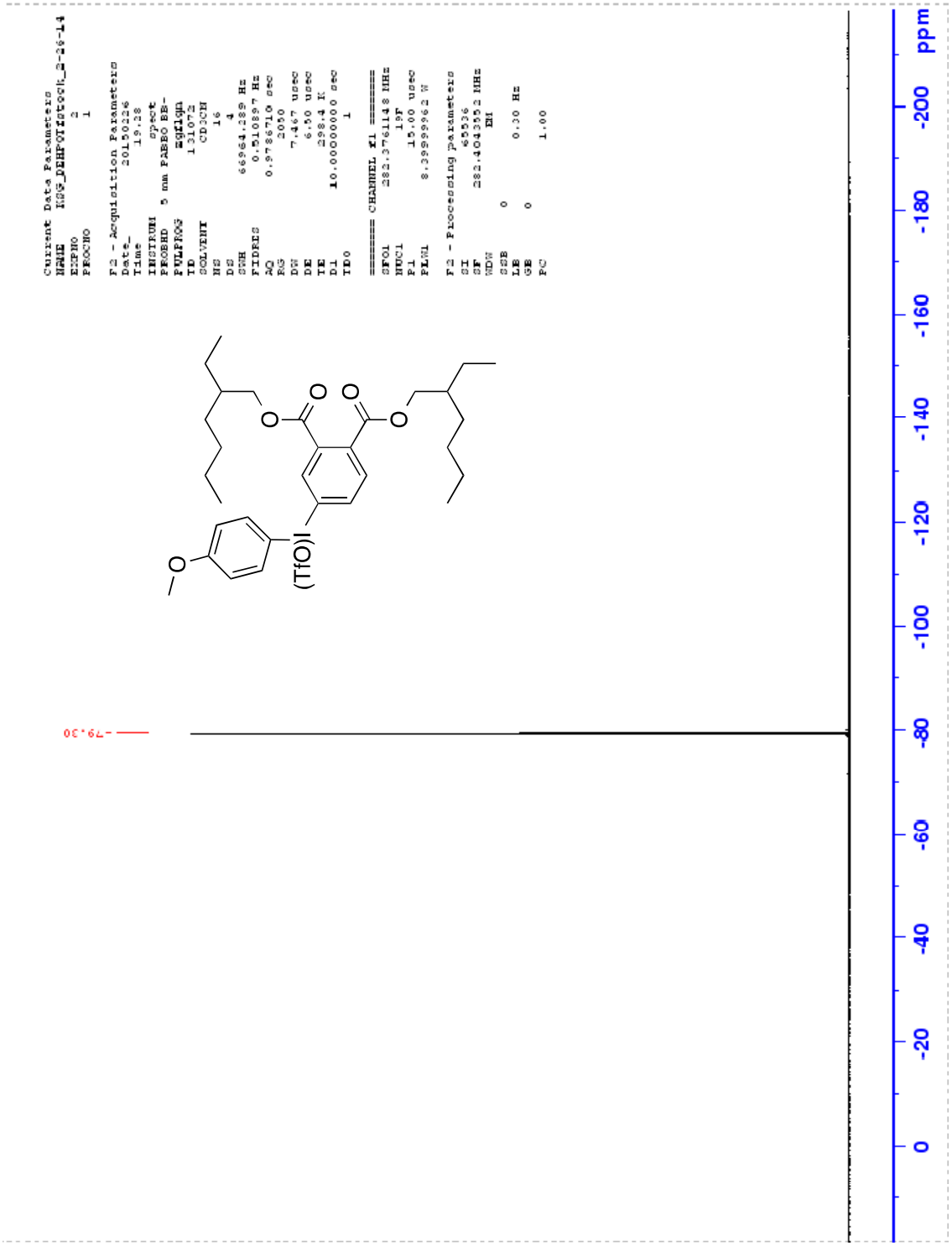

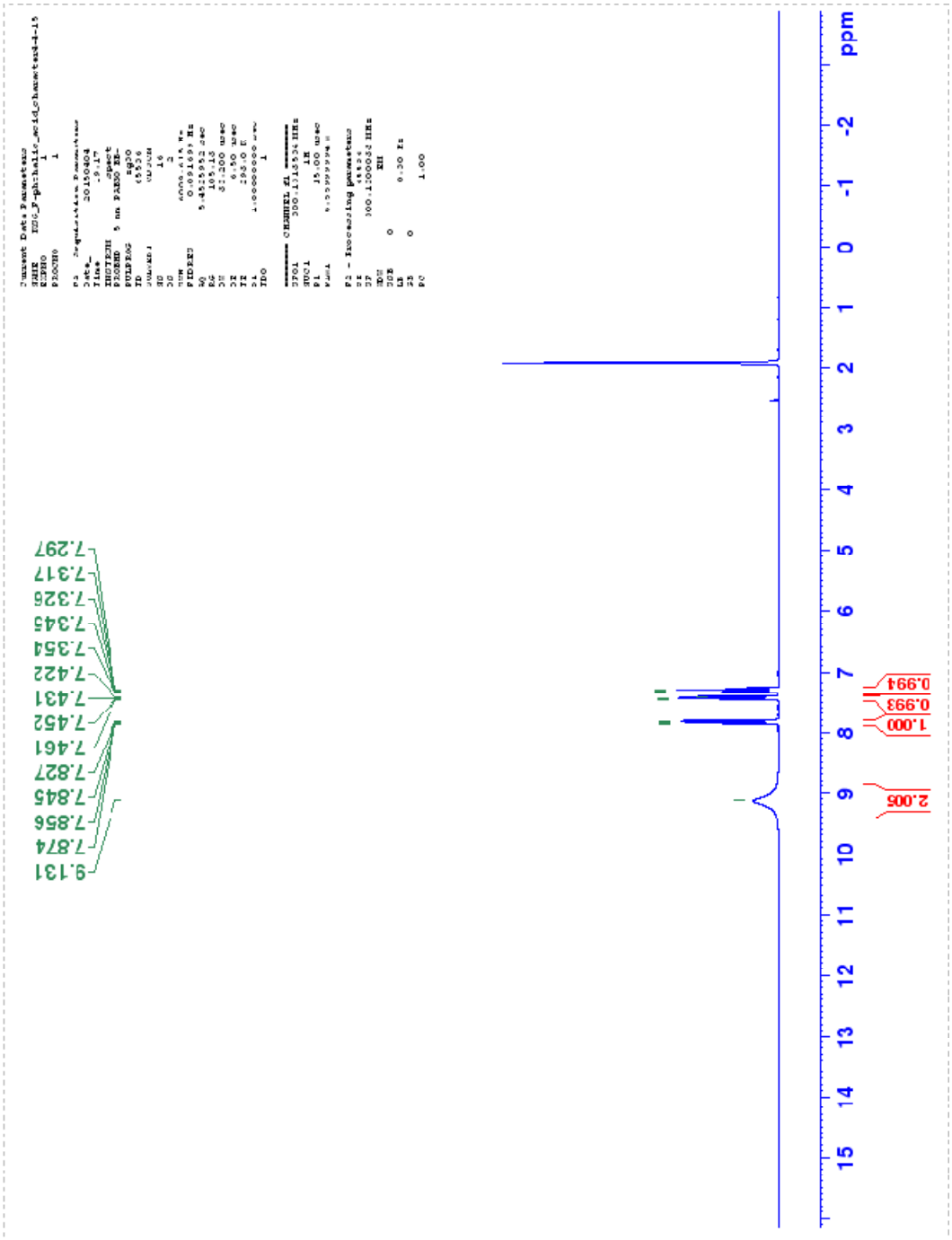
ppm
15
14
13
12
11
10
9
8
7
6
5
4
3
2
1
0
-1
-2
2.005
1.000
0.993
0.994
9.131
7.874
7.856
7.845
7.827
7.461
7.452
7.431
7.422
7.354
7.345
7.326
7.317
7.297

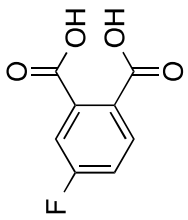

^{13}C NMR Spectrum of 4-fluorophthalic acid

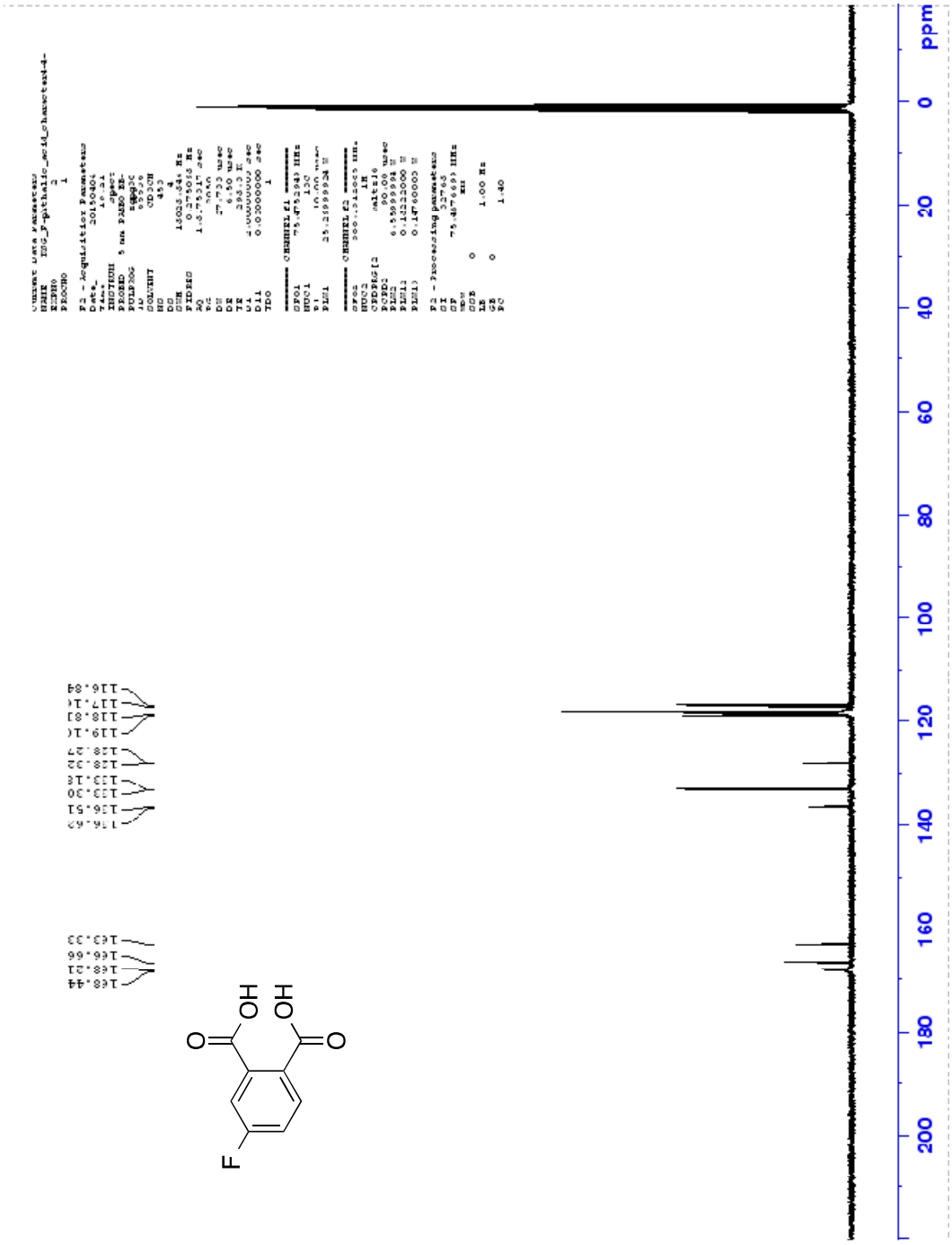
ppm
0
20
40
60
80
100
120
140
160
180
200
OH
OH
O
O
F

^{19}F NMR Spectrum of 4-fluorophthalic acid

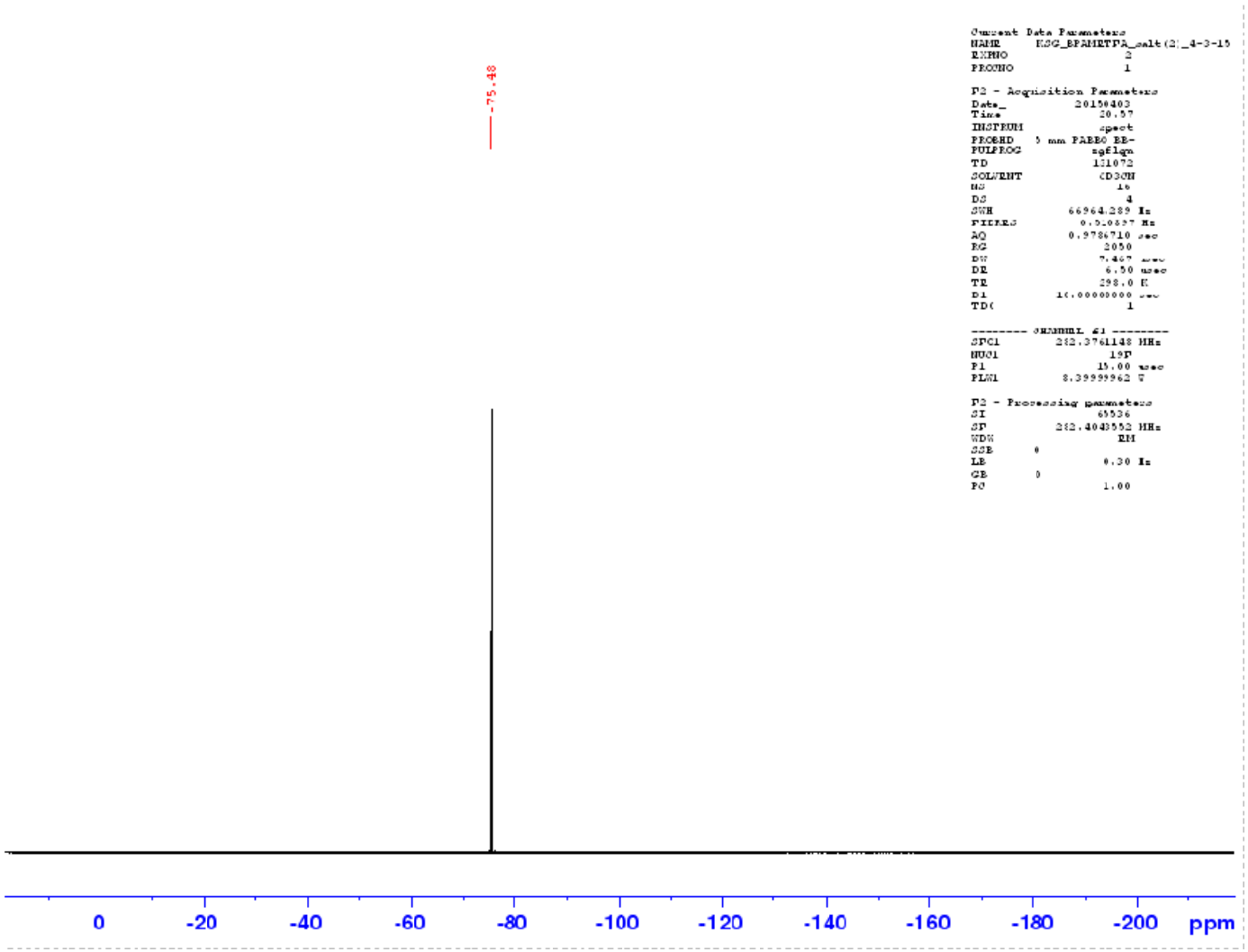

Current Data Parameters
NAME KSG_BPAMETPA_salt(2)_4-3-15
EXPNO 2
PROCNO 1

F2 - Acquisition Parameters
Date_ 20150403
Time 20.57
INSTRUM spect
PROBHD 5 mm PABBO BB-
PULPROG zgflqn
TD 131072
SOLVENT CD3CN
NS 16
DS 4
SWH 66964.289 Hz
FIDRES 0.510837 Hz
AQ 0.9786710 sec
RG 2050
DW 7.467 usec
DE 6.50 usec
TE 298.0 K
D1 10.00000000 sec
TD0 1

======== CHANNEL f1 ========
SFO1 282.3761148 MHz
NUC1 19F
P1 15.00 usec
PLW1 8.39999962 W

F2 - Processing parameters
SI 65536
SF 282.4043552 MHz
WDW EM
SSB 0
LB 0.30 Hz
GB 0
PC 1.00

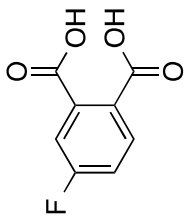

^{1}H NMR Spectrum of bis(2-ethylhexyl) 4-fluorophthalate

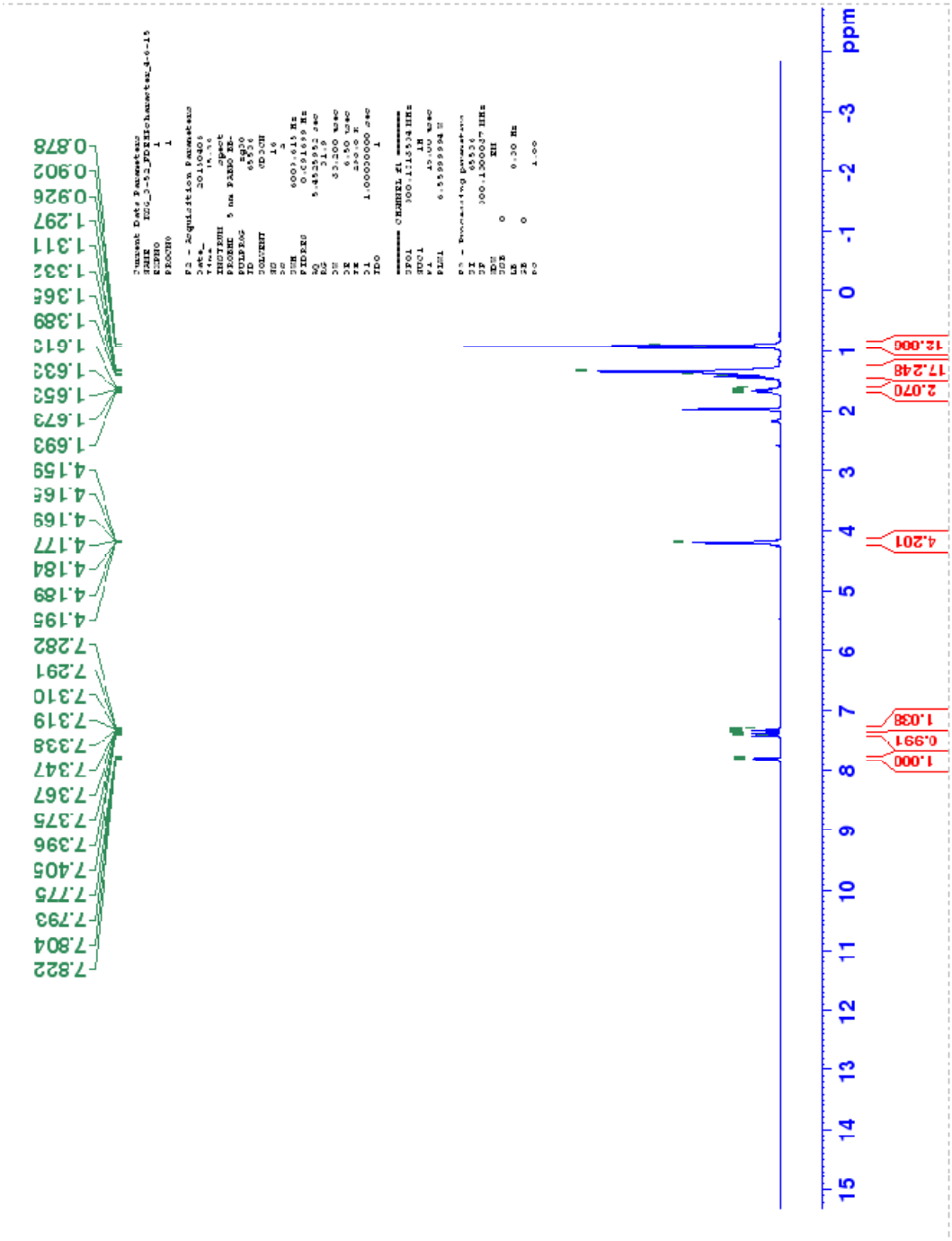
0.878
0.902
0.926
1.297
1.311
1.332
1.365
1.389
1.612
1.632
1.652
1.673
1.693
4.159
4.165
4.169
4.177
4.184
4.189
4.195
7.282
7.291
7.310
7.319
7.338
7.347
7.367
7.375
7.396
7.405
7.775
7.793
7.804
7.822
ppm
12.000
17.248
2.070
4.201
1.038
0.991
1.000

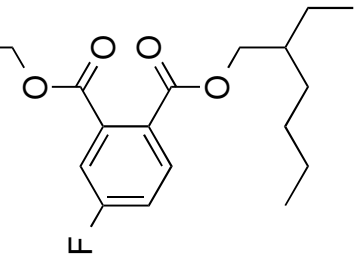

^{13}C NMR Spectrum of bis(2-ethylhexyl) 4-fluorophthalate

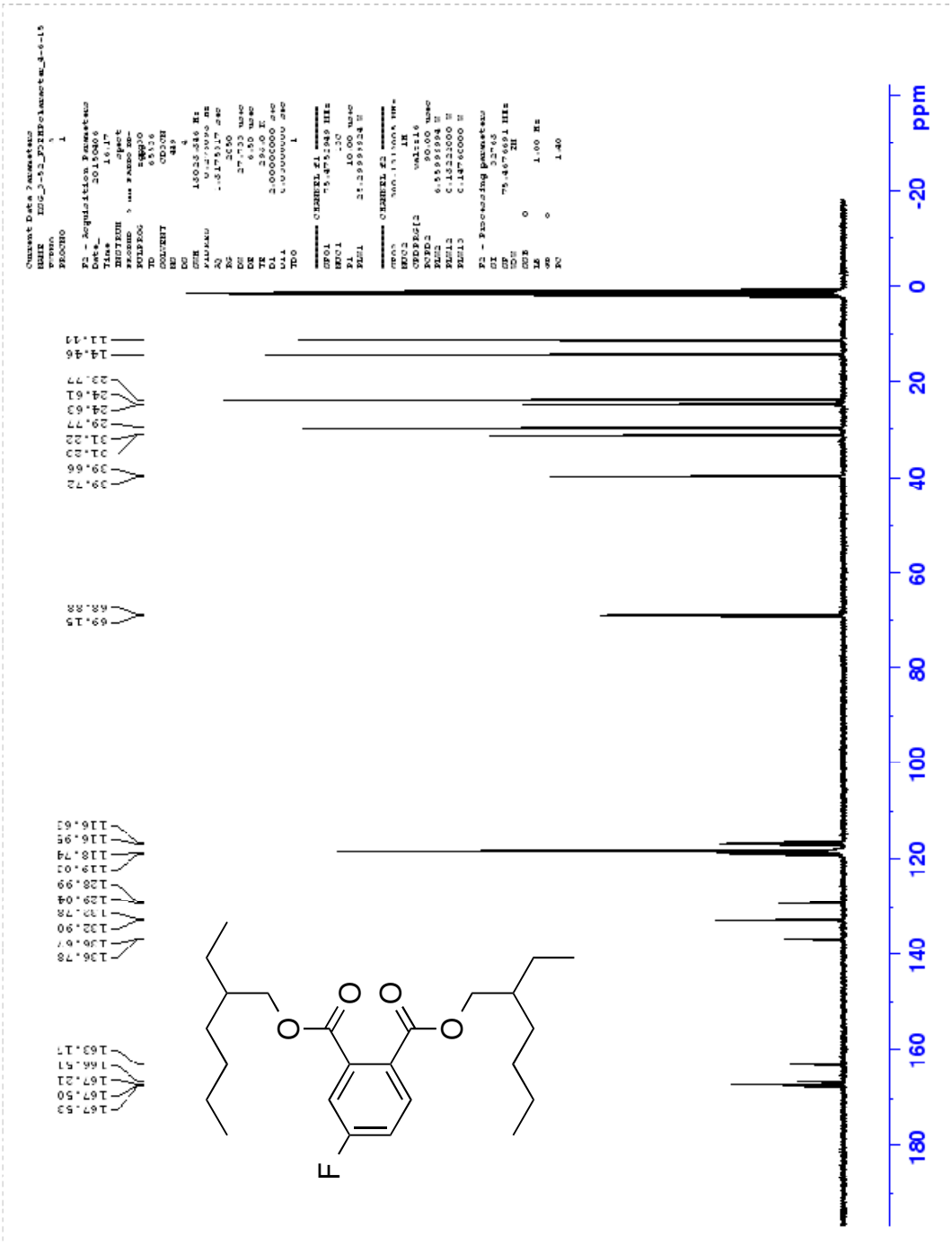
11.44
14.46
23.77
24.61
24.63
29.77
31.22
31.83
39.66
39.72
68.88
69.19
116.61
116.95
118.74
119.03
128.99
129.04
133.78
133.90
136.67
136.78
163.17
166.51
167.21
167.50
167.53
F
O
O
O
O
ppm
180
160
140
120
100
80
60
40
20
0
-20

^{19}F NMR Spectrum of bis(2-ethylhexyl) 4-fluorophthalate

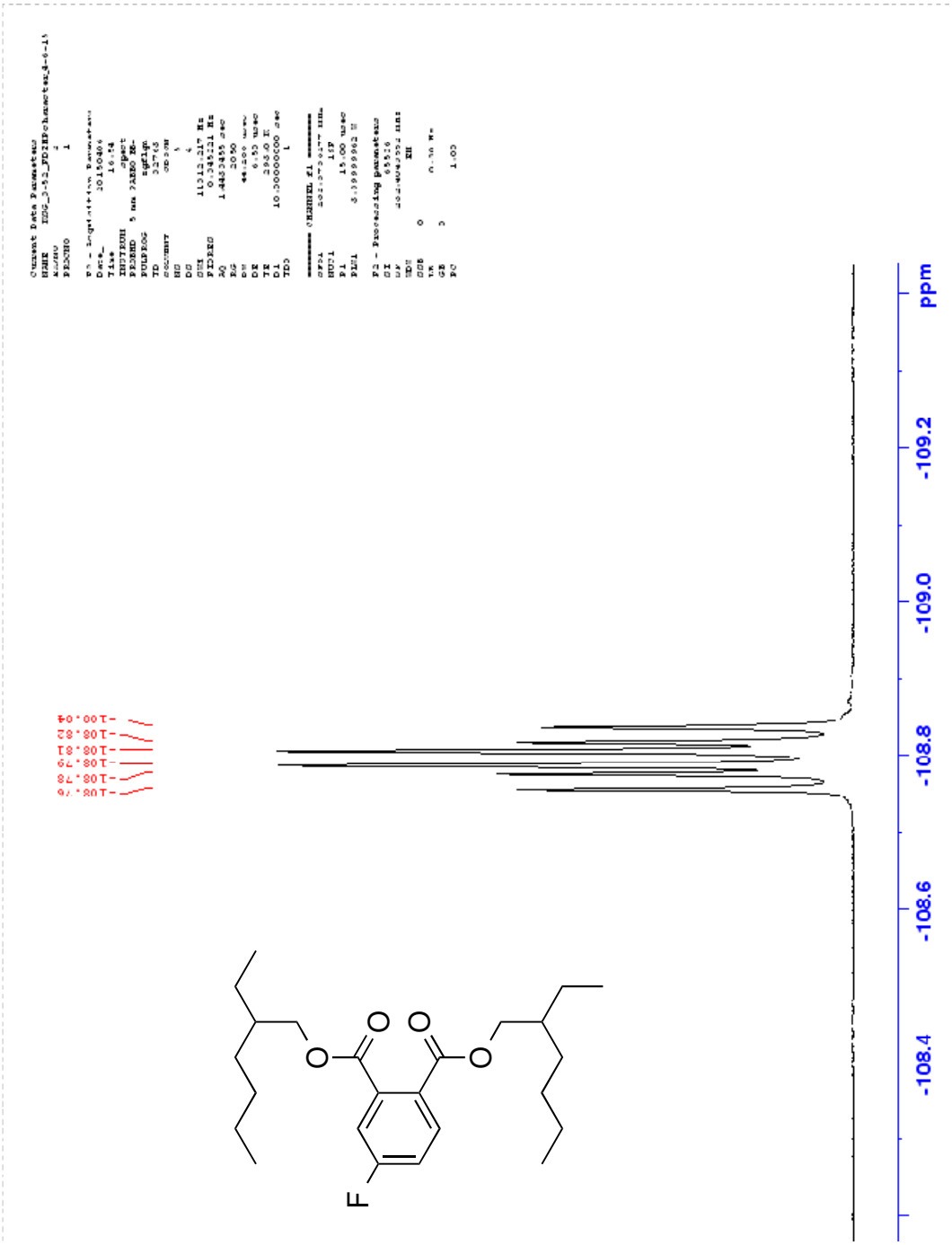
-108.76
-108.78
-108.79
-108.81
-108.82
-108.84
-108.4
-108.6
-108.8
-109.0
-109.2
ppm
F

^{1}H NMR Spectrum of 4,4'-(propane-2,2-diyl)bis(methoxybenzene)

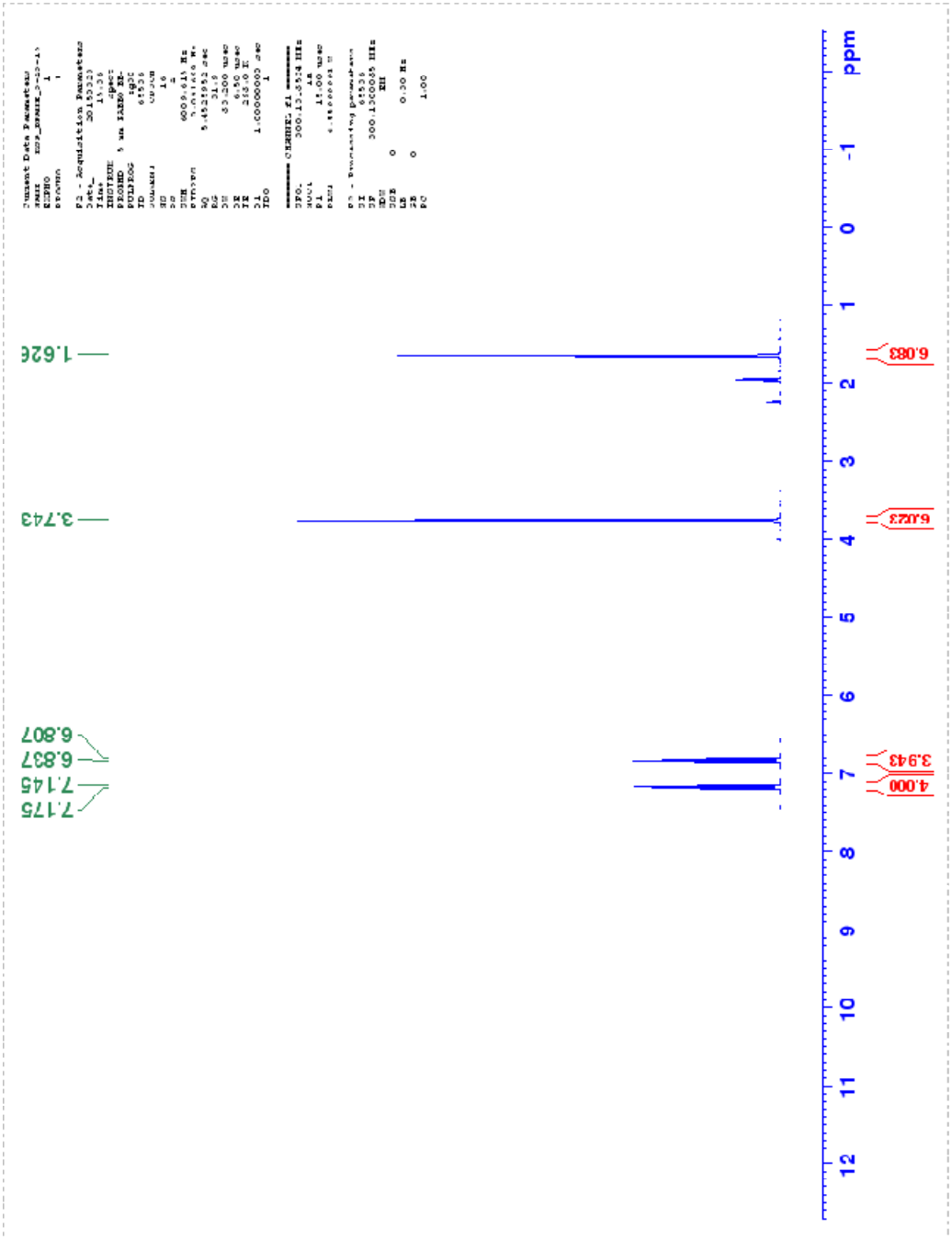
1.626
3.743
6.807
6.837
7.145
7.175
6.083
6.023
3.943
4.000
ppm

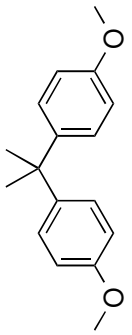

^{13}C NMR Spectrum of 4,4'-(propane-2,2-diyl)bis(methoxybenzene)

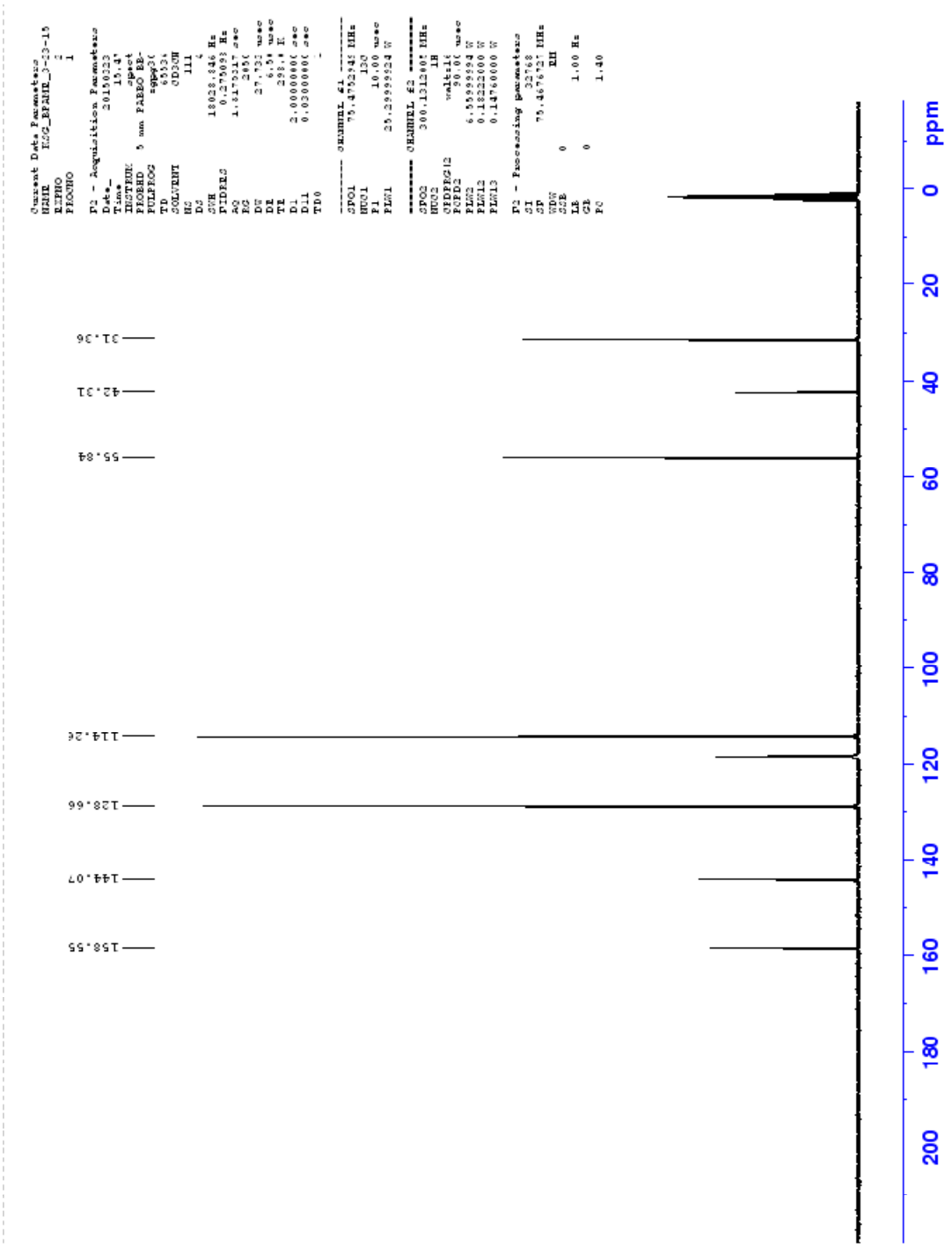
31.36
42.31
55.84
114.26
128.66
144.07
158.55
0
20
40
60
80
100
120
140
160
180
200
ppm

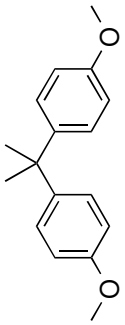

^{1}H NMR Spectrum of 2,2,2-trifluoro-1-((2-methoxy-5-(2-(4-methoxyphenyl)propan-2-yl)phenyl)(4-methoxyphenyl)-λ^{3}-iodanyl)ethan-1-one

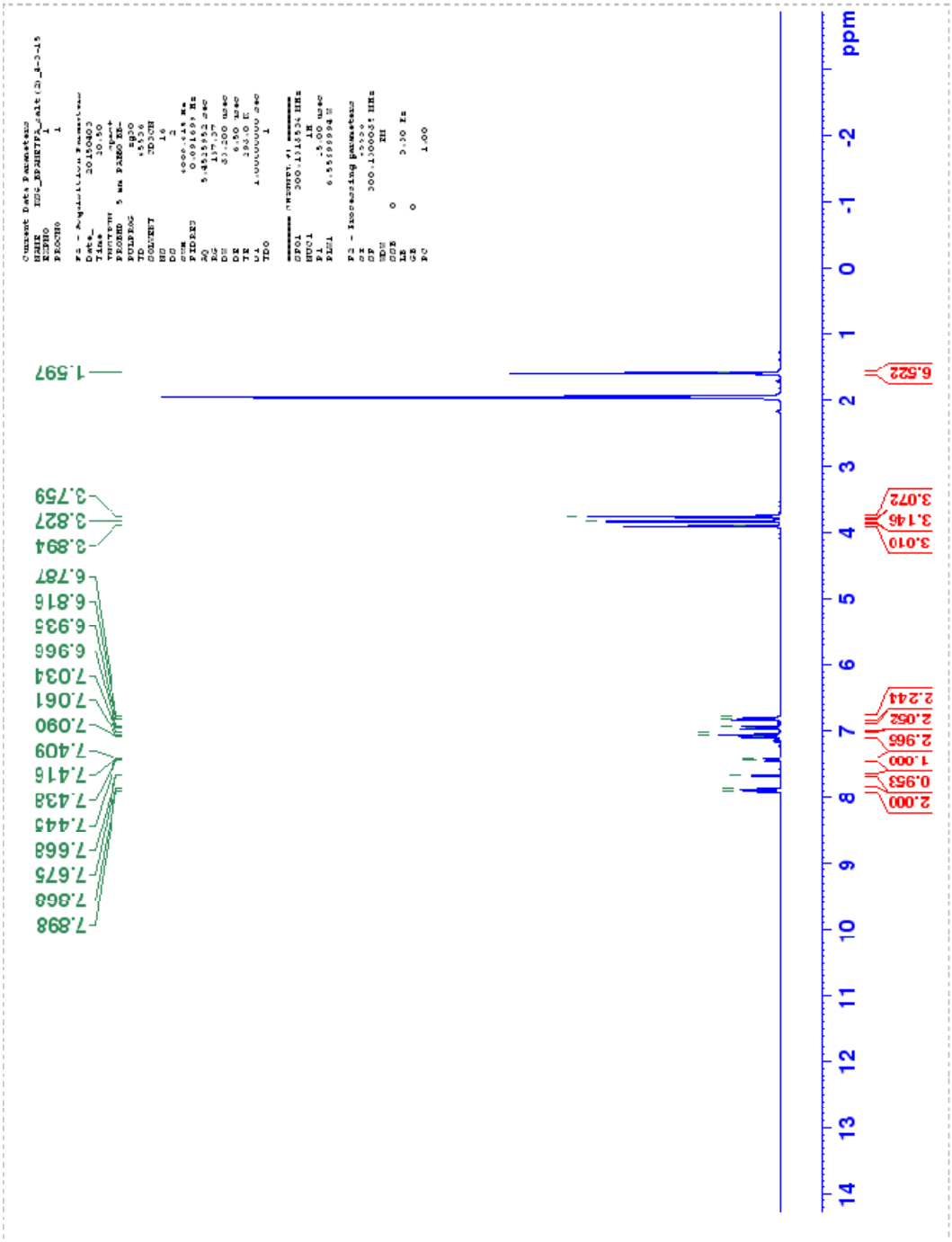
1.597
3.759
3.827
3.894
6.787
6.816
6.935
6.966
7.034
7.061
7.090
7.409
7.416
7.438
7.443
7.668
7.675
7.868
7.898
6.522
3.072
3.146
3.010
2.244
2.062
2.965
1.000
0.953
2.000
ppm

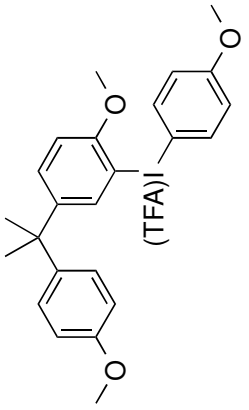

^{13}C NMR Spectrum of 2,2,2-trifluoro-1-((2-methoxy-5-(2-(4-methoxyphenyl)propan-2-yl)phenyl)(4-methoxyphenyl)-□^{3}-iodanyl)ethan-1-one

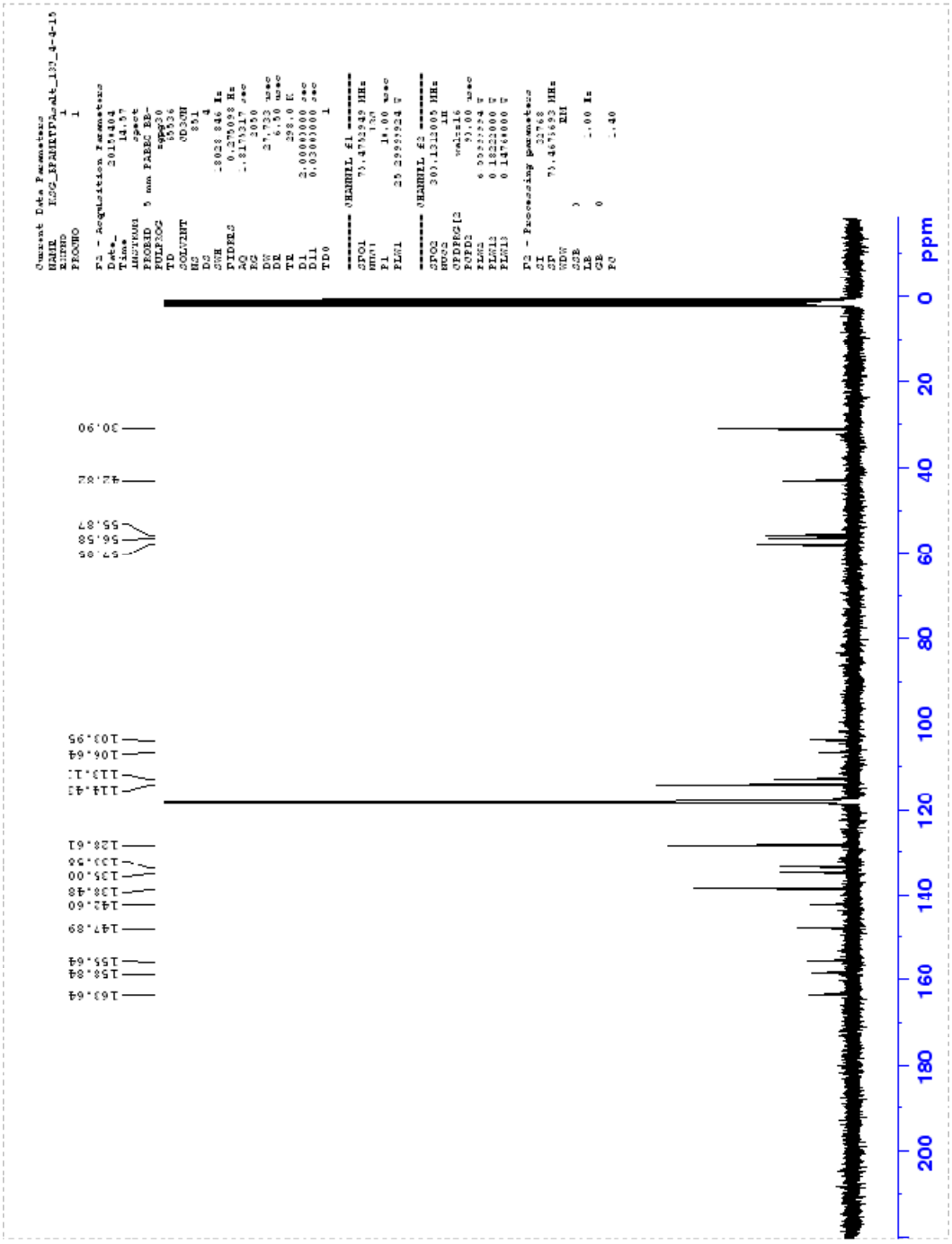
30.90
42.82
55.87
56.58
57.95
103.95
106.64
113.11
114.43
128.61
133.76
135.00
138.48
142.60
147.89
155.64
158.84
163.64
0
20
40
60
80
100
120
140
160
180
200
ppm

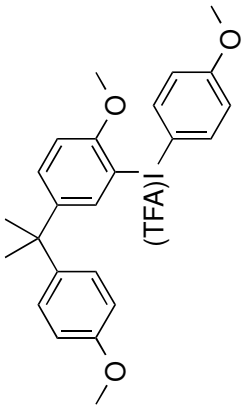

^{19}F NMR Spectrum of 2,2,2-trifluoro-1-((2-methoxy-5-(2-(4-methoxyphenyl)propan-2-yl)phenyl)(4-methoxyphenyl)-λ^3-iodanyl)ethan-1-one

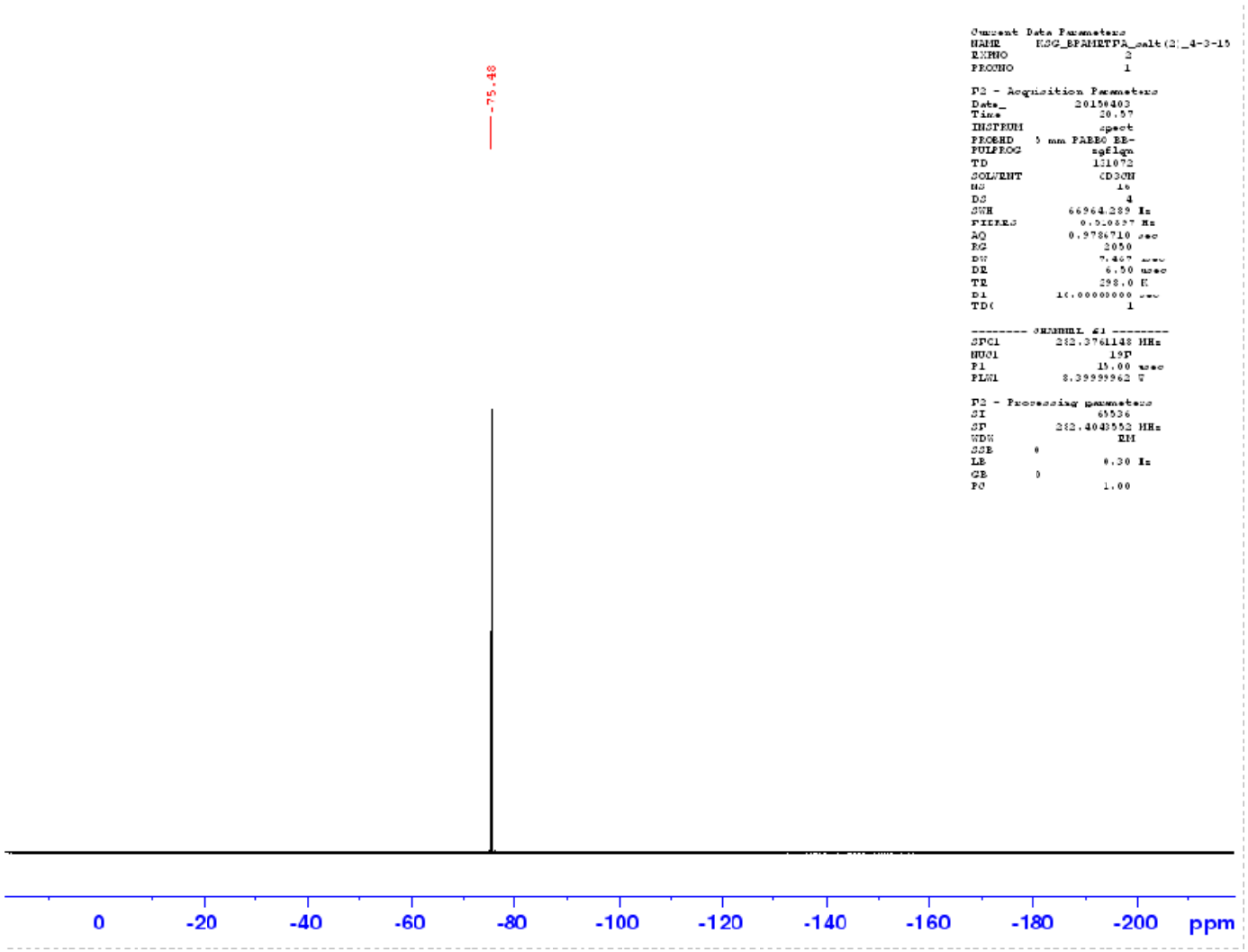
-75.48
Current Data Parameters
NAME KSG_BPAMRTFA_salt(2)_4-3-15
EXPNO 2
PROCNO 1
F2 - Acquisition Parameters
Date_ 20150403
Time 20.57
INSTRUM spect
PROBHD 5 mm PABBO BB-
PULPROG zgflqn
TD 131072
SOLVENT CD3CN
NS 16
DS 4
SWH 66964.289 Hz
FIDRES 0.510837 Hz
AQ 0.9786710 sec
RG 2050
DW 7.467 usec
DE 6.50 usec
TE 298.0 K
D1 10.00000000 sec
TD0 1
-------- CHANNEL f1 --------
SFO1 282.3761148 MHz
NUC1 19F
P1 15.00 usec
PLW1 8.39999962 W
F2 - Processing parameters
SI 65536
SF 282.4043552 MHz
WDW EM
SSB 0
LB 0.30 Hz
GB 0
PC 1.00
0
-20
-40
-60
-80
-100
-120
-140
-160
-180
-200
ppm

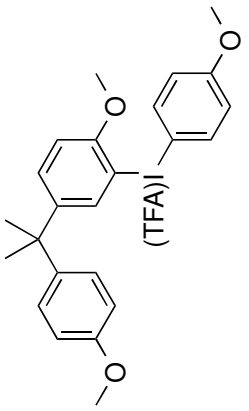

^{1}H NMR Spectrum of 2-iodo-1-methoxy-4-(2-(4-methoxyphenyl)propan-2-yl)benzene

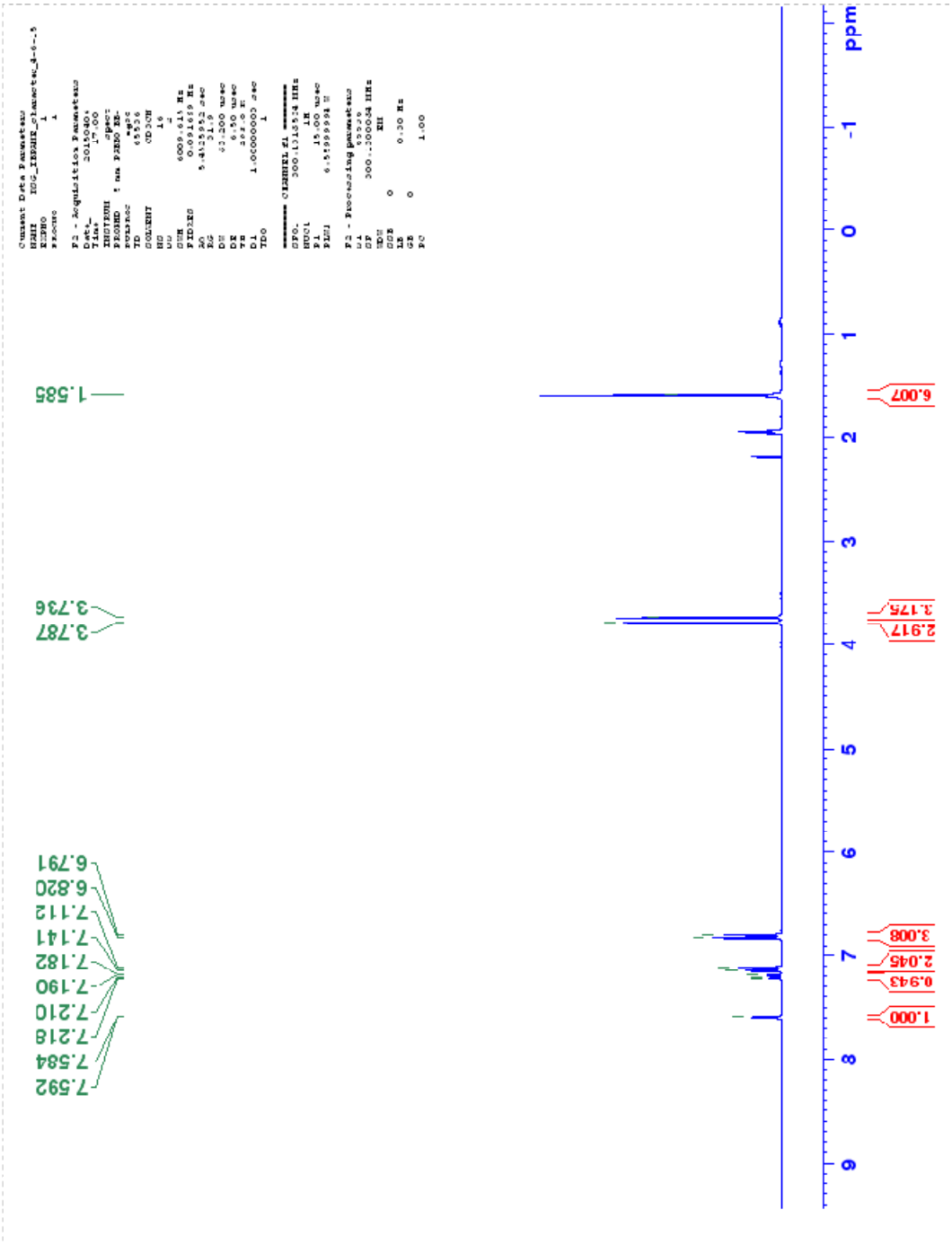
ppm
9
8
7
6
5
4
3
2
1
0
-1
1.585
3.736
3.787
7.592
7.584
7.218
7.210
7.190
7.182
7.141
7.112
6.820
6.791
6.007
3.175
2.917
3.008
2.045
0.943
1.000

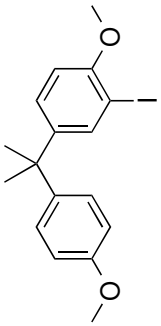

^{13}C NMR Spectrum of 2-iodo-1-methoxy-4-(2-(4-methoxyphenyl)propan-2-yl)benzene

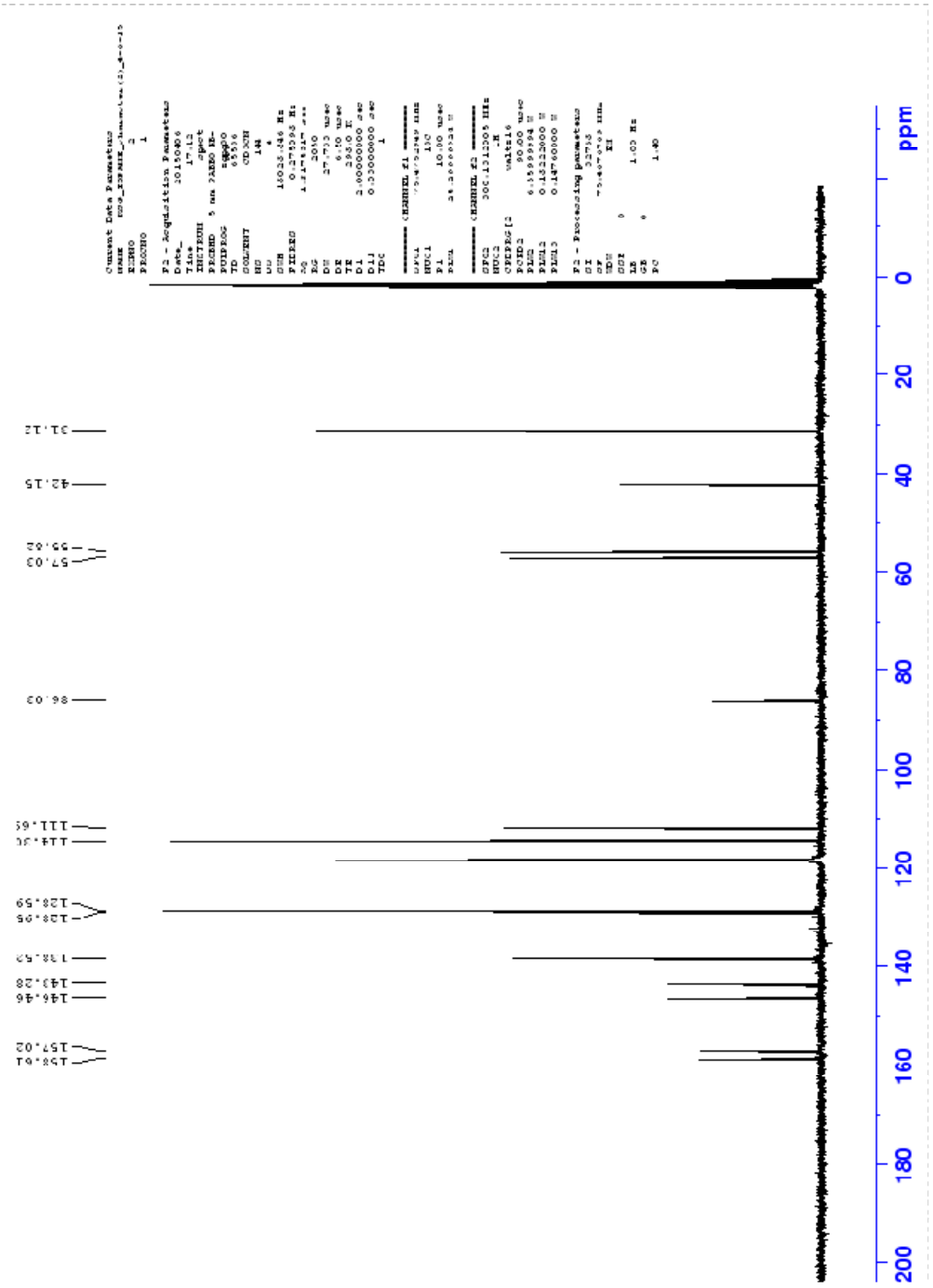
31.12
42.15
57.03
59.62
86.03
111.65
114.35
128.59
128.95
138.53
143.28
146.46
157.02
158.64
ppm
0
20
40
60
80
100
120
140
160
180
200

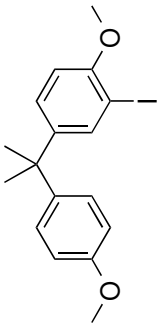

^{1}H NMR Spectrum of 4-(2-(4-hydroxyphenyl)propan-2-yl)-2-iodophenol

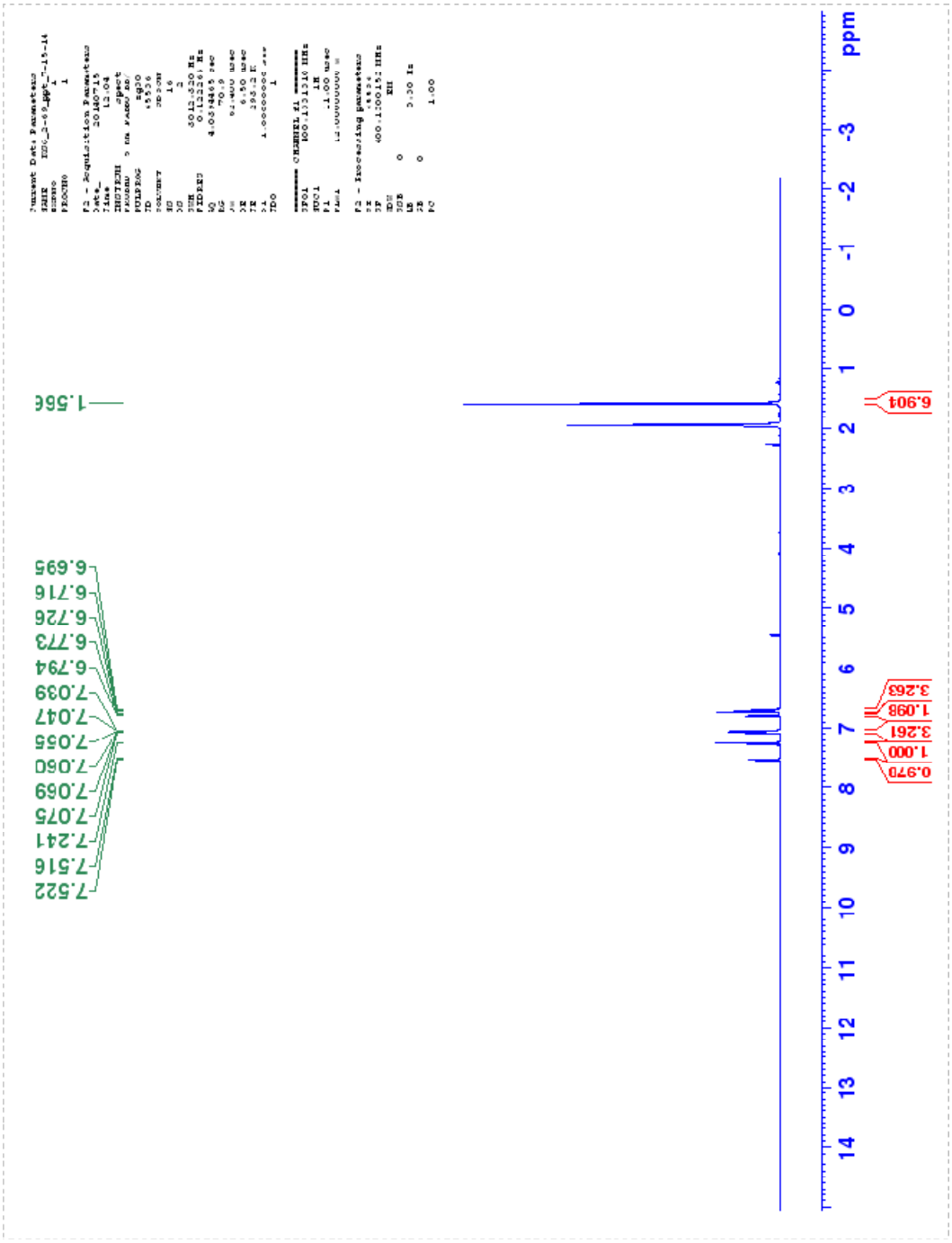
ppm
6.904
0.970
1.000
3.261
1.098
3.263
1.566
6.695
6.716
6.726
6.773
6.794
7.039
7.047
7.055
7.060
7.069
7.075
7.241
7.516
7.522

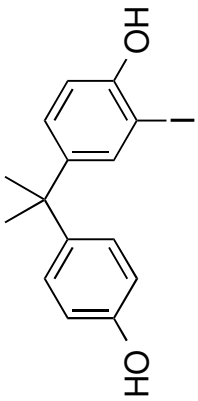

^{13}C NMR Spectrum of 4-(2-(4-hydroxyphenyl)propan-2-yl)-2-iodophenol

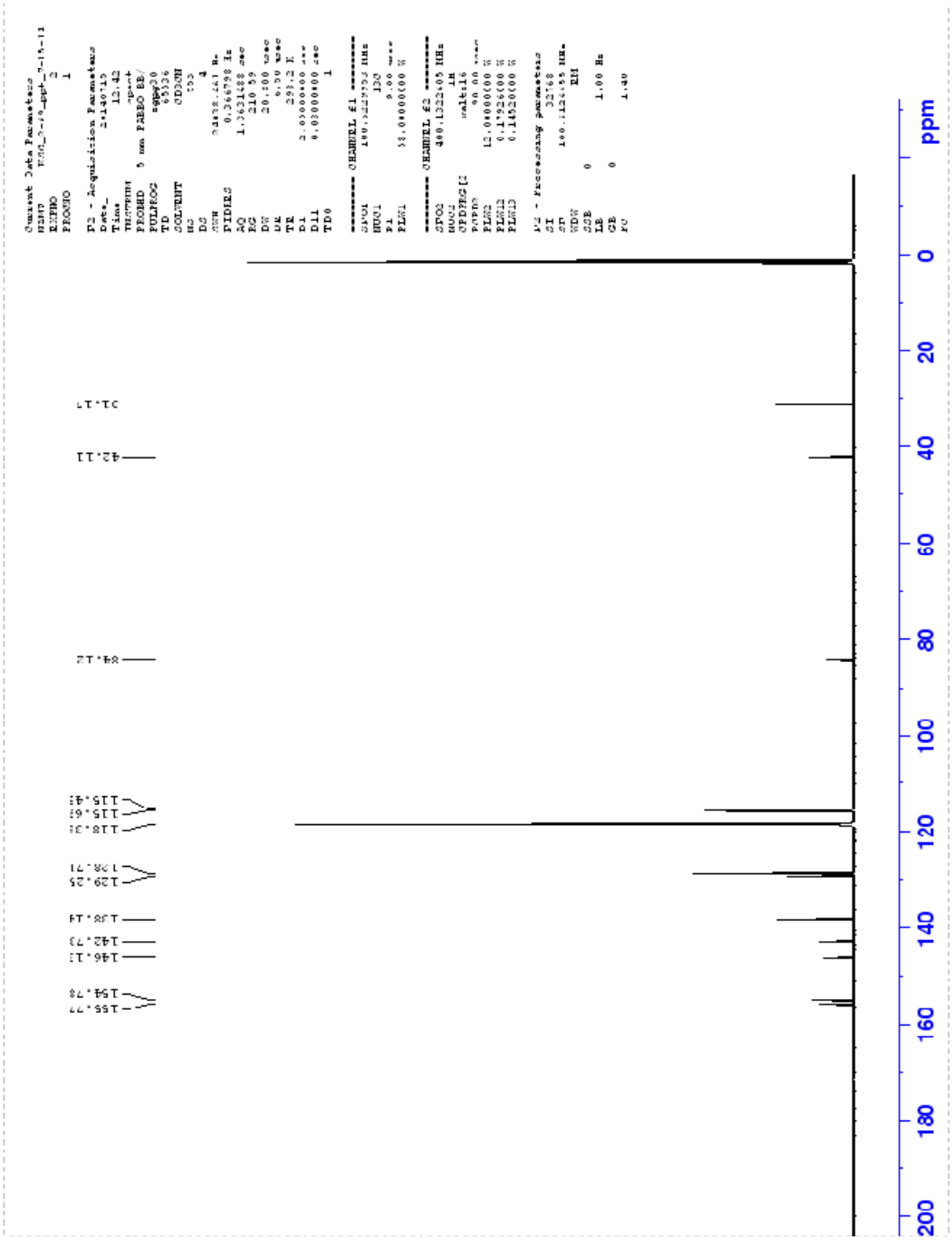
Current Data Parameters
NAME TSC_7-19_pgf_7-19-11
EXPNO 2
PROCNO 1
F2 - Acquisition Parameters
Date_ 20140715
Time 13.42
INSTRUM spect
PROBHD 5 mm PABBO BB/
PULPROG zgpg30
TD 65536
SOLVENT CDCl3
NS 512
DS 4
SWH 24038.461 Hz
FIDRES 0.366798 Hz
AQ 1.3631488 sec
RG 210.59
DW 20.800 usec
DE 6.50 usec
TE 293.2 K
D1 2.00000000 sec
D11 0.03000000 sec
TD0 1
======== CHANNEL f1 ========
SFO1 100.6227793 MHz
NUC1 13C
P1 9.00 usec
PL01 18.04000000 W
======== CHANNEL f2 ========
SFO2 400.1322405 MHz
NUC2 1H
CPDPRG[2 waltz16
PCPD2 90.00 usec
PL02 12.04000000 W
PL012 0.17926000 W
PL013 0.14520000 W
F2 - Processing parameters
SI 32768
SF 100.1234765 MHz
WDW EM
SSB 0
LB 1.00 Hz
GB 0
PC 1.40
194.78
194.77
146.11
142.73
138.54
129.25
128.71
118.38
115.69
115.43
84.12
42.11
31.17
ppm
200
180
160
140
120
100
80
60
40
20
0

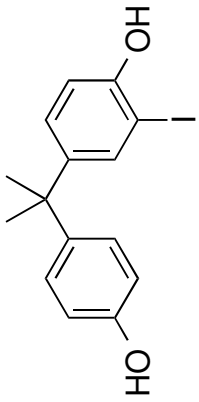

^{1}H NMR Spectrum of 1-(ethoxymethoxy)-4-(2-(4-(ethoxymethoxy)phenyl)propan-2-yl)-2-iodobenzene

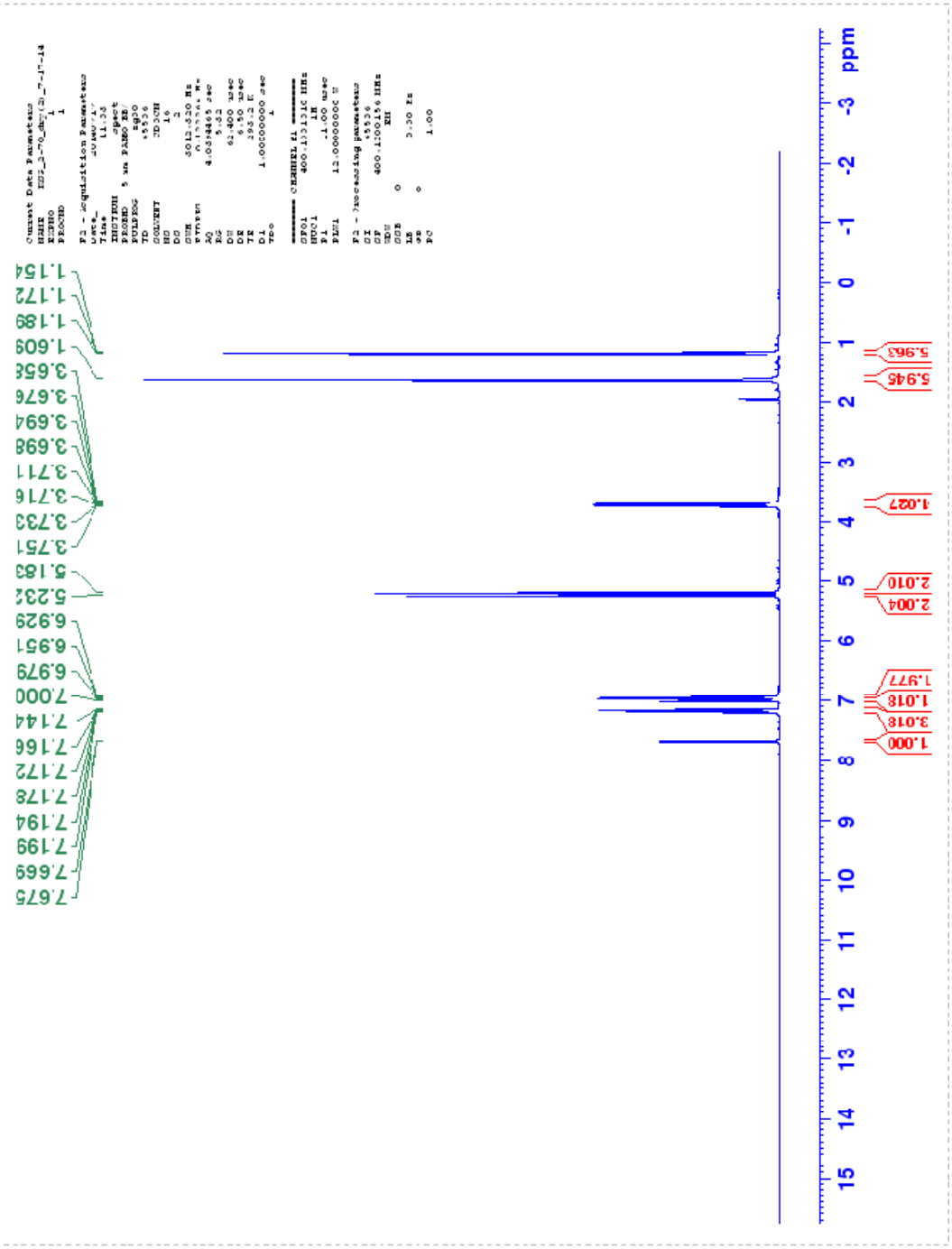
ppm
5.963
5.945
1.027
2.004
2.010
1.977
1.018
3.018
1.000

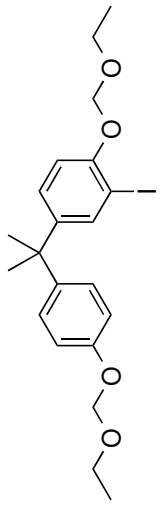

^{13}C NMR Spectrum of 1-(ethoxymethoxy)-4-(2-(4-(ethoxymethoxy)phenyl)propan-2-yl)-2-iodobenzene

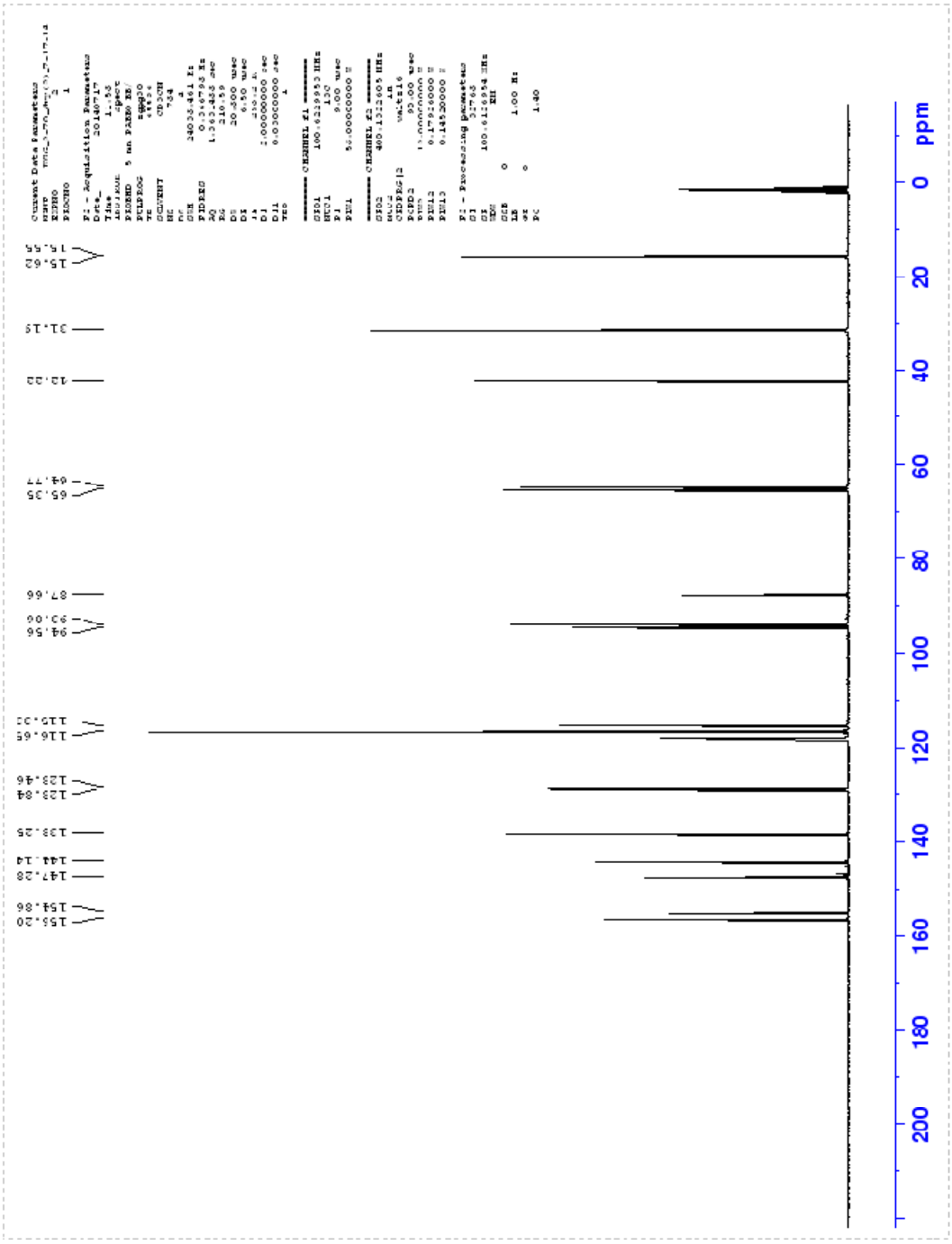
ppm
0
20
40
60
80
100
120
140
160
180
200
15.55
15.62
31.19
42.22
64.77
65.35
87.66
94.56
95.06
116.32
116.65
128.46
128.84
138.25
144.14
147.28
154.86
155.20

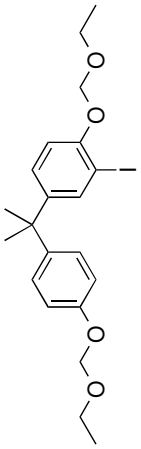

^{1}H NMR Spectrum of (2-(ethoxymethoxy)-5-(2-(4-(ethoxymethoxy)phenyl)propan-2-yl)phenyl)(4-methoxyphenyl)-λ^{3}-iodanyl trifluoromethanesulfonate

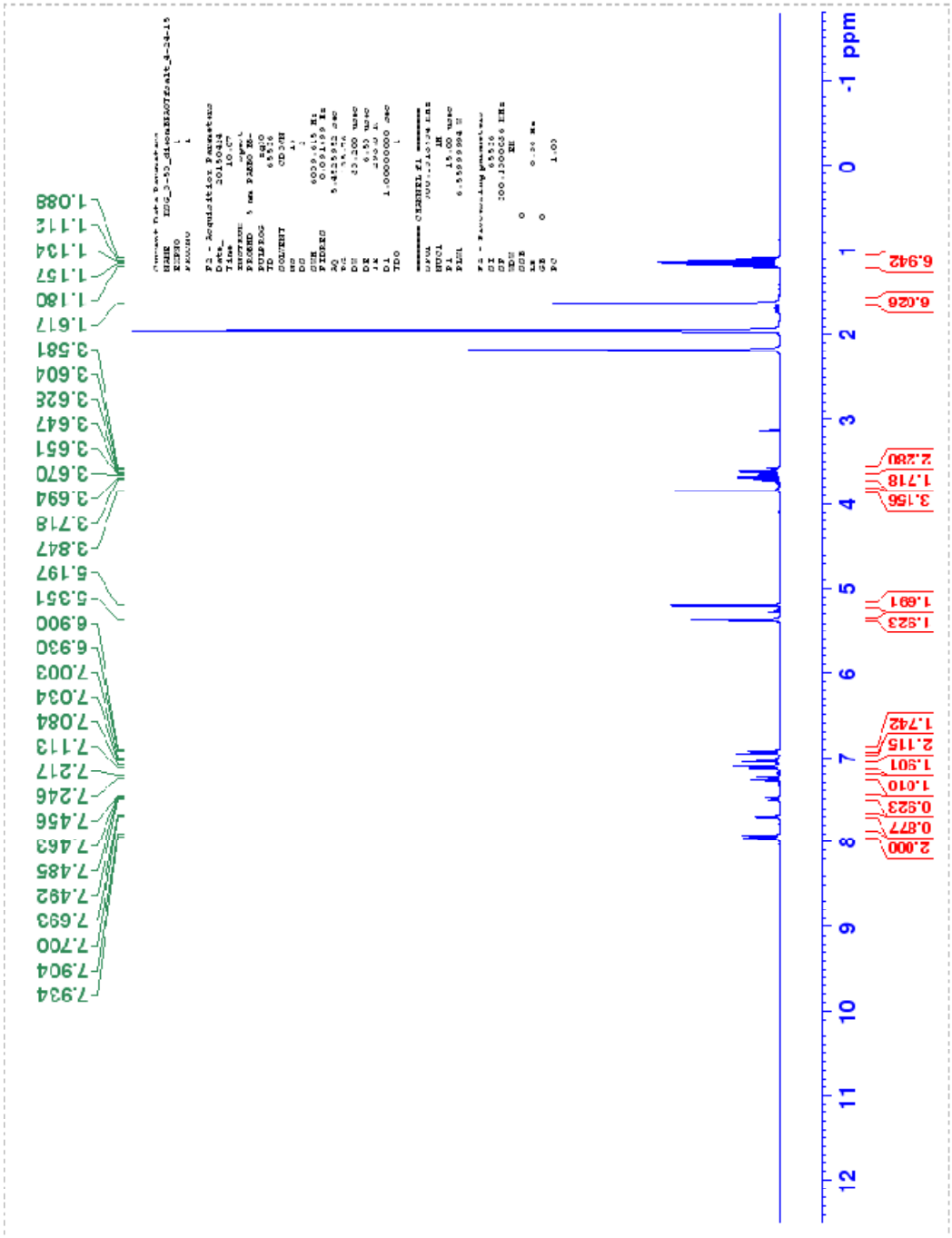
1.088
1.112
1.134
1.157
1.180
1.617
3.581
3.604
3.628
3.647
3.651
3.670
3.694
3.718
3.847
5.197
5.351
6.900
6.930
7.003
7.034
7.084
7.113
7.217
7.246
7.456
7.463
7.485
7.492
7.693
7.700
7.904
7.934
6.942
6.026
3.156
1.718
2.280
1.523
1.691
1.742
2.115
1.501
1.010
0.923
0.877
2.000
ppm

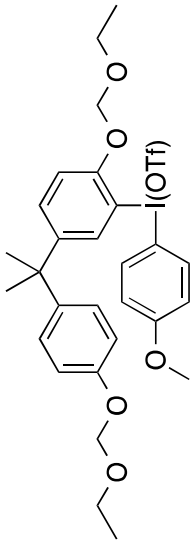

^{13}C NMR Spectrum of (2-(ethoxymethoxy)-5-(2-(4-(ethoxymethoxy)phenyl)propan-2-yl)phenyl)(4-methoxyphenyl)-λ^3-iodanyl trifluoromethanesulfonate

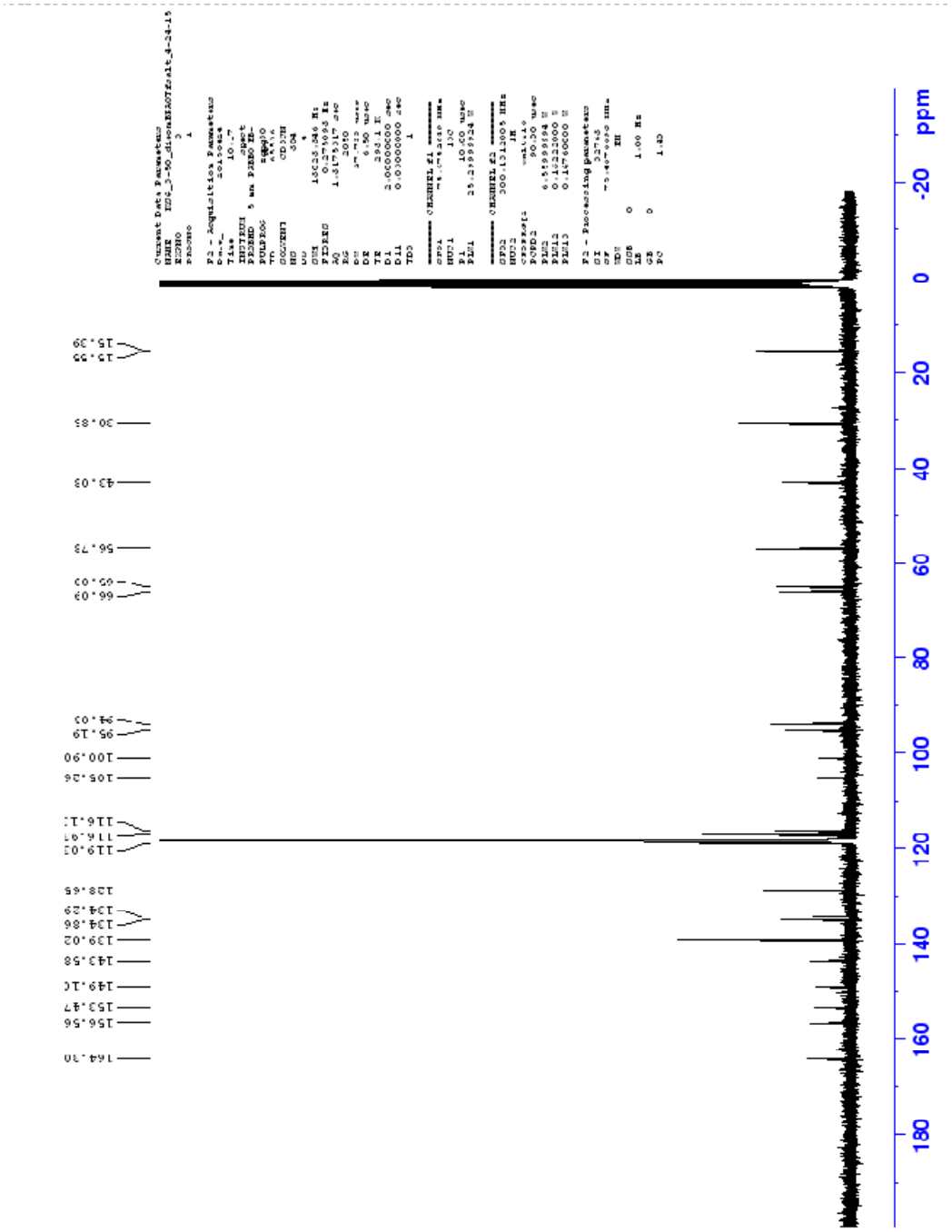
ppm
180
160
140
120
100
80
60
40
20
0
-20
164.30
156.56
153.47
149.10
143.58
139.02
134.86
134.29
128.65
119.02
116.91
116.10
105.26
100.90
95.19
94.03
66.09
65.03
56.73
43.03
30.85
15.99
15.39

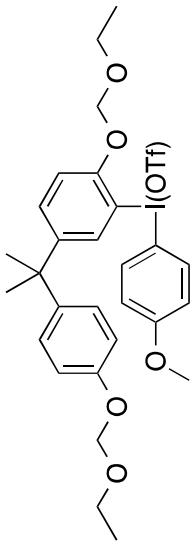
I(OTf)
O
O
O
O
O
O

^{19}F NMR Spectrum of (2-(ethoxymethoxy)-5-(2-(4-(ethoxymethoxy)phenyl)propan-2-yl)phenyl)(4-methoxyphenyl)-λ^3-iodanyl trifluoromethanesulfonate

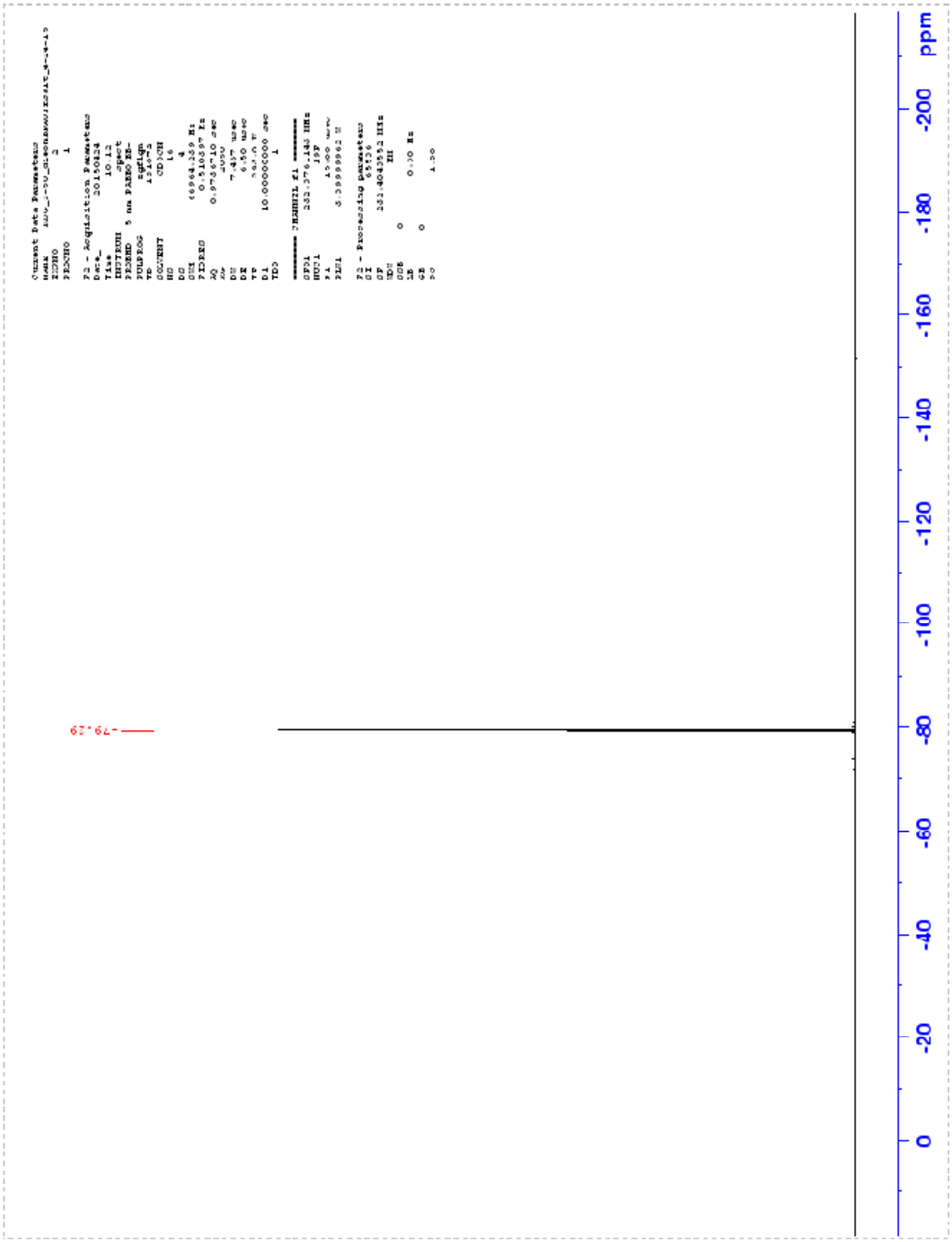
-79.29
0
-20
-40
-60
-80
-100
-120
-140
-160
-180
-200
ppm

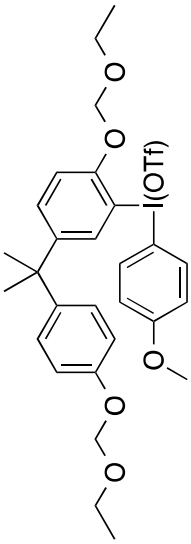

REFERENCES

(1) Ghisari, M.; Bonefeld-Jorgensen, E. C. *Toxicol. Lett.* **2009**, *189*, 67–77.
(2) Bosch, S.; Swarts, S.; Llados, F.; Gray, D. A.; Miles-Richardson, S. *U.S. Dept. Heal. Hum. Serv.* **2002**.
(3) Carlson, K.; Patton, L. *United States Consum. Prod. Saf. Comm.* **2010**.
(4) *World Heal. Organ.* **2010**, 60.
(5) Navarro, R.; Pérez Perrino, M.; Gómez Tardajos, M.; Reinecke, H. *Macromolecules* **2010**, *43*, 2377–2381.
(6) Li, H.; Ding, M.; Yu, J. **2001**, *39*, 251–254.
(7) Richardson, S. D. *Anal. Chem.* **2002**, *74*, 2719–2742.
(8) Penner, N.; Xu, L.; Prakash, C. *Chem. Res. Toxicol.* **2012**, *25*, 513–531.
(9) Solon, E. G. *Chem. Res. Toxicol.* **2012**, *25*, 543–555.
(10) Isin, E. M.; Elmore, C. S.; Nilsson, G. N.; Thompson, R. A.; Weidolf, L. *Chem. Res. Toxicol.* **2012**, *25*, 532–542.
(11) Fodero-Tavoletti, M. T.; Okamura, N.; Furumoto, S.; Mulligan, R. S.; Connor, A. R.; McLean, C. A.; Cao, D.; Rigopoulos, A.; Cartwright, G. A.; O'Keefe, G.; Gong, S.; Adlard, P. A.; Barnham, K. J.; Rowe, C. C.; Masters, C. L.; Kudo, Y.; Cappai, R.; Yanai, K.; Villemagne, V. L. *Brain* **2011**, *134*, 1–12.
(12) Villemagne, V. L.; Furumoto, S.; Fodero-Tavoletti, M. T.; Mulligan, R. S.; Hodges, J.; Harada, R.; Yates, P.; Piguet, O.; Pejoska, S.; Doré, V.; Yanai, K.; Masters, C. L.; Kudo, Y.; Rowe, C. C.; Okamura, N. *Eur. J. Nucl. Med. Mol. Imaging* **2014**, *41*, 816–826.
(13) Li, Z.; Conti, P. S. *Adv. Drug Deliv. Rev.* **2010**, *62*, 1031–1051.
(14) West, C. M. L.; Jones, T.; Price, P. *Nat. Rev. Cancer* **2004**, *4*, 457–469.

(15) Vallabhajosula, S. *Semin. Nucl. Med.* **2007**, *37*, 400–419.
(16) Baudoux, J.; Cahard, D. *Org. React.* **2007**, *69*, 347–669.
(17) Stavber, S.; Zupan, M.; Poss, A. J.; Shia, G. A. *Tetrahedron Lett.* **1995**, *36*, 6769–6772.
(18) Py, S.; Harwig, C. W.; Banerjee, S.; Brown, D. L.; Fallis, A. G. *Tetrahedron Lett.* **1998**, *39*, 6139–6142.
(19) Furuya, T.; Klein, J. E. M. N.; Ritter, T. *Synthesis (Stuttg).* **2010**, *11*, 1804–1821.
(20) Watson, D. A.; Su, M.; Teverovskiy, G.; Zhang, Y.; Garcia-Fortanet, J.; Kinzel, T.; Buchwald, S. L. *Science* **2009**, *325*, 1661–1664.
(21) Pike, V. W.; Aigbirhio, F. I. *J. Chem. Soc. Chem. Commun.* **1995**, 2215.
(22) Stang, P. J. *J. Org. Chem.* **2003**, *68*, 2997–3008.
(23) Carlson, K.; Patton, L. *United States Consum. Prod. Saf. Comm.* **2010**.
(24) Sekizawa, J.; Dobson, S.; Touch, R. J. *World Heal. Organ.* **2003**.
(25) Api, A. M. *Food Chem. Toxicol.* **2001**, *39*, 97–108.
(26) Elsisi, A.; Carter, D.; Sipes, I. G. *Fundemental Appl. Toxicol.* **1989**, *12*, 70–77.
(27) Kurane, R., Suzuki, T., Fukuoka, S. *Agric. Biol. Chem. Tokyo.* **1980,** 44, 529–536.
(28) Kurane, R., Suzuki, T., Fukuoka, S. *Appl. Microbiol. Biotechnol*., **1984,** 29, 378–383.
(29) Nomura, Y., Nakagawa, M., Ogawa, N., Harashim, S., Oshima, Y. *J. Ferment. Bioeng*. **1992,** 74, 333–334.
(30) Saito, T.; Hong, P.; Tanabe, R.; Nagai, K.; Kato, K. *Chemosphere* **2010**, *81*, 1544–1548.
(31) Kayano, Y.; Wantanabe, K.; Matsunaga, T.; Yamamoto, I.; Yoshimura, H. *Biol. Pharm. Bull.* **1997**, *20*, 749–751.
(32) Swan, S. H. *Environ. Res.* **2008**, *108*, 177–184.
(33) Swan, S. H.; Main, K. M.; Liu, F.; Stewart, S. L.; Kruse, R. L.; Calafat, A. M.; Mao, C. S.; Redmon, J. B.; Ternand, C. L.; Sullivan, S.; Teague, J. L.; Drobnis, E. Z.; Carter, B. S.; Kelly, D.; Simmons, T. M.; Wang, C.; Lumbreras, L.; Villanueva, S.; Diaz-Romero, M.; Lomeli, M. B.; Otero-Salazar, E.; Hobel, C.; Brock, B.; Kwong, C.; Muehlen, A.; Sparks, A.; Wolf, A.; Whitham, J.; Hatterman-Zogg, M.; Maifeld, M. *Environ. Health Perspect.* **2005**, *113*, 1056–1061.
(34) Dudič, M.; Císařová, I.; Michl, J. *J. Org. Chem.* **2012**, *77*, 68–74.
(35) White, R. D.; Carter, D. E.; Earnest, D.; Mueller, J. *Food Cosmet. Toxicol.* **1980**, *18*, 383–386.
(36) Sjoberg, P.; Bondesson, U.; Gray, T. J. B.; Ploen, L. *Acta Pharmacol. Toxicol. (Copenh).* **1986**, *58*, 225–233.
(37) Albro, P. W. *Environ. Health Perspect.* **1986**, *65*, 293–298.
(38) Schmid, P.; Schlatter, C. *Xenobiotica* **1985**, *15*, 251–256.
(39) Rubin, R. J.; Schiffer, C. A. *Transfusion* **1975**, *16*, 330–335.
(40) Klimisch, H.; Hellwig, J.; Kaufmann, W.; Jackh, R. *Hum. Exp. Toxicol.* **1991**, *10*, 68.
(41) Barry, Y. A.; Labow, R. S.; Keon, W. J.; Tocchi, M. *Toxicol. Appl. Pharmacolgy* **1990**, *106*, 48–52.

(42) Gillum, N.; Karabekian, Z.; Swift, L. M.; Brown, R. P.; Kay, M. W.; Sarvazyan, N. *Toxicol. Appl. Pharmacol.* **2009**, *236*, 25–38.
(43) Mitchell, F. E.; Price, S. C.; Hinton, R. H.; Grasso, P.; Bridges, J. W. *Toxicol. Appl. Pharmacolgy* **1985**, *81*, 371–392.
(44) Cattley, R. C.; Conway, J. G.; Popp, J. A. *Cancer Lett.* **1987**, *38*, 15–21.
(45) Albro, P. W.; Chapin, Robert, E.; Corbett, J. T.; Schroeder, J.; Phelps, J. L. *Toxicol. Appl. Pharmacol.* **1989**, *100*, 193–200.
(46) Lamb, J. C.; Chapin, R. E.; Teague, J.; Lawton, D.; Reel, J. R. *Toxicol. Appl. Pharmacolgy* **1987**, *88*, 255–269.
(47) Davis, B. J.; Maronpot, R. R.; Heindel, J. J. *Toxicol. Appl. Pharmacolgy* **1994**, *128*, 216–223.
(48) Colon, I.; Caro, D.; Bourdony, C. J.; Rosario, O. *Environ. Health Perspect.* **2000**, *108*, 895–900.
(49) Hill, S. S.; Shaw, B. R.; Wu, A. H. B. *Clin. Chim. Acta* **2001**, *304*, 1–8.
(50) Navarro, R.; Perrino, M. P.; Tardajos, M. G.; Reinecke, H. *Macromolecules* **2010**, *43*, 2377–2381.
(51) Kelber, J.; Achard, M. F.; Garreau-De Bonneval, B.; Bock, H. *Chem. - A Eur. J.* **2011**, *17*, 8145–8155.
(52) Wang, B.; Cerny, R. L.; Uppaluri, S.; Kempinger, J. J.; Dimagno, S. G. *J. Fluor. Chem.* **2010**, *131*, 1113–1121.
(53) Shelby, M. D. *Natl. Toxicol. Program; U.S. Dep. Heal. Hum. Serv.* **2008**, *22*.
(54) Bisphenol A: Information Sheet, 2002, 1–8.
(55) Twaroski, M. *World Heal. Organ.* 2010, 1–16.
(56) Domoradzki, J. Y.; Thornton, C. M.; Pottenger, L. H.; Hansen, S. C.; Card, T. L.; Markham, D. A.; Dryzga, M. D.; Shiotsuka, R. N.; Waechter, J. M. *Toxicol. Sci.* **2004**, *77*, 230–242.
(57) Kolšek, K.; Sollner Dolenc, M.; Mavri, J. *Chem. Res. Toxicol.* **2013**, *26*, 106–111.
(58) Nakamura, S.; Tezuka, Y.; Ushiyama, A.; Kawashima, C.; Kitagawara, Y.; Takahashi, K.; Ohta, S.; Mashino, T. *Toxicol. Lett.* **2011**, *203*, 92–95.
(59) Edmonds, J. S.; Nomachi, M.; Terasaki, M.; Morita, M.; Skelton, B. W.; White, A. H. *Biochem. Biophys. Res. Commun.* **2004**, *319*, 556–561.
(60) Yoo, S. D.; Beom, S. S. *J. Toxicol. Environ. Heal. Part A* **2001**, *64*, 417–426.
(61) Doerge, D. R.; Twaddle, N. C.; Vanlandingham, M.; Fisher, J. W. *Toxicol. Appl. Pharmacol.* **2010**, *247*, 158–165.
(62) Kurebayashi, H.; Betsui, H.; Ohno, Y. *Toxicol. Sci.* **2003**, *73*, 17–25.
(63) Kurebayashi, H.; Harada, R.; Stewart, R. K.; Numata, H.; Ohno, Y. *Toxicol. Sci.* **2002**, *68*, 32–42.
(64) Xin, F.; Jiang, L.; Liu, X.; Geng, C.; Wang, W.; Zhong, L.; Yang, G.; Chen, M. *Mutat. Res. Toxicol. Environ. Mutagen.* **2014**, *769*, 29–33.
(65) Michaela, P.; Mária, K.; Silvia, H.; Lubica, L. *Naunyn. Schmiedebergs. Arch. Pharmacol.* **2014**, *387*, 153–163.
(66) Zhang, L.; Zhang, H. Y.; Ma, C. C.; Zhai, L. L.; Jia, L. H. *Mol. Cell. Toxicol.* **2013**, *9*, 385–391.
(67) Alonso-Magdalena, P.; Vieira, E.; Soriano, S.; Menes, L.; Burks, D.; Quesada, I.; Nadal, A. *Environ. Health Perspect.* **2010**, *118*, 1243–1250.

(68) Khalil, N.; Ebert, J. R.; Wang, L.; Belcher, S.; Lee, M.; Czerwinski, S. A.; Kannan, K. *Sci. Total Environ.* **2014**, *470-471*, 726–732.
(69) Chen, Z. J.; Yang, X. L.; Liu, H.; Wei, W.; Zhang, K. S.; Huang, H. B.; Giesy, J. P.; Liu, H. L.; Du, J.; Wang, H. S. *Arch Toxicol* **2014**.
(70) Rubin, B. S. *J. Steroid Biochem. Mol. Biol.* **2011**, *127*, 27–34.
(71) vom Saal, F. S.; Hughes, C. *Environ. Health Perspect.* **2005**, *113*, 926–933.
(72) Neumann, K. Highly Efficient No-Carrier-Added [18F]-Functionalizations of Electron Rich Arenes and Applications of Hypervalent Iodine, University of Nebraska-Lincoln, 2012.
(73) Schlosser, M.; Marzi, E.; Spitaleri, A.; Mongin, F. *Eur. J. Org. Chem.* **2002**, 2508.
(74) Chen, M.; Buchwald, S. L. *Angew. Chemie - Int. Ed.* **2013**, *52*, 11628–11631.
(75) Kubo, T.; Maezawa, N.; Osada, M.; Katsumura, S.; Funae, Y.; Imaoka, S. *Biochem. Biophys. Res. Commun.* **2004**, *318*, 1006–1011.
(76) Hu, B.; Miller, W. H.; Neumann, K. D.; Linstad, E. J.; Dimagno, S. G. *Chem. A Eur. J.* **2015**, *21*, 6394–6398.